UAB

Universitat Autònoma de Barcelona

STRUCTURAL AND FUNCTIONAL STUDIES OF NSE2, THE SUMO E3 LIGASE OF THE SMC 5/6 COMPLEX

JARA ADELINA LASCORZ LOZANO

2022

Doctoral thesis presented to apply for the Doctor of Philosophy Degree in Biochemistry, Molecular Biology and Biomedicine

This work was performed at the Institut de Biotecnologia i de Biomedicina (IBB) and at the Biochemistry and Molecular Biology Department of the Universitat Autònoma de Barcelona (UAB) under the supervision of
Dr. David Reverter Cendrós and Dra. Nathalia Varejão Nogueira da Paz.

Dr. David Reverter Cendrós   Dra. Nathalia Varejão Nogueira da Paz

Cover illustration by Lucía Sánchez Alba

El azar afortunado suele ser casi siempre el premio del esfuerzo perseverante.

Santiago Ramón y Cajal

Llegar hasta escribir el final de esta tesis ha sido una carrera de fondo, mucho más larga de lo que me planteé en un principio, y el mérito de haber acabado es gracias a toda la gente que me ha acompañado durante todos estos años. Quizá son demasiado largos, pero también ha sido una tesis más larga de lo normal, así que he tenido la suerte de tener a mucha gente a mi lado durante este tiempo.

Sé que mencionar en este apartado a los directores suele ser una formalidad, pero en mi caso estoy realmente agradecida. En las tres fotos que encabezan este apartado (de 2014, 2017 y 2021) hay dos personas que me acompañan permanentemente: David y Nathalia.

David, gracias por la oportunidad de hacer las prácticas de grado aún siendo una estudiante de biología que tenía más bien poca idea de dónde se metía, por contar conmigo para las prácticas de máster y por, finalmente, ofrecerme un contrato para poder hacer el doctorado. Gracias por la paciencia durante todos estos años, pero sobre todo durante los primeros y durante esta etapa final.

Nathalia, no sé ni por dónde empezar a agradecerte todo lo que has hecho por mí. Primero como tutora tanto del máster como ahora de esta tesis, te agradezco toda esa paciencia que tienes para explicarlo todo hasta que quede clarísimo. Gracias por la motivación, la energía positiva que siempre tienes y desprendes a tu alrededor, por estar siempre dispuesta a ayudarme y por los consejos durante todos estos años, algunos con cervezas de por medio. Gracias por tu sinceridad y por enseñarme a confiar en mí misma. Sé que te gusta separar lo profesional de lo personal, pero ambas sabemos que eres una gran amiga.

Además de los directores, hay varias personas que aparecen en las fotos, que han formado parte de EP y que de un modo u otro han contribuido a esta tesis. Con Yang y Pablo comencé los primeros años, y el mérito de no haber perdido la paciencia con la biología molecular es gracias a Yang y a la cantidad de veces que me pasó por alto errores durante aquel verano de las prácticas de grado. Después llegó Bing, trabajador incansable como pocos, del que aprendí que la perseverancia suele dar buenos frutos.

La última foto ya es la del grupo actual, donde aparecen tres personas fundamentales para haber podido llegar hasta aquí: Li Ying, Helena y Lucía. Li Ying, I'm going to miss you a lot! You have been a good friend all these years, and I have learned a lot from you and your culture. I will never forget you, and I still have to go to China to see your hometown! Helena y Lucía, no sé ni qué deciros que no os haya dicho ya, tendréis tres líneas, pero podrían ser tres tesis para cada una. Helena, és un plaer treballar amb tu. Eres dulce, sincera, creativa, inteligente, nunca pones problemas… Como *minion* has sido la mejor con diferencia, ¡pero como predoc eres incluso mejor! Tanto que una parte de esta tesis es directamente tuya, así que gracias se queda corto. Lucía, hace años te dije que serías la primera en los agradecimientos de la tesis, y si te fijas bien has acabado yendo incluso por delante de ellos (¡Gracias de nuevo por el dibujazo!). Qué suerte la mía de conocerte cuando estabas en BioMol y de haberte visto crecer durante estos años como científica, de verdad que ha sido un placer. Pero, sobre todo, qué suerte tenerte como amiga y haber podido compartir tantas cosas contigo durante todos estos años. Os quiero mucho, chicas.

Pero un grupo no se forma sólo con la gente que aparece en las fotos. Durante estos años he tenido la oportunidad de tener varios *minions* de grado o máster, y de todos he aprendido algo y con todos he crecido. Cada uno me ha aguantado en un momento, y todos han tenido un papel importante en algún momento de esta tesis. Muchas gracias a Eric, Ana, Naila, Helena (de nuevo), pero en especial a Jessica. Jess, contigo aprendí muchísimo y espero que fuese mutuo. Me alegro muchísimo de no haber perdido el contacto durante todos estos años, quedar contigo siempre es un placer.

La suerte de tener un laboratorio compartido es que tienes más compañeros/as con los que compartes absolutamente todo, en mi caso durante (casi) toda la tesis ha sido con

el grupo de Salvador Ventura, PDP o PPMC, de dónde también me llevo a muchas y muy buenas personas.

Marcos, no sería justo empezar por otra persona que no fueses tú, que has estado a mi lado (bueno, más bien a mi espalda) todos estos años. Siempre quisiste que esta tesis se alargara para poder acabarla a la vez que tú, y al final casi casi vas a defender tú antes. Cómo hemos crecido en este tiempo, y qué contenta estoy de haberte tenido a mi lado. Muchas gracias por la comprensión en los días difíciles y por las risas en los días fáciles. Voy a echar mucho de menos hasta tu forma de meterte conmigo, pero siempre nos quedará haber hecho el mejor vídeo de Fondue de IBB. Marta, empezamos el mismo día las prácticas de grado una al lado de la otra, hicimos juntas el máster, el doctorado, y al final he acabado la tesis casi dos años más tarde. Muchísimas gracias por todas las confidencias, por el apoyo y por el cariño durante tanto tiempo. Cris, también fuimos compañeras de máster y después de laboratorio, y menos mal que estabas ahí algunas tardes para ayudarme y hacerme compañía cuando ya no había nadie. Muchas gracias por traer la música al lab y por tu manera tan entusiasta de ver la vida.

Cri, Manu, Maria, Alex Mur, Anita, Andrea, gracias por seguir formando parte de mi vida incluso cuando ya no compartimos espacio de trabajo. Alex, medio primo, gracias por haberme hecho más llevadero todo el primer año de doctorado lleno de dudas, nunca podré agradeceros a Jess, Marcos y a ti lo que aprendí de vosotros en los primeros seis meses. Cri, grazie mille per tutto. Eres otra de las personas indispensables durante este tiempo, parece mentira que sólo coincidiéramos seis meses. En Barcelona tienes casa siempre que quieras, ya lo sabes. Maria, gracias por tu alegría, por saber reírte siempre de todo y saber sobre llevar a Marcos. Eres muy grande, Maria, llegarás muy lejos (aunque parece que no nos llevarás a Empuriabrava) y espero que nos lleves contigo, aunque tardemos otro año en volver a vernos. Manu, gracias por recordarme que la vida hay que llevarla con calma, por la devoción al mallorquí, por tantos planes, consejos, paseos con Aníbal, y tantísima ayuda desinteresada. El resto de los agradecimientos te los digo con dos cervezas de por medio. Andrea, gracias por un año de compartir laboratorio, comida, música, disgustos y alegrías, eurovisión, excursiones, café y chocolate… La verdad es que vaya año más completito para ser año de pandemia. Muchísimas gracias por todo el apoyo, Andrea. También agradecer a Susanna todos estos años pendiente de mí, como si fuese una predoc suya más, y a Javi, por estos últimos meses de confusión pre-mudanza y pre-tesis. También me gustaría mencionar a los PDPs que ya no están, pero que me marcaron y me enseñaron muchísimo al principio de esta aventura: Ricardo y Patri.

Además de compartir espacio en el laboratorio, del IBB también me llevo grandes amigos de otros grupos. BioMol fue el grupo que me acogió en los primeros años, y tengo la suerte de llevarme grandes amigos. Sergi, Marina, Lucía (tenías que estar en las dos categorías), Arturo, Ana, Miguel, Luis González. Sergi, eres una de las mejores

personas que puede haber. No tengo palabras para agradecerte todos los consejos y las charlas durante todos estos años que hace que nos conocemos, tanto de ciencia como de la vida en general. Esta tesis habría sido más difícil si tú no hubieras aparecido por ahí en los inicios y me hubieras acompañado todo este tiempo. Marina, eres la bondad hecha persona, y creo que cualquiera al que se lo pregunte me dirá lo mismo. Eres inteligente, buena, dulce, cantas bien, y encima cocinas bien y nos lo demuestras siempre que puedes. Sólo te mereces cosas bonitas en esta vida. Arturo, muchísimas gracias por años de discusiones (científicas o absurdas), cervezas, películas, juegos de mesa y más cervezas, y sobre todo gracias por los ánimos y por darme tanta confianza en mi misma. Os quiero mucho.

Los tiempos cambian, y hace unos meses apareció Enzimo por el sótano para convertirse en nuestros nuevos compañeros de lab. Menos mal que son un grupo creativo como pocos, que tan pronto te montan un detector de movimiento que te canta villancicos como una noria con mecanos dentro de una estufa. Han sido unos meses entretenidísimos, tratando de escribir la tesis mano a mano con Sergi, pero quitándonos los cascos cada dos minutos para chafardear sobre lo que pasaba a nuestro alrededor. Gracias por estar ahí en estos meses de incertidumbre en torno al ataque informático y hacerlo todo más ameno. Mención especial al ex-enzimo Sergi Montané, que el día que entré por la puerta para empezar el doctorado me dijiste "date la vuelta y no mires atrás", y lo he tenido presente todo este tiempo. Sergi, David, Eddi, Marta, Pau y Paula, gracias a todos por hacernos la vida y la convivencia tan fácil, y por estar siempre predispuestos a pedir comida, traer comida, o a ir al sushi.

Por suerte, entre las Fondues, los eternos cafés de desayuno, y las comidas en el patio durante la pandemia, nos ha dado para socializar muchísimo en el patio, por lo que también quiero agradecer el haber estado ahí en un momento u otro (porque cinco años y medio dan para conocer a mucha gente) a otros grupos del IBB. A los chicos de Llevats: Diego, Santo y Marcel, por estar siempre dispuestos a echar un vermut o cerveza y que se acabe alargando. A Inmuno Celular: Adrián, Andrea, Mireia, Alba, porque siempre hay alguien en el patio dispuesto a despotricar entre risas contra lo que sea necesario, mi salud mental durante estos años os está muy agradecida. A NBT, gracias por haber formado el equipo de vóley y de post-vóley, por habernos acoplado en vuestros planes y haber sido una válvula de escape estos últimos meses. Eloi, moltíssimes gràcies en especial a tu, per ser la cola d'aquesta colla de gent amb la mirada pura i brillant. Gràcies pels consells i els ànims aquests mesos! Muchas gracias también a los organizadores de la mejor Fondue hasta la fecha, Xavi, Andros, Santo. Por último, muchísimas gracias a la gente que se encarga de hacernos la vida más fácil: Miguel, Almu, Francisca, Ángels y Paqui.

Tampoco habrían sido lo mismo estos años sin la compañía de la torre del Departamento de Bioquímica, creadores de los Beer-seminars, las barras de la FM-UAB y las fiestas de verano. Gracias infinitas a la otra mitad del grupo de PDP, Jaime, Jordi, Valen, Samu,

Francisca, por todo lo compartido durante estos años de risas y lloros, que no es poco. Gracias por toda la ayuda, por estar siempre disponibles, por celebrarlo absolutamente todo, hasta las no-fiestas-de-verano. Gracias también a Alejandro, por los debates, los aguantes, las quejas, las decisiones tomadas de forma conjunta... Espero que sigamos desayunando juntos aunque sea de vez en cuando en nuestra siguiente etapa, para poder seguir criticando al mundo. Gracias infinitas a Guillem, en el terreno personal y en el laboral, por estar siempre dispuesto a todo y por echar siempre una mano incluso cuando ya no tienes tiempo de nada más. A Pilar y a Gabri, por el apoyo moral durante todo este tiempo, pero sobre todo durante el último año de cuenta atrás constante.

El inicio de todo esto empezó cuando en el verano de 2010 decidí empezar el grado de Biología en esta misma universidad. Si volviese a ese mes de septiembre, le diría a la Jara del pasado que volviese a sentarse con esa chica bajita, tan blanca como yo y que apenas hablaba, y que estaba justo al lado de una chica rubia que no paraba de hablar con todo el mundo y que estaba dispuesta a hacerse amigo de toda la clase. Gracias, Alba y Vicky, por estar conmigo desde el principio y habernos aguantado tal y como somos. El azar de los apellidos quiso que en los grupos de prácticas y problemas nos juntásemos con los mejores amigos que era posible: Alicia, Caste, Marc, Mireia y Lorena. ¿Quién nos iba a decir que diez años después seguiríamos cenando, riéndonos y haciendo planes? Gracias por toda vuestra paciencia conmigo, sobre todo en los últimos meses, y por tener la capacidad de celebrar hasta los no-depósitos. Os quiero, budis.

También el azar acabó formando un piso en la Vila dónde dejamos de ser compañeros de piso y nos hicimos amigos del alma. Aunque empecé la tesis cuando cada una estábamos en una punta del mundo, sin vosotras no habría llegado hasta donde estoy ahora: Angi, Carlos, Mau y Silvia (y Bubi). Durante la tesis, he compartido piso con varias personas, y he tenido la suerte de que una de ellas se mantuviera constante casi hasta el final: Carlos, qué sería de mis últimos diez años sin ti, me has enseñado tanto que estoy segura de que sería una persona totalmente diferente. Te quiero muchísimo. También he tenido la gran suerte de coincidir con Mariví, alguien con quien siempre es un placer hablar y que todo el tiempo con ella se me hace corto. Gracias por ayudarme tanto en los meses en los que estaba flojita.

Para poder llegar a escribir todo esto, y hacerlo con el buen ánimo con el que he tenido la suerte de pasar todos estos años, hace falta tener un buen grupo de gente que te soporte y te aguante al lado. Gracias a los que empezaron siendo compañeros de máster y que acabaron siendo amigos: Elena, Xavi, Javi y Carlota. Elena, has sido un apoyo increíble todos estos años, tanto en casa como a nivel científico. Qué suerte verte y que sea como si no pasase el tiempo. Gracias a mis amigas de Huesca, por hacer que siempre que vuelvo me sienta en casa, y por poder pasar el tiempo hablando de todo y de nada:

Ana, Andrea, Celia, Clara, Elena, Julia, Lara, Laura, Lorena, María, Marta, Mau y Xan. Gracias por estar siempre atentas y por ser un referente para mí en todos los sentidos. Gracias también a Ana Joya y Clara Laliena, por intentar vernos siempre que podemos, aunque vivamos en ciudades distintas, y por mantener viva la amistad, aunque sea a base de tonterías. Gracias también a Malu, Diana, Laura, Mapi, Sara y Elena, porque, aunque no tengáis ni idea de qué hablo si os cuento cosas de la tesis cuando nos vemos en Cimballa, siempre pongáis buena cara y finjáis interés.

Para acabar, he tenido la gran suerte de tener una familia detrás que siempre me ha estado ayudando y que han sido un referente en todos los sentidos, por los que estoy eternamente agradecida. A mis tíos de Barcelona y a Maica, por ayudarme siempre para que no me sintiese sola en esta ciudad desde hace ya once años. Aquí también quiero recordar a Maribel, que en los últimos años ha hecho que tuviese una familia más cerquita de Barcelona. A mis tíos de Zaragoza y a David y Diana, por ser una inspiración tanto en la biología como en cómo afrontar la vida adulta y los primeros trabajos. A la familia Lozano en general, por transmitir siempre alegría y porque cuando nos juntamos parece que sea siempre fiesta. A Pablo y Jari en particular, porque con vosotros la vida se ve de otra forma mucho más bonita. A la yaya Manuela (y a los yayos y yayas que ya no están), por estar siempre pendiente de mi (y de todos), llamándonos a todas horas, y deseándonos que todo nos vaya bien, aunque no acabes de entender si esto es un trabajo, un examen o una oposición. Eres la alegría de la casa.

Gracias a papá, mamá, Lorién y Luzía. Por absolutamente todo. No podría pedir una familia mejor.

Gracias a Carlos, porque sin tu ayuda, tus ánimos, tu comprensión, tu forma de hacerme reír, … Sin ti esta tesis habría sido infinitamente más difícil.

Muitas grazias a toz y totas por tot. Nada de esto habría sido posible sin la gente que está aquí (y más que se me habrán olvidado). Ha sido un placer compartir todos estos años.

Jara

Table of contents

Protein post-translational modification (PTM) by small ubiquitin-like modifier (SUMO) is a widespread manner of regulation of many cellular functions, including as example transcription or DNA damage repair. SUMO belongs to the ubiquitin-like modifiers (UbL) superfamily of proteins, which are constituted by homologous small protein domains that can be attached to protein targets by the formation of an isopeptidic bond between lysine residues in the substrate and the C-terminal tail of the UbL modifier. This reaction requires the participation of an ATP-dependent enzymatic cascade composed by an÷ E1, E2 and E3 enzymes.

Structural Maintenance of Chromosomes (SMC) complexes are ring-shaped heterodimers formed by two SMC proteins and a distinct number of satellite proteins. Eukaryotes contain three SMC complexes: cohesin, which maintains the connection between sister chromatids; condensin, which compacts chromosomes; and the Smc5/6 complex, which promotes chromosome disjunction, among other functions. Nse2 is a subunit of the Smc5/6 complex that possesses SUMO E3 ligase activity by the presence of a SP-RING domain that activates the E2~SUMO thioester discharge on the substrates.

In the present thesis, we first show the design, subcomplex purification, and initial crystallization attempts of truncated constructs of the human Smc5/6 complex. Second, we reveal the enhancement of the SUMO E3 ligase activity of Nse2 upon DNA binding to a positively charged patch in the *arm* domain of Smc5, revealing a potential mechanism to restrict SUMOylation to the vicinity of those Smc5/6-Nse2 molecules engaged on DNA. Third, we present the crystal structure of the Nse2/Smc5 in complex with the E2-SUMO charged thioester, disclosing the structural details of this multiple E2-E3 protein interface. We finally reveal the role of two SIM (SUMO-Interacting Motif)-like motifs in Nse2, which are restructured upon binding the donor and E2-backside SUMO during the E3-dependent discharge reaction, revealing the enzymatic mechanism of the Nse2 SUMO E3 ligase.

°C	Degree Celsius
Amp	Ampicillin
BL21	BL21 (DE3) strain competent cells
BME/βME	β-mercaptoetanol
Chl	Chloramphenicol
Da	Dalton
dsDNA	Double-stranded deoxyribonucleic acid
DTT	Dithiothreitol
E. coli	*Escherichia coli*
EDTA	Ethylenediaminetetraacetic acid
EMSA	Electrophoretic mobility shift assay
FL	Full-length
H. sapiens	*Homo sapiens*
Kan	Kanamycin
kDa	Kilodalton
LB	Luria Broth
MMS	Methyl methane sulfonate
nM	Nanomolar
Nse	Non-Structural maintenance of chromosomes (SMC) element
ON	Over-night

PCR	Polymerase chain reaction
PDB	Protein Data Bank
PTM	Post-translational modification
R2	Rosetta 2 strain competent cells
RING	Really interesting new gene
Rpm	Revolutions per minute
RQ	Resource Q
RS	Resource S
RT	Room temperature
S. cerevisiae	*Saccharomyces cerevisiae*
S. pombe	*Schizosaccharomyces pombe*
SBD	SUMO-binding domains
SBM	SUMO-binding motifs
SCM	SUMO-consensus motifs
SD	Superdex
SDS	Sodium Dodecyl Sulfate
SDS-PAGE	Sodium Dodecyl Sulfate Polyacrylamide Gel Electrophoresis
SIM	SUMO interaction motif
SMC	Structural Maintenance of Chromosomes
ssDNA	Single-stranded deoxyribonucleic acid
SSI	SUMO-SIM interaction
Strep	Streptomycin
SUMO	Small Ubiquitin-like Modifier

UbL	Ubiquitin-like Modifier
WT	Wild-type
XL1B	XL1-Blue strain competent cells
µM	Micromolar

INTRODUCTION
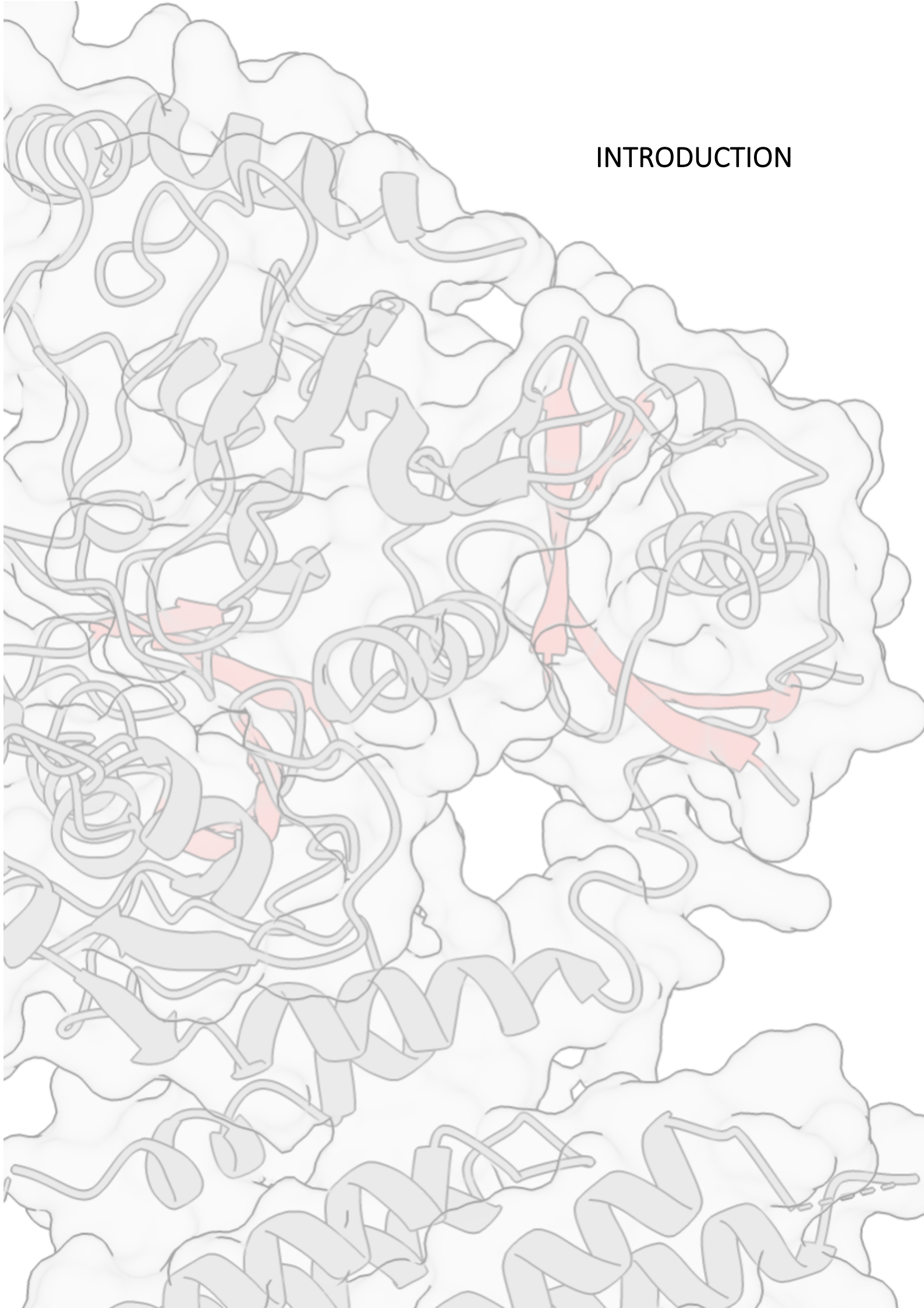
I1. SUMO modification

General introduction

Post-translational modification (PTM) refers to the biochemical modifications after the synthesis of the protein by a ribosome. Mainly, PTMs occurs by decorating proteins with functional groups (such as acetate, phosphate, lipids, or carbohydrates), which alter the localization or activities of proteins or induce structural changes. These modifications suppose an important role in cellular signaling and regulation. Moreover, PTMs can also occur by the covalent attachment to other proteins, such as the ones belonging to the ubiquitin family (like ubiquitin, SUMO, Nedd8, ISG15, among others).

Small Ubiquitin-like MOdifier (SUMO) is a small protein of about 100 amino acids which belongs to the ubiquitin-like modifiers (UbL) superfamily of proteins. The protein post-translational modification by SUMO is called SUMOylation and it demands the covalent conjugation of SUMO to the side chains of lysine residues in the target proteins. Differently of the classical protein destination upon ubiquitination, SUMOylation does not signal proteins for degradation but suppose an important manner of regulation of many cellular functions inside the cell, regulating the function of hundreds of proteins involved in multiple cellular pathways, having in most instances essential roles for their correct function (Cubeñas-Potts & Matunis, 2013; Droescher, Chaugule, & Pichler, 2013; Flotho & Melchior, 2013). It has been well reported that many of the SUMO-modified proteins are transcription factors and other nuclear proteins involved in the maintenance of chromatin structure and DNA repair (Bergink & Jentsch, 2009). This activation by SUMO requires the action of three enzymes, E1, E2 and E3, and it could be reversed by SUMO specific proteases, which are also responsible for the initial SUMO maturation.

The SUMOylation pathway

SUMO is a member of the ubiquitin-like modifiers (UbL) superfamily of proteins, which are all formed by homologous small protein domains that can be attached to protein targets by forming an isopeptidic bond between ε-amino groups of lysine side chains in

the substrate and the UbL modifier's C-terminal tail, which has a di-glycine motif (Cappadocia & Lima, 2018; Flotho & Melchior, 2013; Welchman, Gordon, & Mayer, 2005). SUMO modification is conserved among all eukaryotes and hundreds of distinct substrates have been identified inside cells. Indeed, SUMOylation is involved in a wide range of processes, including DNA replication, nuclear trafficking, chromatin organization, response to stress or cancer (García-Rodríguez, Wong, & Ulrich, 2016; Hay, 2005; Müller, Ledl, & Schmidt, 2004).

Although SUMO is a small protein, different variants are observed in distinct organisms: while yeast and invertebrates have only one single SUMO protein named Smt3, vertebrates have several SUMO proteins. Mammals express three active SUMO proteins: SUMO2 and SUMO3 that share 97% sequence identity, and SUMO1 that only shares 47% sequence identity with the formers (Flotho & Melchior, 2013; Hay, 2005). To be noticed, SUMO1 is commonly conjugated to substrates under natural cell conditions, while all other SUMO paralogs are preferentially conjugated in response to stress (Liang *et al.*, 2016; Saitoh & Hinchey, 2000; Wei *et al.*, 2008). All the SUMO proteins are synthesized as precursors that need to be matured by specific SUMO proteases to expose the conserved C-terminal di-glycine motif (-Gly-Gly) prior to their use in SUMOylation (Li & Hochstrasser, 1999; Reverter & Lima, 2004).

The SUMO modification pathway consists of a three-steps enzymatic cascade dependent of ATP energy that activates SUMO and promotes the formation of the isopeptidic bond with lysine residues of specific substrates (Hershko & Ciechanover, 1998; Varejão *et al.*, 2020) (Figure I1. 1). The first step starts with the unique heterodimeric E1-activating enzyme (Sae1/Sae2 in humans), which activates C-terminal glycine of SUMO via ATP consumption and loads it into a conserved E1 cysteine by forming a high energy thioester bond (Lois & Lima, 2005; Schulman & Wade Harper, 2009). Then, SUMO is transferred to another sole E2-conjugating enzyme (Ubc9 in all species) through another thioester bond with the E2 active site cysteine (Cys93) (Johnson & Blobel, 1997; Liu, Lois, & Reverter, 2019; Olsen & Lima, 2013). Finally, the charged-E2 (E2~SUMO thioester) can either transfer directly SUMO to one or more lysines in the target substrate by mono-, multi- and poly-SUMOylation (Yunus & Lima, 2006), or it can be enzymatically stimulated by an

E3-ligase enzyme, which enhances the transfer to the substrate by several fold (Pichler *et al*., 2017; Streich & Lima, 2014).

Interestingly, SUMO conjugation is a reversible process performed by the same SUMO-specific proteases used in the initial maturation process (Hickey, Wilson, & Hochstrasser, 2012; Yeh, 2009) that can cleave off the isopeptidic bond between the substrate and SUMO, allowing SUMO to be reused in another conjugation cycle. Thus, SUMO conjugation is a highly dynamic process in which the presence of SUMO is tightly regulated in the cell by a balance between conjugation and deconjugation.
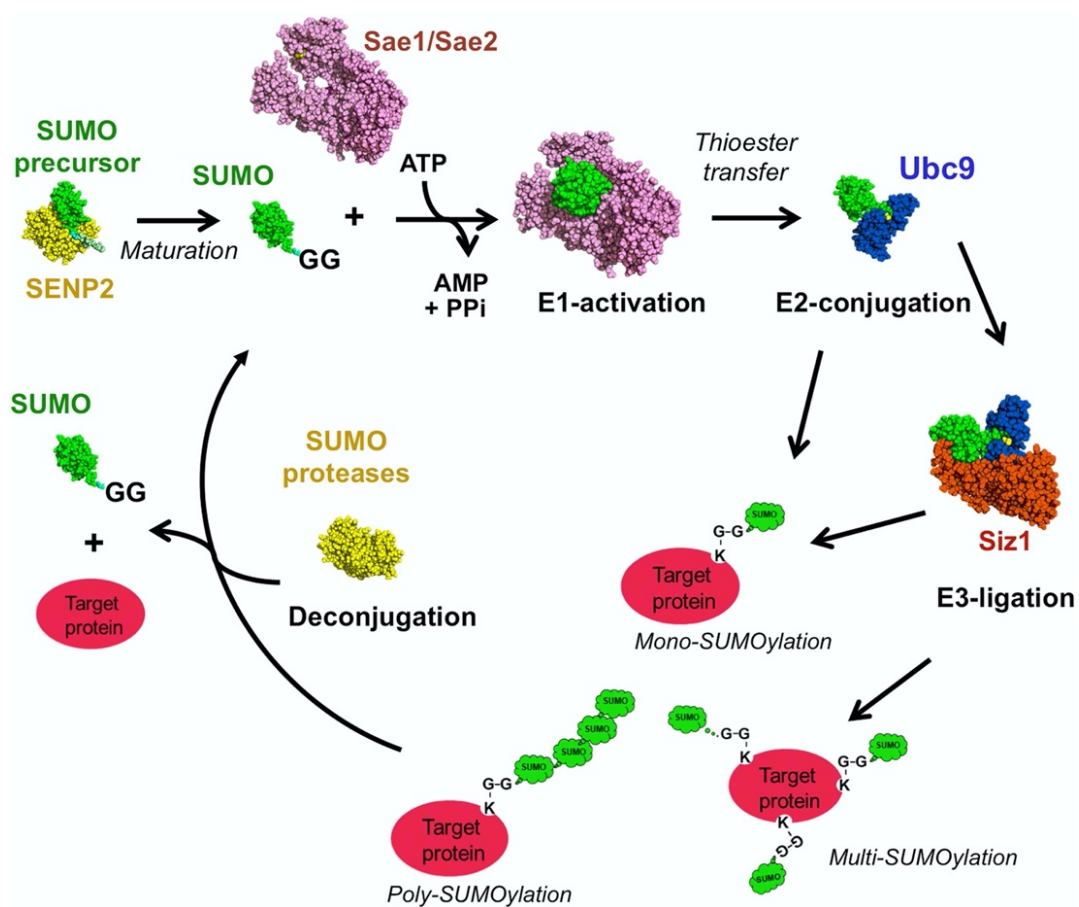
Figure I1. 1 SUMO conjugation pathway (Varejão et al., 2020)

Scheme depicting structures of the dedicated enzymes of the catalytic cascade that lead to the formation of SUMO conjugates. The ATP-dependent E1-activating enzyme activates the SUMO precursor (previously proteolytically processed leaving a Gly-Gly motif at the C-terminus) by the formation of a high energy thioester-bond between the SUMO C-terminus and an internal Cys (Sae1–Sae2, PDB: 1Y8R, 3KYC). Then SUMO-E1-thioester can be iso-energetically transferred to a Cys residue from the E2 conjugating enzyme (Ubc9∼SUMO, PDB: 5JNE). The E2-SUMO-thioester can discharge SUMO on one or several lysine residues from target substrates forming covalent isopeptidic bonds. E2-SUMO discharge can be stimulated by the action of a SUMO E3 ligase enzyme (Siz1-SUMO-Ubc9 structure, PDB 5JNE). Poly-SUMO chains can also be formed on target substrates. Finally, SUMO conjugation can be reversed by the action of a particular SUMO protease family (SENP2-SUMO, PDB: 2IO0), which can either cleave off SUMO precursors and SUMO conjugated substrates.

Conjugation mechanism

The correct geometry of the E2 active site is essential for its catalytic activity by fixing the E2~SUMO thioester in a right orientation. The ε-amino group of the lysine substrate attacks the E2-SUMO thioester bond in the catalytic process, creating an isopeptidic bond between the lysine ε-amino and the C-terminus of SUMO. The conserved Ubc9 active site is formed by the residues Tyr87, Cys93, Asn85, and Asp127 (Reverter & Lima, 2005; Yunus & Lima, 2006).

In addition to the catalytic cysteine (that stablishes the thioester bond), Asp127 assists the reaction by reducing the pKa of the ε-amino group facilitating the SUMO discharge (Figure I1. 2) (Yunus & Lima, 2006). Moreover, Asn85 helps to keep the correct geometry of the active site to promote the catalytic reaction (Berndsen *et al.*, 2013).

In the absence of an E3 enzyme, it has been proposed that the E2~SUMO thioester is highly mobile, displaying multiple conformations that hinders the SUMO discharge on the substrate lysine (Page *et al.*, 2012; Pruneda *et al.*2011). Thus, the ability of E3 ligases to fix and orient the E2~UbL thioester in a productive conformation to promote discharge on the substrate lysine is a major and common mechanism in all ubiquitin and SUMO E3 ligases.
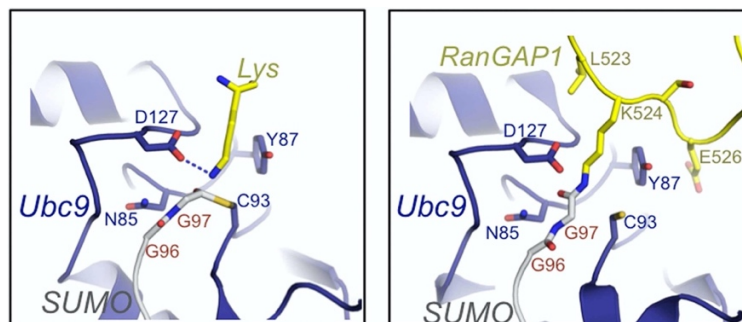
Figure I1. 2. Molecular model for SUMO conjugation (Varejão et al., 2020).

Left, structural model displaying the thioester bond between the active site Cys93 and the C-terminal Gly97 of SUMO1. The catalytic reaction of SUMO conjugation implies the discharge of E2~SUMO thioester on the attacking substrate lysine (yellow stick model). Important residues in the Ubc9 active site are depicted in stick configuration. The model is based on the PDB 1Z5S. Right, structure of the isopeptidic bond between SUMO C-terminal Gly97 and the lysine from RanGAP1, based on the complex between RanGAP-SUMO1-Ubc9-IR1-M (PDB: 1Z5S). Residues in the Ubc9 active site are shown in blue stick configuration. Residues of the SCM in RanGAP1 are shown in yellow stick configuration.

Substrate specificity and SUMO-consensus motifs (SCM)

As previously indicated, SUMO can be also attached to target lysines without the use of an E3 ligase, relying only the action of E2. Ubc9 can directly transfer SUMO to substrate lysines by direct interaction with a SUMO consensus motif (SCM), formed by ΨKxE (Ψ being hydrophobic with a preference for Ile or Val and x is any amino acid residue) (Bernier-Villamor *et al.*, 2002; Sampson *et al.*, 2001), although some variations of this motif have been also reported (Matic *et al.*, 2010). The role of unspecific SUMO conjugation (i.e. in exposed lysines that are not embedded in SCMs) under stress conditions remains obscure, but it could contribute to compensate protein instability under those circumstances (Psakhye & Jentsch, 2012; Ranjha *et al.*, 2019).

Moreover, additional PTMs such as phosphorylation may regulate SUMO conjugation to SCM in some cases, which is called "phosphorylation-dependent SUMO motif" (PDSM) (Hietakangas *et al.,* 2006; Mohideen *et al.*, 2009). Interestingly, proteomics analyses have recently revealed that the cross-talk between SUMO and phosphorylation plays an important role in the regulation of numerous target proteins (Hendriks *et al.*, 2017; Hendriks & Vertegaal, 2016). Thus, whether E3 ligases are present or absent, the conjugation reaction is influenced by the peculiarities of the SCM target, which can be regulated by other PMTs (phosphorylation), altering the interaction of the E2 enzyme.

The SUMO-interacting motif (SIM)

Once conjugated to proteins, SUMO often regulates their functions by recruiting other cellular proteins. Recruitment is achieved by non-covalent interactions between SUMO and motifs known as SUMO Interaction Motifs (SIMs). The presence of SIMs in a protein group can promote a velcro or glue effect, holding together large molecular assemblies (Lascorz *et al.*, 2021).

A SUMO-Interacting Motif is a short sequence of residues that directly interact with the SUMO surface in an extended conformation (Song *et al.*, 2004), and only few types have been reported so far (Hecker *et al.*, 2006; Minty *et al.*, 2000; Song *et al.*, 2004; Song *et al.*, 2005). (Figure I1. 3A). SIMs are normally located in loops between secondary

structure elements and adopt the characteristic extended β-like conformation upon binding to SUMO (Reverter & Lima, 2005; Song *et al.*, 2004, Song *et al.*, 2005). SIMs can interact with free SUMO or SUMOylated proteins.

Figure I1. 3. The SUMO-Interacting Motif (SIM) (Lascorz et al., 2021).

A) Cartoon representation of the secondary structure elements of a SIM motif (blue) in contact with the SUMO surface (red). Negative and positive charges indicate the SIM acidic region and SUMO surface patch, respectively. Stick representation of the basic amino acid of the SUMO surface patch.
B) Sequence alignment of SIMs from some proteins described in the text. Dotted line indicates the hydrophobic core (blue), adjacent to acidic residues (red) and potential phospho-serine residues (orange).

The main core of the canonical SIM is composed of 3 to 4 consecutive hydrophobic amino acids with the following sequence combinations: ΨΨΨΨ, ΨxΨΨ or ΨΨxΨ (where Ψ corresponds to Val, Ile or Leu; and x to Asp, Glu, Ser or Thr) (Figure I1. 3B). It forms an extended β-strand backbone interaction with the central SUMO β-sheet and wedges its hydrophobic side-chains in a pocket formed between the α-helix and the β-sheet on the SUMO structure (Reverter & Lima, 2005; Song *et al.*, 2004). This hydrophobic core of SIMs is usually surrounded by acidic residues, such Asp or Glu, which interacts with a positive patch area on the SUMO surface, increasing the affinity for SUMO (Figure I1. 3B).

Prediction of SIM motifs is not an easy task since the presence of the hydrophobic residues is not always required (Figure I1. 3B and Figure I1. 4). Thus, despite differences in the 'canonical' SIM motif composition, the extended β-strand is always present in all cases when these sequences interact with SUMO. It is important to mention here that depending on the location of the negative charged residues of SUMO, the formed β-sheet with SIM can be either parallel or antiparallel (Figure I1. 4).

The E2 conjugation

The catalytic activity of the E2-conjugating enzyme comprises both the SUMO thioester transfer from the E1-enzyme and the formation of an isopeptidic bond on the substrate. The presence of E3 ligases improves SUMO conjugation by stabilizing the E2~SUMO thioester in a productive conformation for discharge on the incoming substrate lysine (Zheng & Shabek, 2017). As a result, Ubc9 (E2) interacts with a variety of protein surfaces, including one in the E1-activating enzyme, several SUMO E3 ligases, SUMO and other surfaces in specific substrates, providing substrate-dependent specificity (Stewart *et al.*, 2016).

Direct binding of Ubc9 to other areas on the substrate is another manner to fix a productive conformation of the E2~SUMO thioester and provide substrate specificity. RanGAP1, the first SUMO substrate discovered, has a high-affinity region outside of the SCM that stabilizes the association with Ubc9 and improves SUMO conjugation activity (Bernier-Villamor *et al.*, 2002; Sampson *et al.*, 2001; S. Zhu *et al.*, 2009). Another example of a direct substrate contact with Ubc9 is proliferating cell nuclear antigen (PCNA), where direct substrate binding favors specific conjugation at Lys127 on PCNA in the absence of an E3 enzyme (Streich & Lima, 2016).

Also, the presence of SIM motifs in the substrate, which can bind the E2~SUMO thioester, provides an indirect way to offer specificity and regulate the interaction between E2 and the substrate. The PML protein, Daxx (death domain associated protein), USP25 and USP28 (ubiquitin specific proteases), and BLM (Bloom's syndrome helicase) are all examples of this process (Lin *et al.*, 2006; Meulmeester *et al.*, 2008; Zhen *et al.*, 2014; J. Zhu *et al.*, 2008).

Finally, PTMs as SUMOylation, phosphorylation, and acetylation can also affect the binding to Ubc9, changing the affinity of the substrate with the E2~SUMO thioester (Hsieh *et al.*, 2013; Knipscheer *et al.*, 2008).

SUMO E3 ligases mechanism

The SUMO substrate specificity is a critical issue in the field, since there are less than ten genes identified that encode SUMO E3 ligases, in contrast to ubiquitin, with 600 putative E3 ligases encodes in the human genome. These SUMO E3 ligases enzymes act mainly as catalysts by enhancing the discharge of E2~SUMO thioester in the substrate lysines (Berndsen & Wolberger, 2014; Pichler *et al*., 2017). Only a few cases of specific interactions between SUMO E3 ligases and substrates have been described (Pichler *et al*., 2017). As previously indicated, the interaction between the E2~SUMO thioester and the substrate lysine in the context of a SCM motif is the basis of SUMO specificity. Thus, in the absence of a clear SCM, SUMO conjugation is probably dependent on the occurrence of a substrate lysine close to the SUMO conjugation machinery. This could explain the large amount of conjugated SUMO substrates under stress conditions (Hendriks *et al*., 2017). The "SUMO spray" theory is based on the idea that locally concentrated SUMO ligases promiscuously modify a group of proteins requiring a large degree of flexibility in the SUMOylation machinery that gives the ability of SUMO enzymes to target simultaneously spatially related groups of substrates (Psakhye & Jentsch, 2012).

In human, SUMO has only nine *bona fide* E3 ligases, including five SP-RING, three ZNF451 and RanBP2, which should provide specificity to more than 6000 substrates (Hendriks *et al*., 2017). Figure I1. 4 describe different types and forms of interaction between the E2, SUMO and the SIM of the E3. The crystal structure of the RanBP2-Ubc9-RanGAP1-SUMO complex shown on Figure I1. 4A, revealed how the E3 IR1-M optimally positions the E2~SUMO thioester for the nucleophilic attack by the substrate lysine (Reverter & Lima, 2005). For the first time, that structure showed the interaction of the E3 ligase with the SUMO moiety of the E2~SUMO thioester, forming a non-covalent SIM–SUMO interface that fixes the SUMO-thioester linkage in an ideal orientation for the formation of isopeptidic bonds, reducing the number of conformations of the E2~SUMO.

In addition to the donor SUMO-SIM association, a second SUMO-SIM interaction has been observed in SUMO E3s. This was first reported for the SUMO E3 ligase ZNF451 (Figure I1. 4B), which is characterized by the presence of a tandem of two SIMs separated by a PLPR motif in the N-terminal region of the protein (Cappadocia, Pichler, & Lima,

2015; Eisenhardt *et al.*, 2015). In a similar way as the RanBP2, the SIM1 binds the donor SUMO, meanwhile the SIM2 binds a second SUMO located at the backside of the E2 enzyme. Both SIMs are essential for the E3 ligase activity, highlighting the role for the backside SUMO, probably aiding to fix the E2~SUMO thioester in a productive conformation.
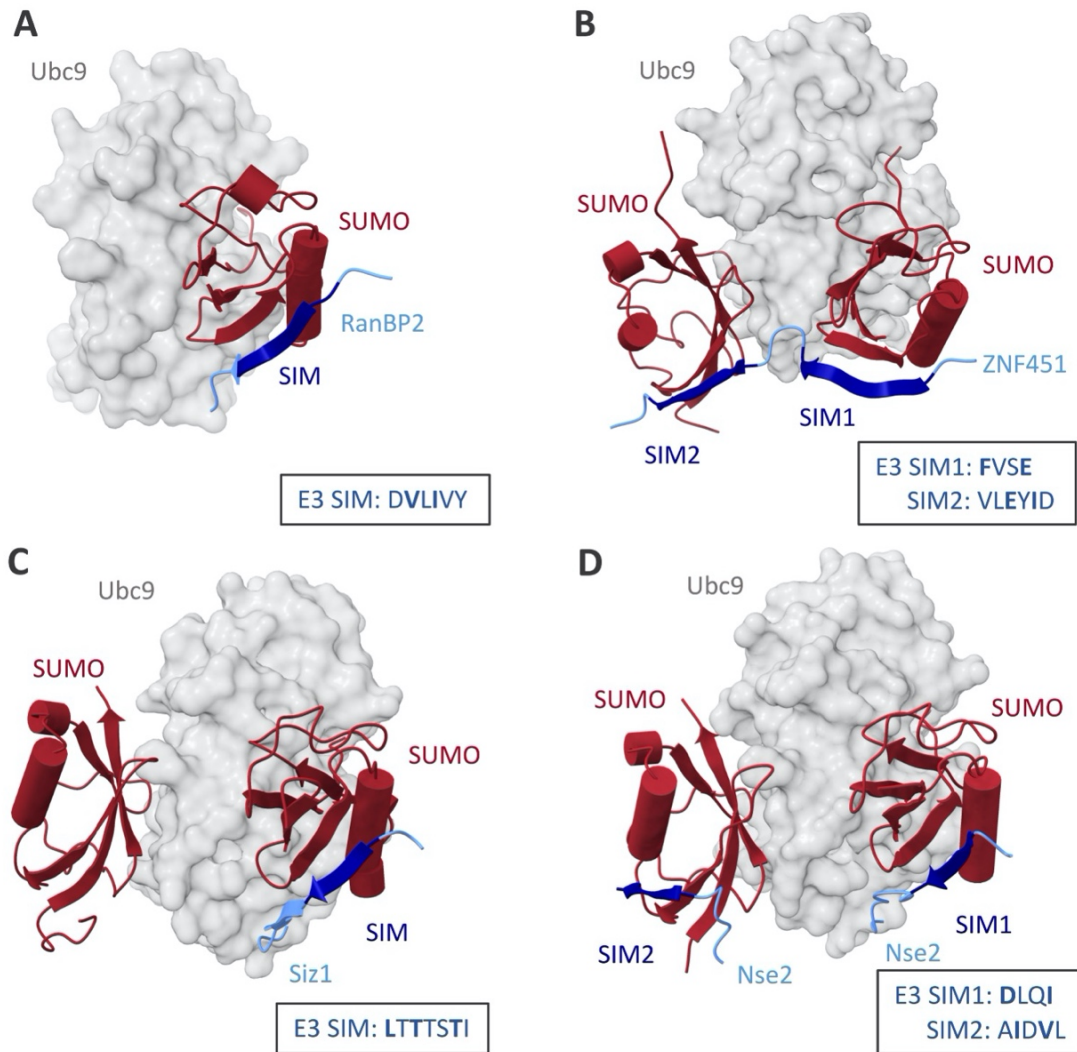
Figure I1. 4. Structural comparison of E2-SUMO thioester complexes with SIMs in SUMO E3 ligases (Lascorz et al., 2021).

A) Structure of the product complex between Ubc9/RanGAP1-SUMO/RanBP2 (PDB: 1Z5S). Ubc9 is shown as a gray surface. Donor SUMO and SIM of RanBP2 are shown in a cartoon representation (red and blue, respectively).
B) Structure of the product complex between ZNF451/Ubc9-SUMO/SUMO-backside (PDB: 5D2M). Ubc9 is shown as a gray surface. Donor SUMO, backside SUMO and double SIM of ZNF451 are shown in a cartoon representation (red and blue).
C) Structure of the product complex between Ubc9/PCNA-SUMO/Siz1 (PDB: 5JNE). Ubc9 is shown as a gray surface. Donor SUMO, backside SUMO and SIM of Siz1 are shown in a cartoon representation (red and blue).
D) Structure of the Nse2/Ubc9-SUMO/SUMO-backside complex (PDB code 7P47). Ubc9 is shown as a gray surface. Donor SUMO, backside SUMO, SIM1 and SIM2 of Nse2 are shown in a cartoon representation (red and blue). Sequences of all SUMO E3 ligases SIMs are indicated (in dark blue side chains binding the SUMO hydrophobic groove).

Finally, the SP-RING family of SUMO E3 ligases contains a conserved RING domain similar to the most abundant family of ubiquitin E3 ligases. The yeast founding members Siz1 and Siz2 (Johnson & Gupta, 2001), the mammalian PIAS1 to PIAS4 (Kahyo *et al.*, 2001; Kotaja *et al.*, 2002; Sachdev *et al.*, 2001; Sapetschnig *et al.*, 2002; Schmidt & Müller, 2002), and a component of the SMC5/6 complex conserved from yeast to humans named Nse2 or Mms21 (Andrews *et al.*, 2005; Potts & Yu, 2005; Zhao & Blobel, 2005), are all members of this family. The SP-RING domain is similar to the ubiquitin RING domain, however it only coordinates one Zn^{2+} ion rather than two (Duan *et al.*, 2009; Yunus & Lima, 2009).

Inside this family, two examples confirm the role of a second SUMO bound to the E2 backside. The first example is observed in the structure of the Siz1 ligase in complex with a SUMO-linked E2 and its substrate PCNA (Figure I1. 4C). This crystal structure revealed the interaction of the E2~SUMO thioester with a non-canonical SIM in Siz1, which positions the donor SUMO in an optimal catalytic conformation, similar to RanBP2 and ZNF451 (Streich & Lima, 2016). Interestingly, a second SUMO was also observed at the E2 backside, resembling the interaction observed in ZNF451 E3 ligase (Figure I1. 4C). Moreover, Siz1 also contains a second SIM located C-terminally to the SP-RING domain (not observed in the crystal structure), which probably interacts with the backside SUMO contributing to the stabilization of the E2~SUMO thioester in a productive conformation.

The second example is observed in the Nse2/Mms21 SUMO E3 ligase from the Smc5/6 complex, where the yeast ortholog also contains two SIMs playing a relevant role in conjugation (Bermúdez-López *et al.*, 2015). The crystal structure of the complex formed by Nse2-Smc5-E2~SUMO thioester will be presented and further discussed on Chapter III (Varejão*, Lascorz*, *et al.*, 2021). In few words, two SIM-SUMO interactions are observed: a "non-canonical" SIM binds the E2-attached donor SUMO; and a C-terminal "canonical" SIM binds the E2-backside SUMO (Figure I1. 4D).

I2. SMC complexes

General introduction

Structural Maintenance of Chromosomes (SMC) complexes are multimeric protein complexes involved in many aspects of chromosome dynamics and structural organization. The SMC complexes are formed by dimeric SMC proteins present in all prokaryotic and eukaryotic organisms. Each dimer of SMC proteins is associated with other accessory proteins that add important structural and functional properties to the complexes.

SMC complexes are recognized as fundamental proteins that regulates the structural and functional organization of chromosomes, from simple organisms, like bacteria, to complex organisms like animals or plants. Their protein sequence and function have been highly conserved in evolution (Losada & Hirano, 2005; Nasmyth & Haering, 2005).

In contrast to prokaryotes, where SMC proteins are homodimers, in eukaryotes we can find six different SMC proteins that form three different SMC complexes, consisting on heterodimers of two SMC proteins: SMC1/3 known as cohesin, SMC2/4 known as condensin, and the SMC5/6 complex, which has no nickname (Figure I2. 1) (Hirano, 2006; Jeppsson *et al.*, 2014; Nasmyth & Haering, 2005).
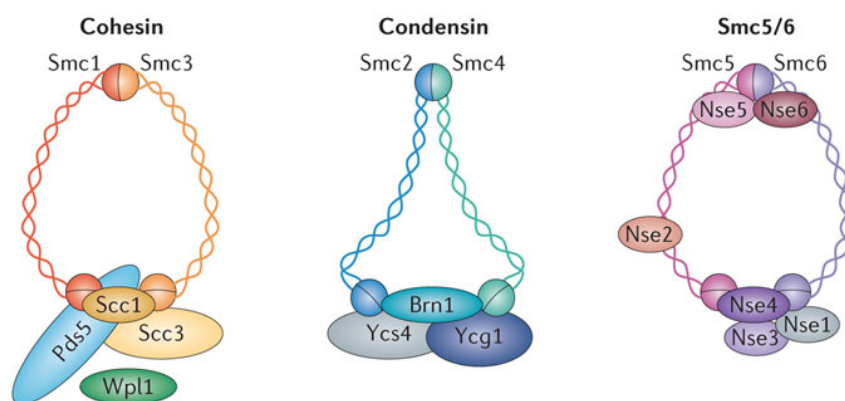
Figure I2. 1. Model of the three different SMC complexes (Jeppsson et al., 2014).

The three different SMC complexes: Smc 1/3 or cohesin, Smc 2/4 or condensin and Smc5/6.

All SMC proteins have a common structural scaffold formed by globular domains in the N- and C-terminal creating an ATPase domain (named as _heads_), connected by a long coiled coil region (named as _arm_ domain), bended by another globular domain (named as _hinge_), located at the middle of the protein (Figure I2. 2). The dimer formation, either in homodimers prokaryotes or heterodimers eukaryotes, is made by a strong association between two _hinge_ domains, while the _heads_ domains are associated through other proteins (named as non-SMC-elements or Nse), creating a large quaternary structure with ATPase activity.
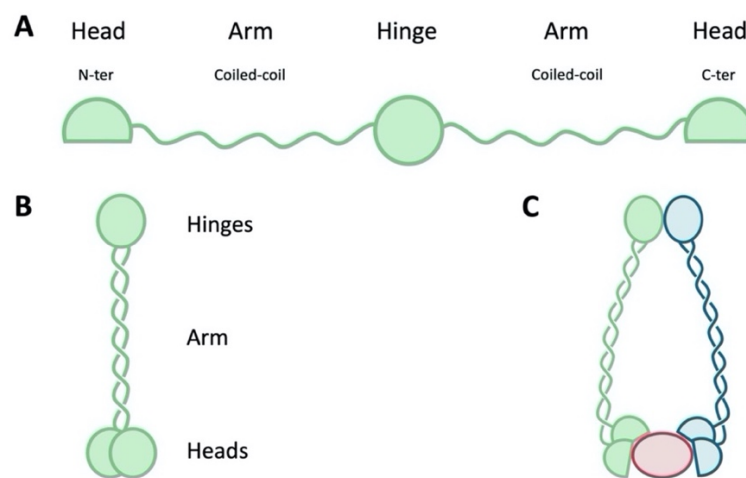
**Figure I2. 2. Schematic model of the structural organization of the SMC proteins.**

A) Representation of the different parts of the full-length SMC, from the N-terminal to the C-terminal.
B) Model of the folded SMC protein.
C) Representation of the two SMC proteins forming the SMC complex.

In addition to the SMC dimer, some satellite proteins in each complex, interact with the _heads_ domain, as shown in Figure I2. 1:

-The cohesin complex is formed by four subunits: Smc1, Smc3 and the two non-SMC proteins Scc1, an α-kleisin subunit, and Scc3.

- The condensin complex is constituted by five subunits, being Smc2, Smc4 and three non-SMC proteins: Brn1, Ycs4 and Ycg1.

- The SMC5/6 complex is constituted by eight subunits: Smc5, Smc6 and at least four non-SMC elements (Nse): Nse1, Nse3, Nse4, Nse2 and occasionally Nse5 and Nse6.

The SMC complexes are essential in many cell functions, including chromosome segregation, transcription, or replication (Nasmyth & Haering, 2005). These functions are normally carried out by ATP-hydrolysis, that enable the DNA interaction with the complex (Kanno *et al.*, 2015). The absence of any of these complexes in cells, will lead to an abnormal segregation of chromosomes, as shown in Figure I2. 3.

The main role of cohesin is to maintain the union between sister chromatid in the metaphase, by holding together the DNA of the two chromatids (Michaelis, Ciosk, & Nasmyth, 1997). Moreover, cohesin is involved in other functions like homologous recombination or transcription regulation (Jeppsson *et al.*, 2014). On the other hand, the main role of condensin is to maintain bounded the different regions of the chromatid to assure the chromosome's compaction (Hirano, 2006) and to organize the mitotic chromosomes avoiding tangle up structures during segregation (Hirano & Mitchison, 1994). The role of Smc5/6 complex will be described in the next section.
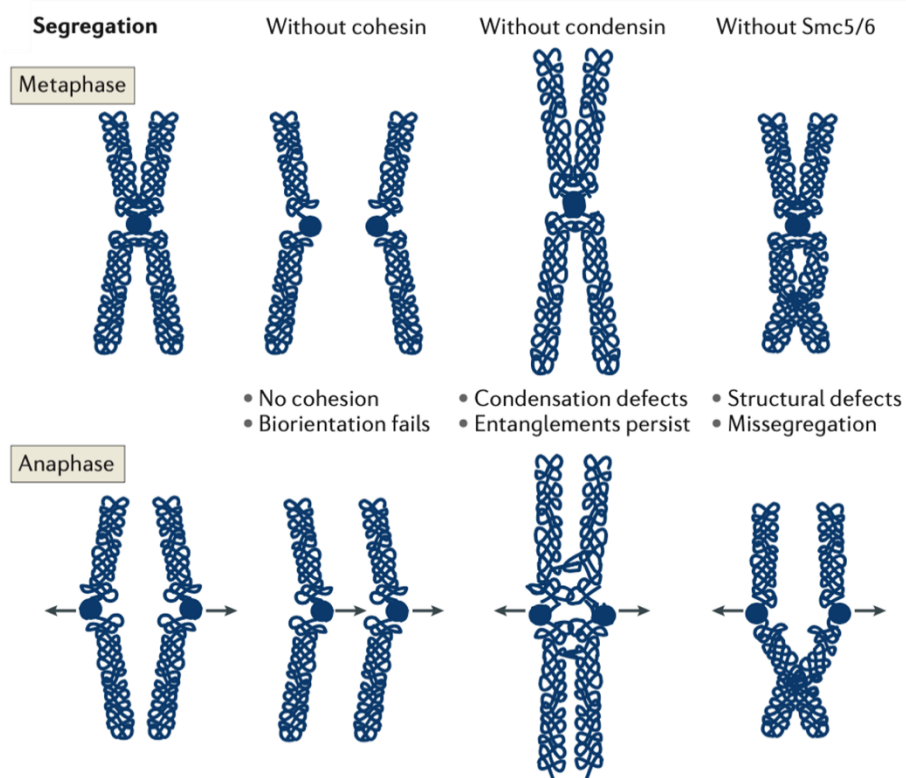
Figure I2. 3. Scheme of the different roles of the three SMC complex, from Jeppsson et al. 2014.

The cohesin (SMC1/3) holds the two sister chromatids allowing the correct alignment and segregation of the chromosomes, the condensin (SMC2/4) facilitates the separation of the sister chromatids at anaphase by assisting the compactation of them, and, although the function of SMC5/6 complex in chromosome stability remains to be understood, there is further evidence that the lack of this complex leads to structural defects of the chromosomes.

The SMC5/6 complex

The SMC5/6 complex is constituted by eight subunits: the two main SMC proteins, Smc5 and Smc6; and at least four non-SMC proteins, Nse1, Nse3, Nse4, Nse2 and occasionally Nse5 and Nse6.

This complex was first identified in *Schizosaccharomyces pombe* (Lehmann *et al.*, 1995). Human orthologs were subsequently identified and were shown to be particularly abundant during meiosis (Fousteri & Lehmann, 2000). Subsequently, its architecture and its important role in DNA repair were defined (Sergeant *et al.*, 2005; Zhao & Blobel, 2005).

Likely cohesin and condensin, the Smc5/6 complex is conserved and essential for cell survival. Important roles include the DNA reparation by homologous recombination (Murray & Carr, 2008), the DNA ribosomal replication (Torres-Rosell *et al.*, 2005), genome stability, and more recently, DNA compaction (Gutierrez-Escribano *et al.*, 2020; Serrano et al., 2020).

Structural organization of the Smc5/6 complex

Although the Smc5/6 complex is conserved in all the eukaryotes, their quaternary organization between organisms show some differences. In all, the Smc5 and Smc6 act as the main long protein scaffold of the complex with the non-Smc-elements (Nse) around them. The difference between organisms is the organization of the Nse proteins. For example, initially, in *S. cerevisiae* as in *S. pombe*, the location of Nse5 and Nse6 was controversial: whilst in *S. pombe* they are located close to the ATPase *heads* domains, in *S. cerevisiae* there was a discrepancy that located the Nse5 and Nse6 proteins close to the *hinges* of Smc5/6 (Duan *et al.*, 2009), whereas others located them close to the *heads*, similar to *S. pombe*. However, recent CryoEM and crosslinking studies (Hallett *et al.*, 2021; Taschner *et al.*, 2021; Yu *et al.*, 2021) provide strong structural evidence supporting their location next to the *heads* domains, so it seems that this position would be more plausible.
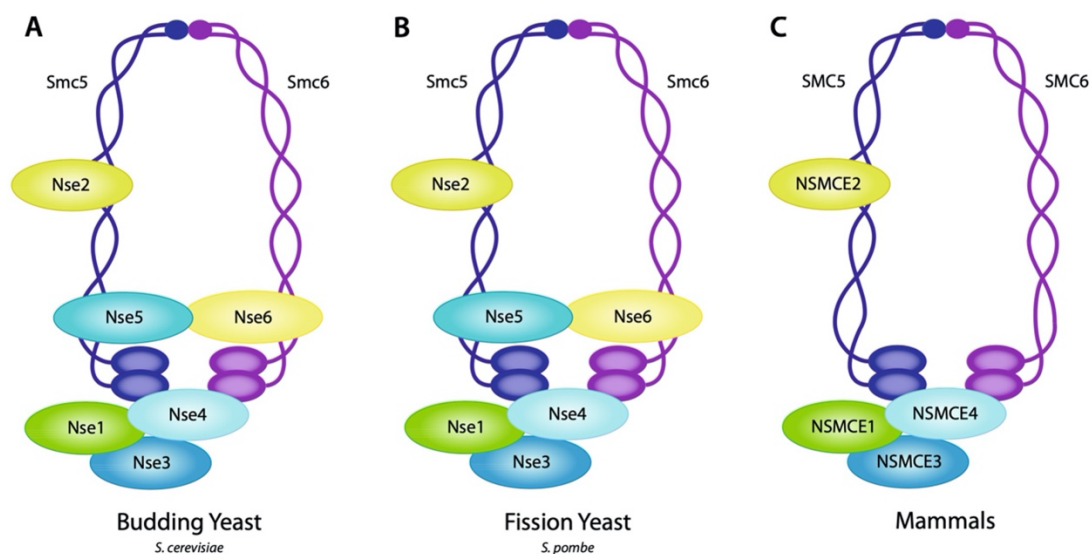
Figure I2. 4. Schematic figure of the structure and composition of the Smc5/6 complexes from S. cerevisiae, S. pombe and mammals, adapted from Verver et al., 2016.

The Smc5/6 complex is conserved from yeast to humans, the two main proteins fold and interact at their central *hinge* domains. The N- and C-terminal create a domain, forming a ring-like structure which is closed by several non-SMC elements: Nse1, Nse3, and Nse4. The SUMO ligase Nse2 is bound to the coiled coil region of Smc5. Recent studies have located the Nse5 and Nse6 at the ATPase domain in budding yeast (**A**), as well as in fission yeast (**B**), but homologs have not been identified in mammals (**C**).

All the complexes from different organisms shown in Figure I2. 4 have a similar structural organization. The Nse4 protein, a kleisin subunit that bridges Smc5/6 *heads* domains (Palecek *et al*., 2006), is found in all of them. Nse4 also binds Nse1 and Nse3 (J. J. Palecek & Gruber, 2015), forming a subcomplex that interacts with the *heads* domain.

The Nse2 or Mms21 protein is another key subunit with non-globular structure that is essential for the complex stabilization and SUMO E3 ligase activity. Interestingly, Nse2 is the only protein that does not interact with a globular *head* domain of Smc5 or Smc6, but instead interacts with the *arm* region of Smc5, binding to the middle of the coiled coil region (Duan, Sarangi, *et al*., 2009).

Despite being a complex known for a long time and considering all the advances that have been made in technologies to study the protein structure, the detailed atomic tridimensional structure of the complex components remains unknown. Only a few subcomplexes from different organisms have been solved at the molecular level by X-ray crystallography, as shown in Figure I2. 5 and described in the following paragraph.

From *Saccharomyces cerevisiae*, two structures have been solved:

- The Smc5 *arm* domain bound to Nse2 (PDB: 3HTK), which was the first structure solved of the complex by Duan *et al.*, 2009.

- The Nse5-Nse6 crystal structure (PDB: 7OGG), revealed by Taschner *et al.*, 2021, coinciding at the same time with the CryoEM structure (PDB: 7LTO) solved by Yu *et al.*, 2021. These two structures have been essential in localizing the Nse5-Nse6 heterodimer in the Smc5/Smc6 complex.

From *Schizosaccharomyces pombe*, one structure is known:

- The Smc5-Smc6 *hinges* domain (PDB: 5MG8), which gives information related to the interaction between Smc5 and Smc6, discovered by Alt *et al.*, 2017.

From *Homo sapiens*, one structure has been solved:

- The heterodimer with Nse3/Nse1, also known as MAGE-G1, (PDB: 5WY5) which has been solved by Doyle *et al.*, 2010 and revealed the Ubiquitin E3 ligase activity. Moreover, the structure with of Nse1/Nse3 together with Nse4 has also been solved recently (Jo *et al.*, 2021).
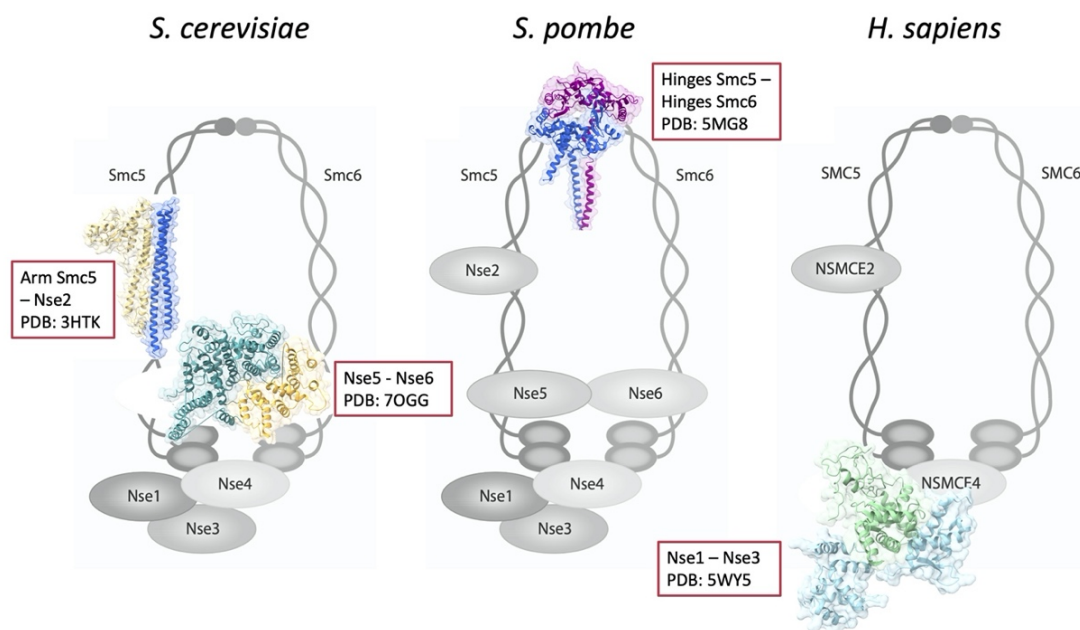
Figure I2. 5. Scheme adapted from Verver et al., 2016, showing the known tridimensional structures.

Scheme of the Smc5/6 complexes in *S. cerevisiae*, *S. pombe* and *H. sapiens* with the different structures already known. In *S. cerevisiae,* the structure of the Arm/Smc5 with Nse2 (PDB: 3HTK) has been revealed by Duan *et al.* in 2009, and the Nse5-Nse6 crystallographic structure (PDB: 7OGG) has been discovered by Taschner *et al.* in 2021, parallel to the CryoEM structure (PDB: 7LTO) solved by Yu *et al.* in 2021. The only known structure of the *hinges* was solved in *S. pombe* by Alt *et al.* in 2017, showing the interaction between the *hinges* of Smc5 and Smc6 (PDB: 5MG8). In *H. sapiens*, only the structure of the Nse1 and Nse3 proteins is solved (PDB: 5WY5), by Doyle *et al.* in 2010.

Properties and functions of Smc5/Smc6 complex

The enzymatic activity of the Smc5/6 complex constitute an important difference compared to the other two complexes, cohesin and condensin, where the ATPase activity of the *heads* is the only enzymatic activity. The Smc5/6 complex has two enzymatic activities: ubiquitin and SUMO E3 ligase, provided by two subcomplexes formed by Nse subunits: Nse1-Nse3-Nse4 and Nse2 bound to Smc5 *arm*. These enzymatic activities are essential for Smc5/6 function but are absent in cohesin and condensin.

Nse1 contains a RING (Really Interesting New Gene)-like domain characteristic of ubiquitin E3 ligases (Doyle *et al.*, 2010), and confers ubiquitin ligase activity (Palecek & Gruber, 2015; Pebernard *et al.*, 2008) but only in complex with Nse3. Nse3 is the member of the melanoma associated antigen (MAGE) protein family (Barker & Salehi, 2002). Nse1 and Nse3 both have a pair of winged-helix domains that allows their heterodimerization (Doyle *et al.*, 2010). The subcomplex is also composed with the Nse4 kleisin protein, which binds the *heads* of the Smc5 and Smc6 proteins (Palecek *et al.*, 2006). Moreover, the function of the subcomplex formed by Nse1, Nse3 and Nse4 is involved in the DNA binding activity of the complex (Zabrady *et al.*, 2016).

The Nse2 subunit attached to the *arm* region of Smc5 provides SUMO E3 ligase activity by the presence of its RING-like domain (Doyle *et al.*, 2010; Duan, Sarangi, *et al.*, 2009; Potts & Yu, 2005). In addition to this enzymatic activity, Nse2 plays an essential stabilization role for the complex (Andrews *et al.*, 2005). The activation of the Nse2/Mms21 E3 ligase in yeast cells requires the binding of ATP to Smc5/6 at the *head* domain of the complex (Bermúdez-López *et al.*, 2015). This subcomplex provides to Smc5/6 the capacity to SUMOylate external substrates and also to auto-SUMOylate (Bermúdez-López *et al.*, 2016).

The Nse5-Nse6 subcomplex function is related to DNA repair (Pebernard *et al.*, 2006), but its specific role remains unclear. Recent studies indicate a role of this subcomplex in the ATPase activity of the Smc5/6 complex, as a negative regulator (Hallett *et al.*, 2021; Taschner *et al.*, 2021). They suggest that the inhibition of the ATP hydrolysis could modulate DNA substrate binding (Taschner *et al.*, 2021).

The Nse2 or Mms21 subunit: a SUMO E3 ligase

Nse2, also known as Mms21, was evidenced from a screen in *S. cerevisiae* for mutants sensitive to MMS (Prakash & Prakash, 1977)and was later shown to be one of the non-Smc-elements proteins of the Smc5/6 complex, docked into the coiled coil region of Smc5 (Zhao & Blobel, 2005). Nse2 is a member of Siz/PIAS (SP) family of E3 SUMO ligases, as it contains the characteristic catalytic SP-RING domain at its C-terminus (Andrews *et al.*, 2005; Potts & Yu, 2005; Zhao & Blobel, 2005). Its presence is essential for the structural stabilization of the complex and, by that, essential for cell viability (Duan, *et al.*, 2009). Besides, it has been demonstrated that its SUMO E3 ligase activity is required in the DNA repair processes.

It has been demonstrated that this subunit has important roles in the maintenance of chromosome integrity (Ampatzidou *et al.*, 2006; Behlke-Steinert *et al.*, 2009; Bermúdez-López *et al.*, 2015; Branzei *et al.*, 2006; Chavez *et al.*, 2010; Zhao & Blobel, 2005). Interestingly, the activation of the Nse2 SUMO ligase promotes the SUMOylation of different targets in the cohesin complex (Almedawar *et al.*, 2012; McAleenan *et al.*, 2012; Potts *et al.*, 2006), the Smc5/6 complex, including Nse2 itself (Bermúdez-López *et al.*, 2015), and in the STR complex (Sgs1–Top3–Rmi1) (Bermúdez-López *et al.*, 2016; Bonner *et al.*, 2016).

The structure of Nse2 from *S. cerevisiae* was solved by x-ray crystallography on 2009 (Duan, Sarangi, *et al.*, 2009), and it evidences the presence of two defined regions. As shown in Figure I2. 6, Nse2 interacts with the Smc5 *arm* coiled coil domain through two extended helixes at N-terminal region, whereas its C-terminal region contains the SP-RING domain. Moreover, the structure reveals three distinct parts at the C-terminal domain: an internal flexible Loop domain (T158-K179), the RING domain (T183-D238) and the C-terminal α-helix (P239-K258) (Figure I2. 6). It is important to mention that the last nine residues (R259-L267) cannot be observed in the structure since no defined electron density was present, indicating that the C-terminal tail of Nse2 is disordered due highly flexibility.

The interaction between Nse2 and Smc5 is essential for cell viability, as defects in cell growth have been observed when this interaction is not present (Bermúdez-López *et al*., 2015; Duan, Sarangi, *et al*., 2009). In contrast, even though the C-terminal domain is not essential for viability, it is essential for DNA damage repair (Bermúdez-López *et al*., 2015).
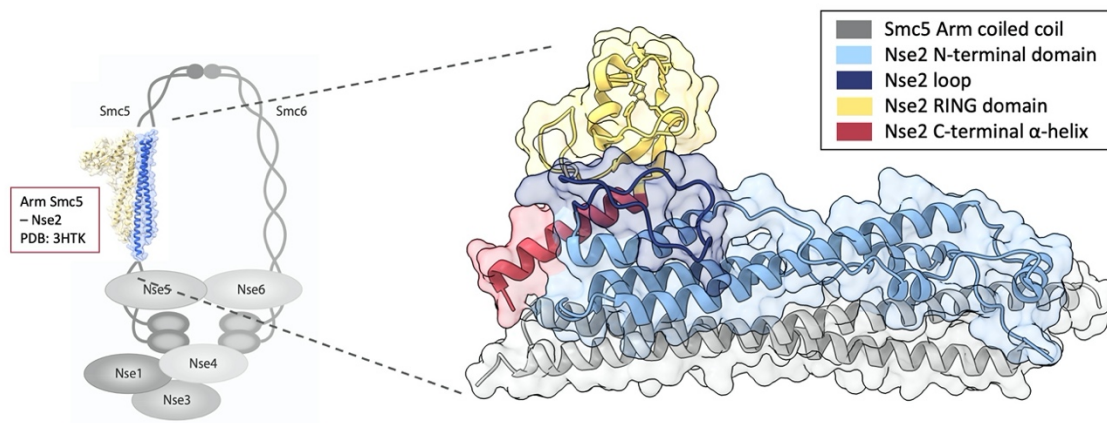
Figure I2. 6. Structure of the Nse2 protein in complex with the Smc5 coiled coil domain (PDB: 3HTK).

Schematic representation of the Arm/Smc5 coiled coil with Nse2 (PDB: 3HTK) structure, revealed by Duan *et al*., 2009. The Smc5 *arm* domain (gray) is interacting with Nse2 (light blue) by the coiled coil domain. The different domains of Nse2, loop (dark blue), RING (yellow) and the C-terminal α-helix (red) are indicated.

As previously indicated, the RING domain of Nse2 provides SUMO E3 ligase activity to the Smc5/6 complex. The restriction of this Nse2 SUMO E3 ligase activity could lead to the development of some human pathologies, such as primordial dwarfism, extreme insulin resistance, or gonadal failure (Payne *et al.*, 2014). This study corroborates the idea that losing the role of Nse2 in DNA damage repair causes dwarfism by reducing replicative stress tolerance (Payne *et al.*, 2014). However, the C-terminal truncations of Nse2 in patients indicate that it is the stabilization of the whole complex and not the E3 ligase activity responsible for the pathology (Jacome *et al.*, 2015). It is interesting to note that C-terminal helix of human protein is shorter than one exhibited by its yeast counterpart, showing also low sequence identity, more details will be further addressed on the next chapters

DNA binding in the Smc5/6 complex

Despite the different functions, all SMC complexes have a common property: they all organize chromosomes by topologically enveloping DNA within their ring-shaped structure. Certainly, some studies on the interaction of DNA with cohesin suggest that this complex may interact with one or more DNA molecules (Cuylen *et al.*, 2011; Haering *et al.*, 2008). DNA binding depends on the ATPase activity of the *heads* domains, which controls the conformation of DNA fibers inside the SMC ring. For example, it has been shown that the Smc5/6 complex of *S. cerevisiae*, in addition to being ATP-dependent, DNA binding is sensitive to differences in salt concentration, indicating that as in cohesin and condensin, the Smc5/6 complex is also capable to interact with DNA (Kanno *et al.*, 2015).

Smc5/6 participates in essential chromosome transactions during DNA replication and repair when loaded into chromatin. *In vitro*, the Smc5 and Smc6 subunits strongly bind DNA through several binding regions located in the *hinge*, the *head* and the *arm* regions (Alt *et al.*, 2017; Roy & D'Amours, 2011; Roy, Siddiqui, & D'Amours, 2011). It has been proposed that the complex has a high affinity for single-stranded DNA (Roy, Dhanaraman, & D'Amours, 2015). Nevertheless, *in vivo*, the remaining six non-SMC-elements (Nse proteins) subunits seems to modulate the binding of DNA to the Smc5/6 complex. The subcomplex formed by Nse4-Nse1 and Nse3 contains a positive patch region that might act as a DNA-binding surface and mediates Smc5/6 loading onto chromatin (Zabrady *et al.*, 2016). Moreover, it has been recently demonstrated that Nse5/6 modulates DNA binding by direction inhibition of Smc5/6 ATPase (Hallett *et al.*, 2021; Taschner *et al.*, 2021).

Chapter I: Structural approaches into the human Smc5/6 complex

- To design and produce different truncate constructions of the human Smc5/6 complex.

- To solve the three-dimensional structure of different domains of human Smc5/6 complex using protein crystallography.

- To study the role of the C-terminal region of the human Nse2 protein by *in vitro* SUMOylation assays.

Chapter II: DNA activates the Nse2/Mms21 SUMO E2 ligase in the Smc5/6 complex

- To characterize the role of DNA in the Nse2 SUMO E3 ligase activity.

- To identify the key residues in the interaction between DNA and Smc5/Nse2 by *in vitro* and *in vivo* SUMOylation assays.

- To analyze the influence of DNA binding in the structure of the Smc5/Nse2 complex.

Chapter III: Insights into the structure and mechanism of the Nse2 E3 SUMO ligase

- To purify and crystallize the complex between the Smc5-Nse2 and the E2-SUMO thioester mimetic.

- To solve the tridimensional structure of the Smc5-Nse2/E2-SUMO complex.

- To characterize the role of the SIMs domain of Nse2 and its relation with the SUMO E3 ligase activity by *in vitro* SUMOylation activities.

CHAPTER I:
STRUCTURAL STUDIES OF
THE HUMAN SMC5/6
COMPLEX
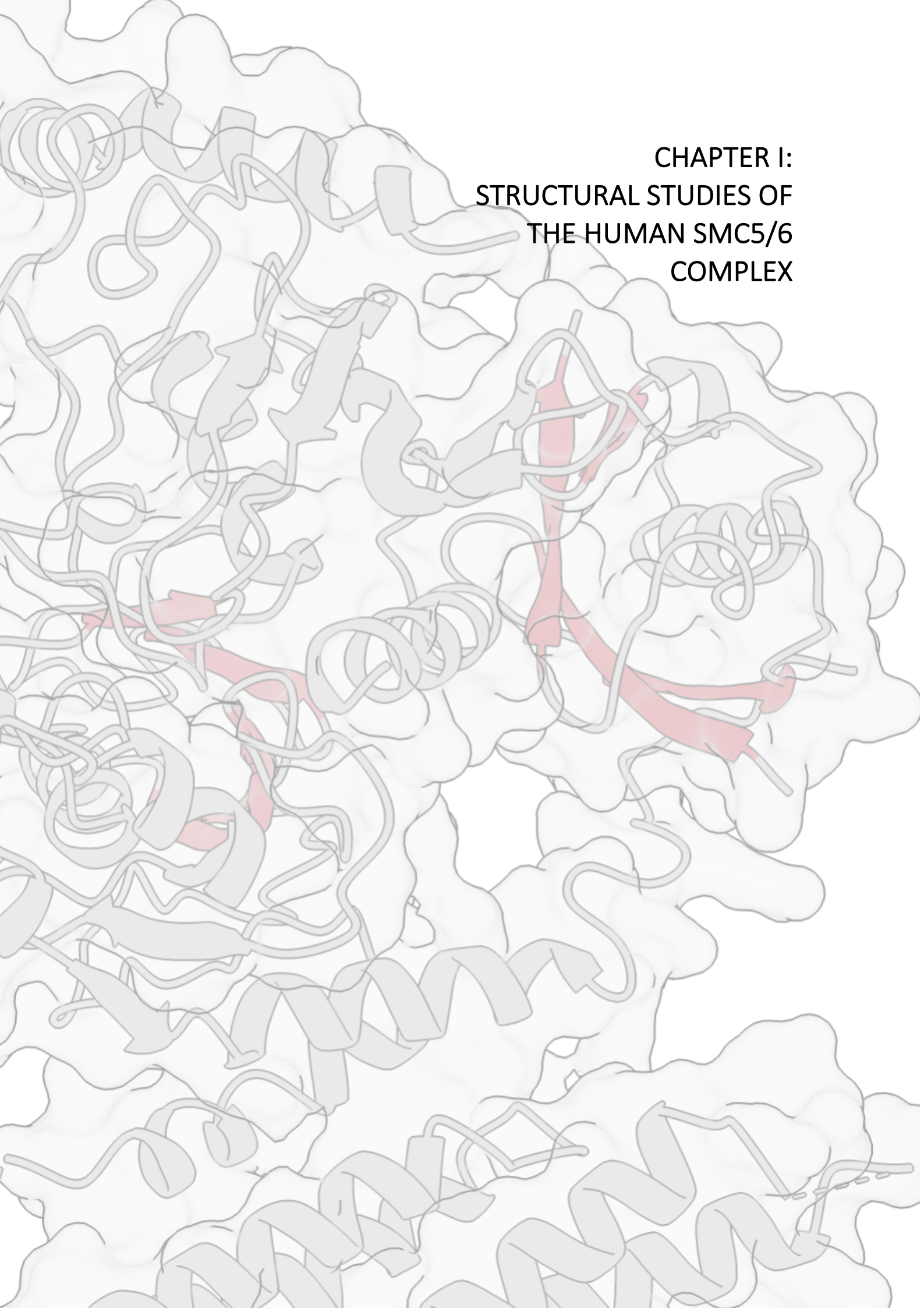
CI.1 Introduction

The determination of the tridimensional structure of the Smc5/6 complex might represent a breakthrough in order to gain insights on the molecular basis on how this complex executes its function. However, due to the large molecular weight and intrinsic flexibility of the Smc5/6 complex, the main approach used over the last years consisted to work with subcomplexes of the Smc5/6 complex. During the development of this thesis, four crystal structures of different organisms have been solved based on this approach, as shown in Figure CI. 1.
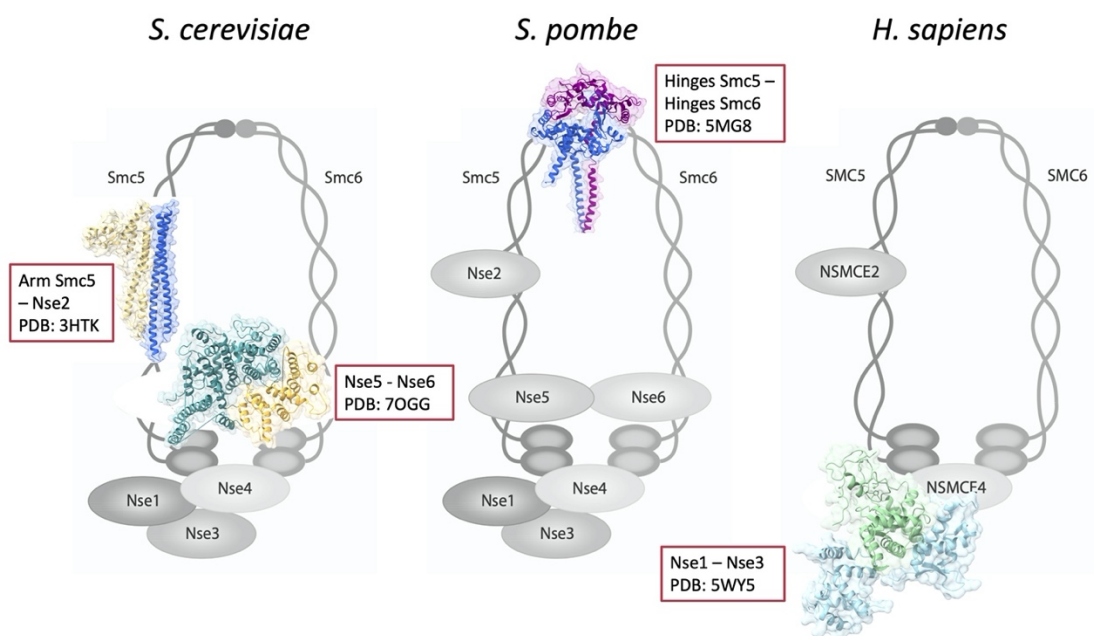
Figure CI. 1. Scheme adapted from Verver et al., 2016, highlighting the crystallographic structures.

Scheme of the Smc5/6 complexes in *S. cerevisiae*, *S. pombe* and *H. sapiens* with the different structures already known. In *S. cerevisiae*, the structure of the Arm/Smc5 with Nse2 (PDB: 3HTK) has been revealed by Duan *et al.* in 2009, and the Nse5-Nse6 crystallographic structure (PDB: 7OGG) has been discovered by Taschner *et al.* in 2021, in parallel with the CryoEM structure (PDB: 7LTO) solved by Yu *et al*. in 2021. The only known structure of the *hinges* was solved in *S. pombe* by Alt *et al.* in 2017, showing the interaction between the *hinges* of Smc5 and Smc6 (PDB: 5MG8). In *H. sapiens*, only the structure of the Nse1 and Nse3 proteins is solved (PDB: 5WY5) (Doyle *et al.* in 2010).

Due to the high complexity of the Smc5/6 complex and the numerous unsuccessful attempts to solve the structure through x-ray crystallography, recent studies using Transmission Electron Microscopy (TEM) and mainly CryoEM have been reported to gain knowledge on the structural organization (Hallett et al., 2021; Taschner *et al*., 2021; Yu

et al., 2021). Unfortunately, none of these studies have enough atomic resolution to reach a definitive conclusion about the structure of this complex. Therefore, additional studies are still required in this direction.

In this chapter, we focused on the analysis of the human Smc5/6 complex, both to disclose how this complex is organized in human and to compare it with the yeast counterpart. We have produced different subcomplexes of Smc5/6 and attempted the determination of their structure by X-ray crystallography. Furthermore, we have performed SUMOylation activities assays in order to know the enzymatic role of Nse2, particularly of its C-terminal tail region.

CI.2 Results

Design and molecular cloning

Smc5 and Smc6 are long proteins with an inner structural complexity due to its elongated conformation formed by long coiled coils connecting different globular domains. We assumed that it would be difficult to obtain crystals of these proteins because of the flexibility of these long coiled coil conformation. Therefore, we decided to design short versions of each globular domains (*heads* or *hinges*) along with coiled coils of different lengths, associated in some instances to other Nse (Non-Smc-elements) subunits (Nse2 or Nse4).

Since the SMC5/6 complex has low sequence homology with other SMC proteins, we have used the COILS / PCOILS server (Biegert *et al*., 2006; Lupas, Van Dyke, & Stock, 1991; Zimmermann *et al*., 2018) to predict the boundaries of the coiled coil. Providing an aminoacidic sequence as an input, this software estimates the probabilities for each residue in the protein to belong to a coiled coil region through sequence alignments against a large database of proteins classified as coiled coils.

As shown in (Figure CI. 2), using PCOILS, it was possible to predict the boundary residues of the *head* N-terminal, the first *arm*-coil, the *hinge*, the second *arm*-coil and *head* C-terminal domains. Notably, the program also predicted the disruption regions inside the coiled coil *arms*, also found in other SMC proteins (Beasley *et al*., 2002). Therefore, based on the results obtained in COILS/PCOILS program, we initially designed six constructs of SMC5 and five constructs of SMC6 to be expressed in *Escherichia coli*. These constructs including *heads*, *hinges* and *arms* are summarized in Figure CI. 3.
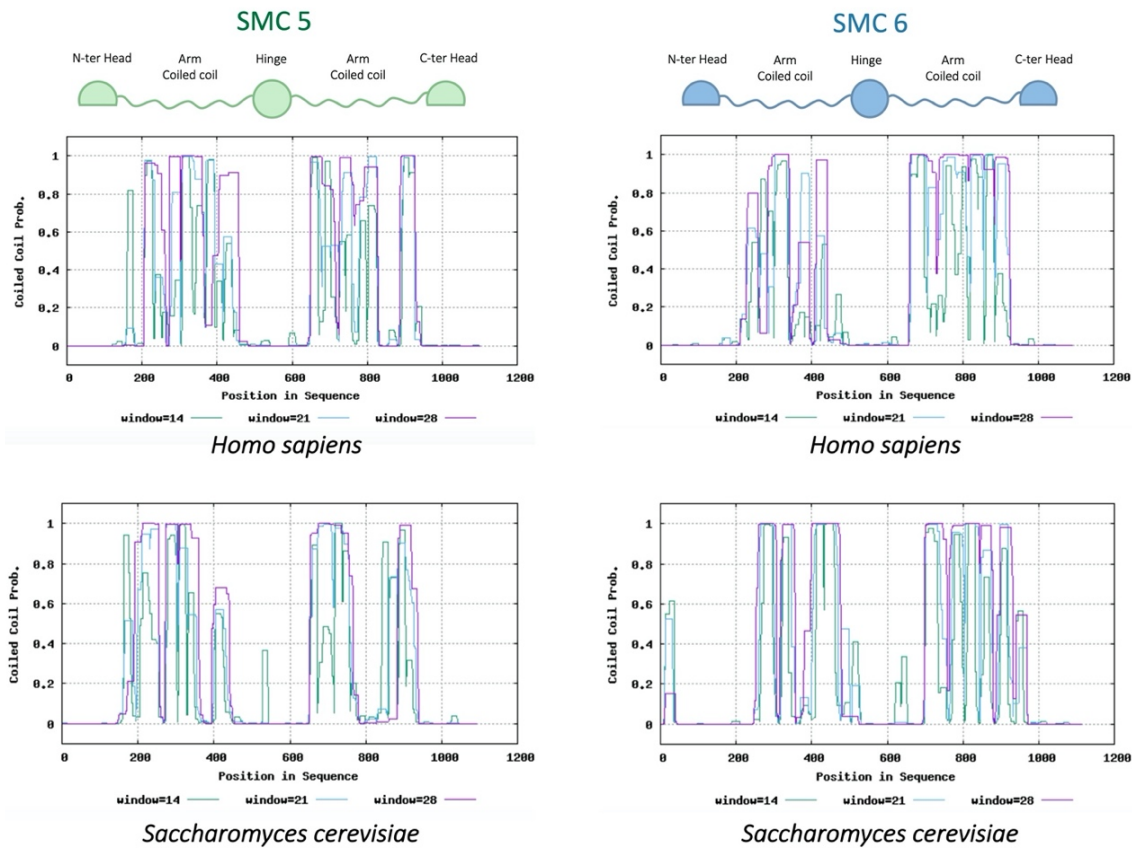
Figure CI. 2. PCOILS prediction of the structure of the Smc5 and Smc6 proteins.

Probability of finding coiled coil regions in the different sequences of Smc5 (left) and Smc6 (right). Above, diagrams with *H. sapiens* proteins. Below, diagrams corresponding to the *S. cerevisiae* sequences.
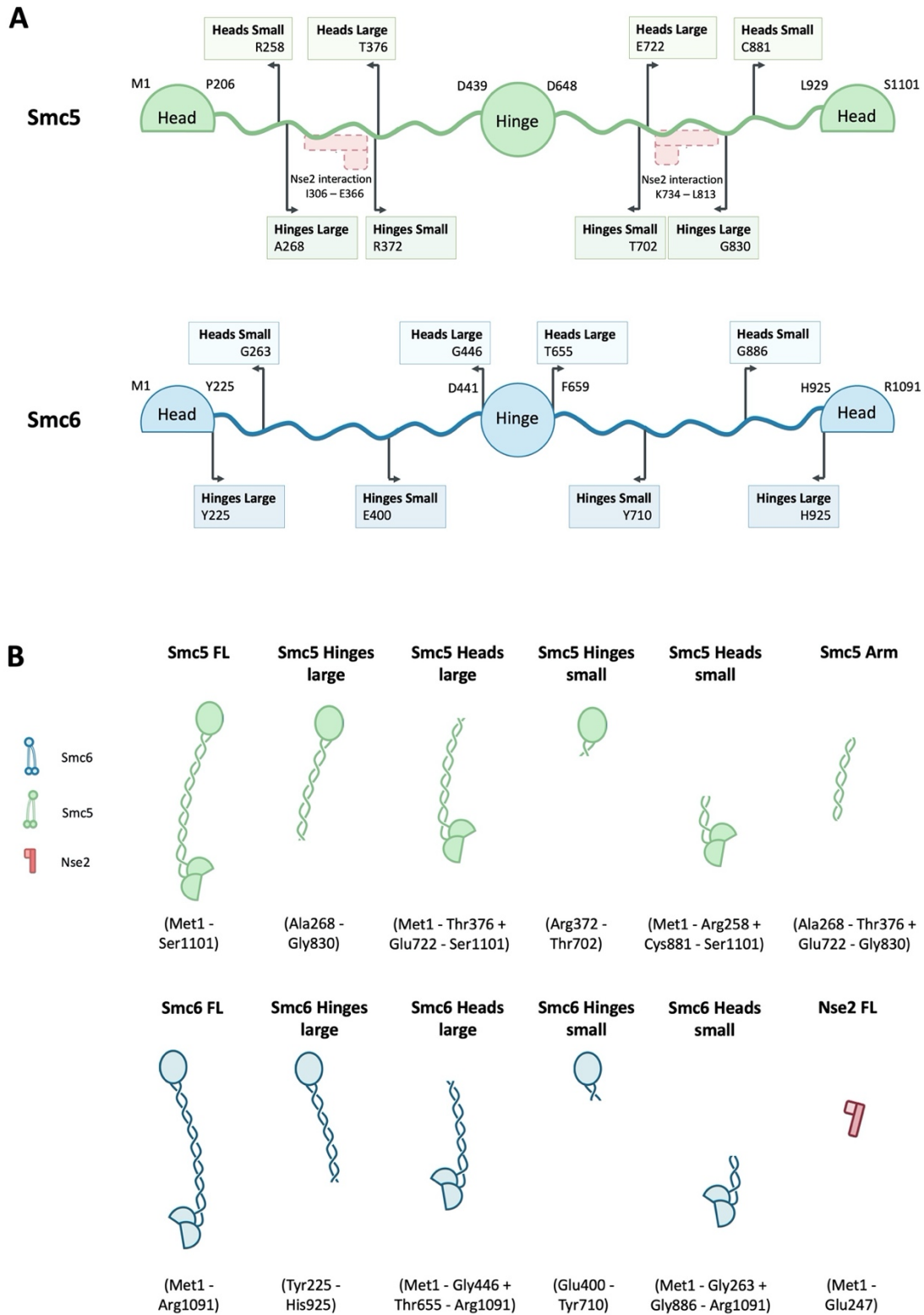
Figure CI. 3. Schemes of the different constructs designed

A) Representation of the data obtained in the PCOILS in relation to the structural conformation of Smc5 and Smc6. The range of amino acids of the different constructions is indicated.

B) Different Smc5 and Smc6 constructs designed. The construct length (with the amino acids at their respective position in the full-length protein) is indicated below each scheme.

To obtain all these constructs, PCR reactions were conducted with human Smc5, Smc6 and Nse2 cDNA clones and subcloned in expression plasmids. The details of the results obtained for all constructs are summarized in the table below (Table CI. 1).

Table CI. 1. Cloning details of the different Smc5 and Smc6 constructs

Construction name		Data			Cloning			
		Base pair	Amino acids	kDa	PCR	Cloning site	Plasmid and antibiotic	Sequenciation
SMC 5	FL	3303	1101	129	OK	BamHI - NotI	pET28a (K)	OK
	Hinges small	990	330	40	OK	BamHI - NotI	pET28a (K)	OK
	Hinges large	1686	562	67	OK	BamHI - NotI	pET28a (K)	OK
	Heads small	1434	478	55	OK	BamHI - NotI	pET28a (K)	OK
	Heads large	2265	755	88	OK	BamHI - NotI	pET28a (K)	OK
	Arm	666	222	26	OK	BamHI - NotI	pET28a (K)	OK
SMC 6	FL	3276	1092	126	OK	SalI - NotI	pCDFDuet (S)	OK
	Hinges small	930	310	36	OK	SalI - NotI	pCDFDuet (S)	OK
	Hinges large	2100	700	82	OK	SalI - NotI	pCDFDuet (S)	OK
	Heads small	1404	468	54	No	SalI - NotI	-	-
	Heads large	2646	882	98	No	SalI - NotI	-	-
NSE 2	FL	744	248	28	OK	NdeI - BamHI	pET15b (A)	OK

Expression and purification

Once we obtained the different constructs of Smc5 and Smc6 in the selected plasmids, we transformed and co-transformed different constructs combinations in *E. coli* expression strains, usually Rosetta2 (R2). Co-transformation was performed using a selection method by combination of two or more antibiotics. We also run expression tests to assess the expression levels of these proteins before to proceed with a large-scale purification.

First, we checked each protein alone prior to the co-expression of two or more proteins. The Smc5 and Smc6 full length (FL) were difficult to produce due to their irregular conformation. On the other hand, the expression of Smc5 FL in combination with Nse2 was successful, probably due to an increase in stability caused by the interaction of Nse2 with the *arm* region of Smc5 FL. Also, we were able to co-express correctly other combinations. Thus, we chose the best candidates to perform large-scale co-expressions (Figure CI. 4).

The co-expression and purification results of each combination of Smc5, Smc6 and Nse2 constructs are summarized in Table CI. 2. As shown, we initially tried to purify nine subcomplexes.
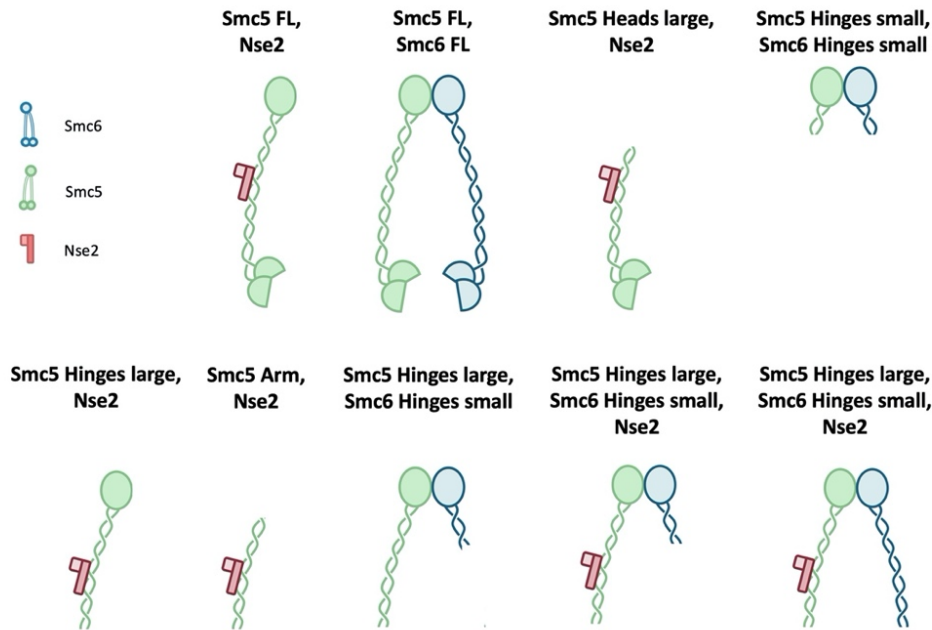
Figure CI. 4. Schemes of the different combinations of the constructs of Smc5, Smc6 and Nse2.

Table CI. 2. Expression and purification results of the different combinations of Smc5, Smc6 and Nse2 constructs, with details about the purification process.

Name	Data	Expression and purification				
	kDa	R2 plasmid + antibiotic	Expression test	Expression	Purification	Results
Smc5 FL + Nse2	130 + 28	pET28a (K) + pET15b (A) (C)	OK	OK 3L 30 °C 3h	Could not be purified	-
Smc5 FL + Smc6 FL	130 + 126	pET28a (K) + pCDFDuet (S) (C)	Could not be expressed			-
Smc5 hinge S + Smc6 hinge S	40 + 36	pET28a (K) + pCDFDuet (S) (C)	OK	OK 3L 20 °C ON	Metal Affinity Chromatography + Size Exclusion Chromatography (pH 7.5) + Ion Exchange Chromatography	OK
				OK 2L 20 °C ON	Metal Affinity Chromatography + Size Exclusion Chromatography (pH 7.0)	OK
				OK 2L 20 °C ON	Metal Affinity Chromatography + Size Exclusion Chromatography (pH 7.5)	OK
				OK 2L 20 °C ON	Metal Affinity Chromatography + Size Exclusion Chromatography + **Methylation process** + SEC (pH 7.5 + 5% glycerol)	OK
Smc5 hinge L + Nse2	67 + 28	pET28a (K) + pET15b (A) (C)	OK	OK 4L 20 °C ON	Metal Affinity Chromatography + Size Exclusion Chromatography (pH 7.0)	Lost in SEC
				OK 4L 20 °C ON	Metal Affinity Chromatography + Size Exclusion Chromatography (pH 7.5)	Lost in SEC
Smc5 heads L + Nse2	88 + 28	pET28a (K) + pET15b (A) (C)	OK	OK 4L 20 °C ON	Metal Affinity Chromatography + Size Exclusion Chromatography (pH 7.0)	Lost in SEC
Smc5 hinge L + Smc6 hinge S + Nse2	67 + 36 + 28	pET28a (K) + pCDFDuet (S) + pET15b (A) (C)	Not conclusive	OK 6L 20 °C ON	Could not be purified	-
				OK 6L 20 °C ON	Metal Affinity Chromatography + Size Exclusion Chromatography (pH 8.0) + Ion Exchange Chromatography	Not conclusive
Smc5 Arm + Nse2	26 + 28	pET28a (K) + pET15b (A) (C)	OK	OK 4L 20 °C ON	Metal Affinity Chromatography + Size Exclusion Chromatography	OK
				OK 6L 20 °C ON	Metal Affinity Chromatography + Size Exclusion Chromatography (pH 8.0) + Ion Exchange Chromatography	OK
Smc5 hinge L + Smc6 hinge S	67 + 36	pET28a (K) + pCDFDuet (S) (C)	OK			
Smc5 hinge L + Smc6 hinge L+ Nse2	67 + 82 + 28	pET28a (K) + pCDFDuet (S) pET15b (A) (C)	OK	OK 6L 20 °C ON	Could not be purified	-

As shown in Table CI. 2, the most promising combination was Smc5 hinges small + Smc6 hinges small. Since the expression tests of this combination was successful, we performed several purifications attempts. We tried several conditions: varying the pH between 7.0 and 7.5, changing the reducing agent (βME, DTT or TCEP), or with the addition of 5% glycerol into the purification buffer. We also changed the purification steps to optimize the purification yield. The results of these experiments are shown in Figure CI. 5.
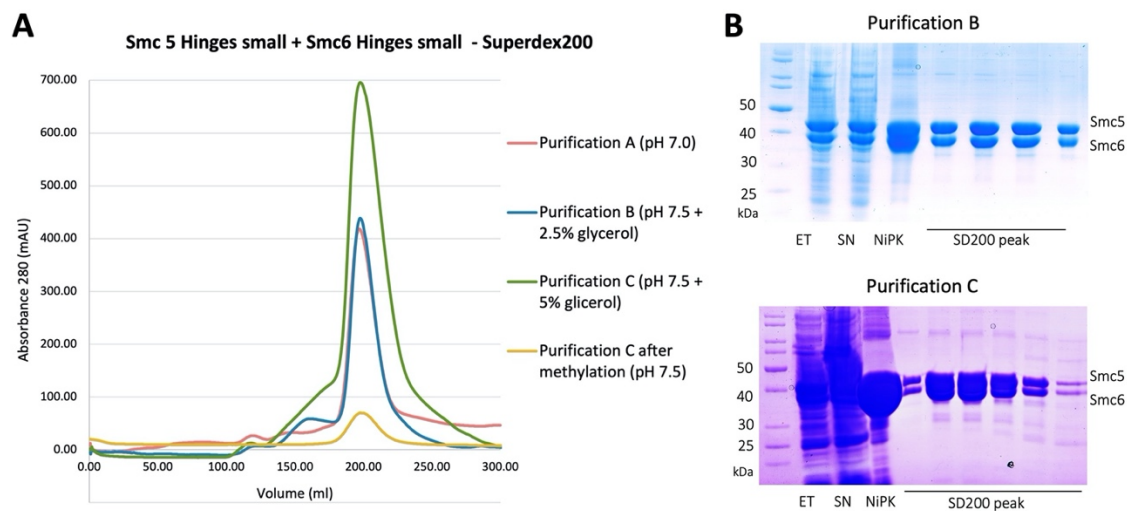
Figure CI. 5. Different large-scale purifications of Smc5 hinges small + Smc6 hinges small construct.

A) Size-exclusion chromatography (Superdex200 or SD200) elution profiles of different purifications of the Smc5 and Smc6 hinges small construct. On purification A (red), the buffer used was 20 mM Hepes pH 7.0, 250 mM NaCl, 2mM DTT. On purification B (blue), the buffer was changed to 20 mM Hepes 7.5, 250 mM NaCl, 2,5% glycerol and 0.5 mM TCEP, but the result was similar to purification A. On purification C (green), the buffer was changed again to 20 mM Hepes 7.5, 250 mM NaCl, 5% glycerol and 0.5 mM TCEP, and after the SD200 we tried a methylation process to improve the crystallization. The protein obtained after this process, was purified again (yellow) using 20 mM Tris pH 7.5, 200 mM NaCl and 1mM TCEP as the buffer. The protein was pure after this last purification, although we lost some protein in the process.
B) Two SDS-PAGE of the purifications showing the results of the size-exclusion chromatography. ET: total extract after breaking the cells, SN: supernatant, NiPK: sample eluted in a Nickel-affinity column, SD200 peak: samples obtained in the Superdex200 peak shown at Figure CI.5A around 200 ml.

In addition, due to the good results obtained with the initial [268/376-722/830]Arm/Smc5 + Nse2 construct, we decided to create new constructs with a minimal *arm* length that could still bind Nse2, as it was previously done in yeast (Duan *et al.*, 2009). For this purpose, we reanalyzed the results obtained in the PCOILS prediction map to produce shorter versions of Arm/Smc5, and we compared the results with the structure of *S. cerevisiae* Arm/Smc5+Nse2 (PDB: 3HTK). This comparison gave us some insight on the minimal *arm*

boundaries that interact with Nse2. Accordingly, we have shortened the *arm* domain from four different points: from the N- and C- terminal ends of both strands of the coiled coil, as shown in Figure CI. 6A.
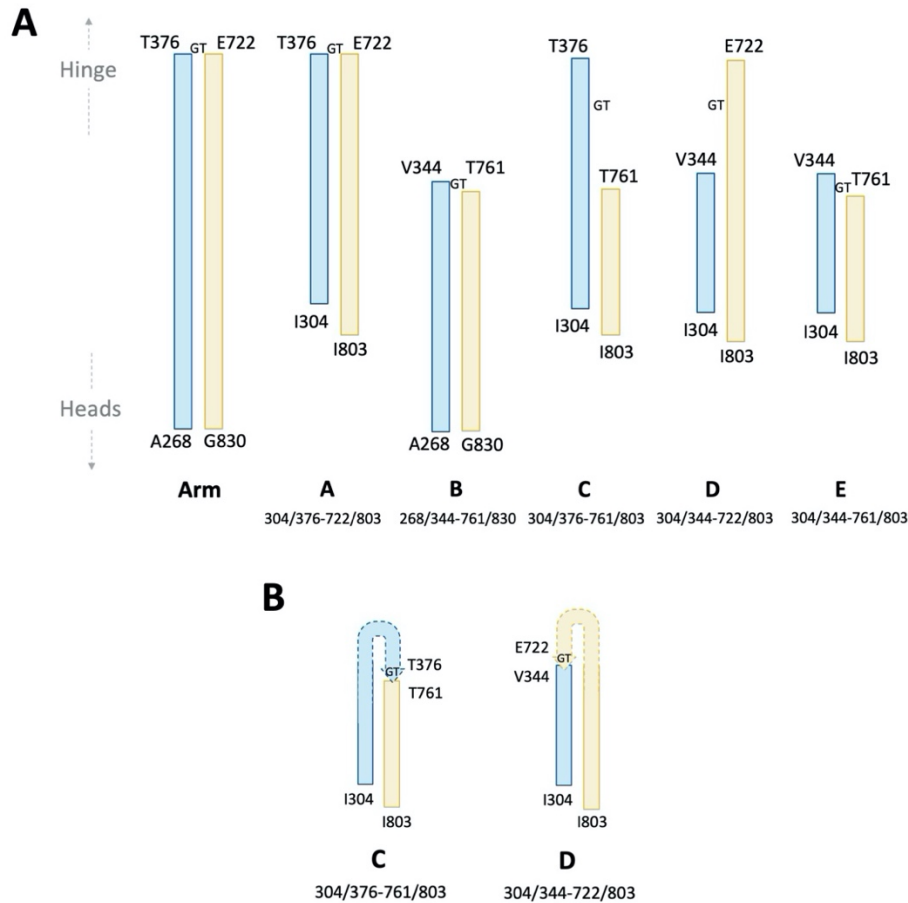
Figure CI. 6. Scheme of the different Smc5 arm constructs designed to obtain a shorter arm region.

A) Design of constructs of Smc5 comprising only the *arm* domain. The amino acids number where the new five constructs were truncated are indicated.
B) Hypothetical fold of the asymmetric extended sequences between the coils, assuming they can adopt a flexible loop form.

The initial Arm/Smc5 construct had two starting points to form the coiled coil region, one starting at A268 and finishing at T376 and the other one starting at E722 and finishing at G830. The region of Nse2 that interacts with Smc5 is predicted to be between the I306 and E366 in one coiledcoil, and K734 and L813 in the other coiled coil. Therefore, we expected to narrow down the size of the newly designed *arms* towards the Nse2 binding site (Figure CI. 6A). First, we designed two versions from the *heads* or from the *hinge* sides:

-**A**: I304 to T376 plus a connecting GlyThr linker and the region from E722 to I803. We named it $^{304/376-722/803}$Arm/Smc5.

-**B**: A268 to V344 plus a GlyThr linker plus the region from T761 to G830. This was named as $^{268/344-761/830}$Arm/Smc5.

To determine if these new *arm* constructs could bind to Nse2, the two proteins were co-expressed and co-purified with Nse2. We assumed that if the elution peak obtained by Size Exclusion Chromatography (SEC) displayed an expected molecular weight for the complex, there was indeed interaction between the two proteins. This was the case for $^{304/376-722/803}$Arm/SMC5 (Figure CI. 7A, construct A). We further purified the complex by ion exchange chromatography (RQ). As observed on an SDS-PAGE, the complex was purified to the homogeneity with two bands with the expected molecular weight.

Once we defined the starting point from the *head* side of the coiled coil (amino acids 304 and 803), we next tested three new *arm* constructs now shortening them from the *hinges* side (Figure CI. 6A):

-**C**: I304 to T376 plus the GlyThr linker and the region ranging from T761 to I803. This was named $^{304/376-761/803}$Arm/SMC5.

-**D**: I304 to V344 plus the GlyThr connecting linker and the region from E722 to I803. This construct was named $^{304/344-722/803}$Arm/SMC5.

-**E**: I304 to V344 plus the GlyThr linker and the region from E761 to I803. This last construct was named $^{304/344-761/803}$Arm/SMC5.

It is important to note that the apparent asymmetry between the N- and C-term coils sequences of the new *arms* constructs may not be a problem for the proper folding of the constructs, since we hypothesize that the regions connected by the GlyThr linker could adopt flexible conformations (Figure CI. 6B).
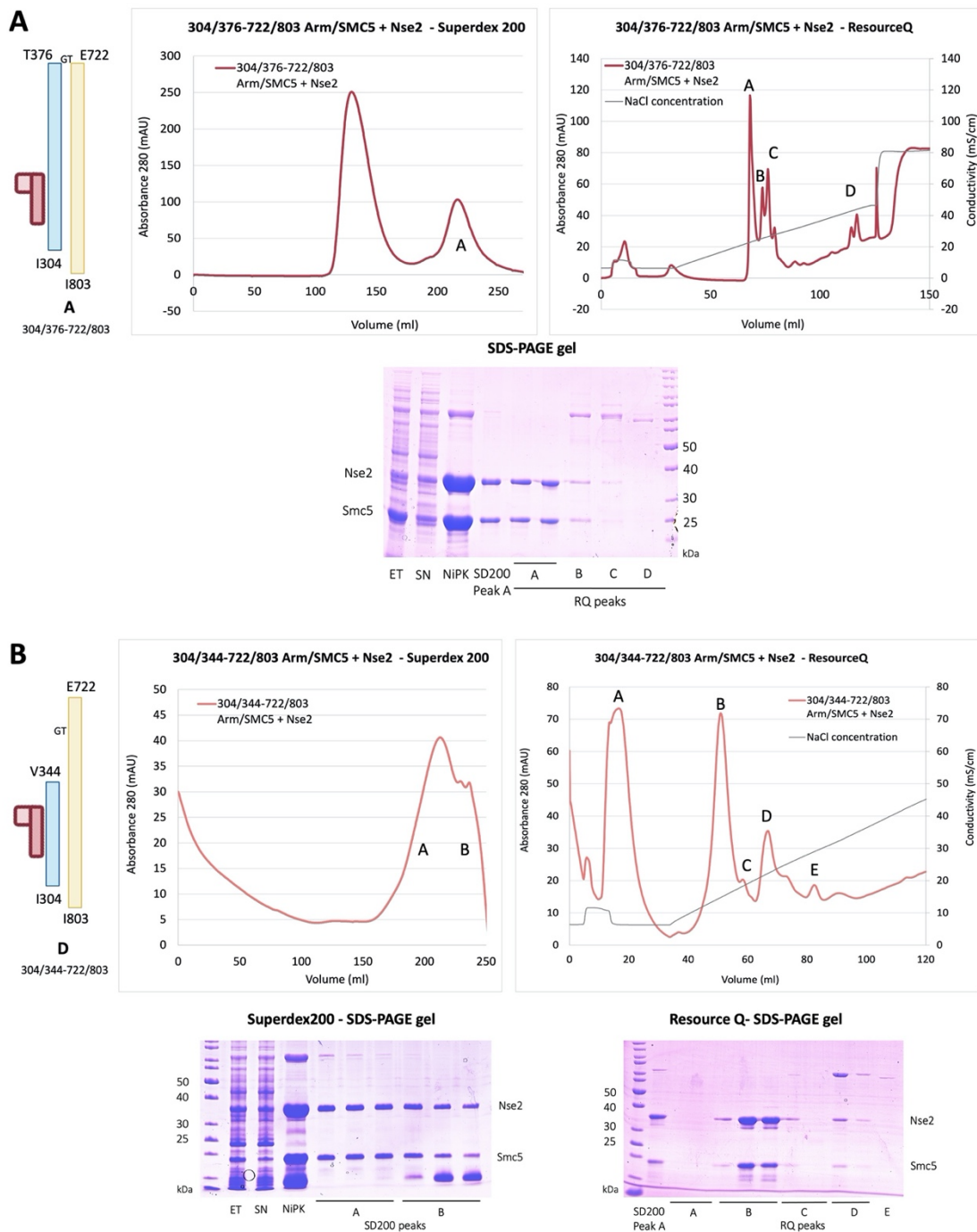
Figure CI. 7. Successful purifications to obtain a new version of a shorter Smc5 arm.

A) Purification of the construct A named as [304/376-722/803]Arm/SMC5 with Nse2 in different steps: size-exclusion chromatography, ion-exchange chromatography and the SDS-PAGE gel to check the results of the purification. ET: total extract; SN: supernatant; NiPK: sample eluted from the Nickel-affinity column; SD200 peak B: sample corresponding from 210 to 240 ml of Superdex200 purification; RQ peaks: samples eluted at different points of the ion-exchange purification.

B) Purification of the construct D named as [304/344-722/803]Arm/SMC5 with Nse2: size-exclusion chromatography, ion-exchange chromatography and the SDS-PAGE gels to confirms the results. ET: total extract; SN: supernatant; NiPK: sample eluted from the Nickel-affinity column; SD200 peak B: sample eluted from of Superdex200 purification; RQ peaks: samples eluted at different points of the ion-exchange purification.

After several attempts using these three constructs, we noticed that only the [304/344-722/803]Arm/SMC5 bound to Nse2 could be purified to homogeneity after SEC and RQ **(Figure CI. 7B**, construct D). Since, the purification quality of the construct D was very similar to the construct A **(Figure CI. 7A-B)**, together with the observation that the constructs B, C and E did not elute with Nse2 in a SEC experiments, led us to conclude that the region of C-terminal coil ranging from E722 to T761 is essential to bind Nse2. Interestingly, the previously published structure (PDB 3HTK) shows that this region of the initial part of the second coil, corresponding to E722-T761, is located in the binding site to the globular part of Nse2 (i.e. the SP-RING domain) (data not shown).

In summary, we are able to produce three stable heterodimers formed by different Smc5 *arm* + Nse2 with Nse2: the initial [268/376-722/830]Arm/SMC, the [304/376-722/803]Arm/SMC5, and the [304/344-722/803]Arm/SMC5. Thus, we achieved our first goal restricting the length of *arm* to the Nse2 binding region.

Crystallization approaches

Once the constructs are successfully purified, they become good candidates for crystallization. We performed several crystallizations attempts with different construct combinations, as shown in Table CI. 3.

Table CI. 3. Data of the crystallization attempts with the different complexes. Concentration, temperature, or types of plates used to obtain crystals of the different constructs are detailed on the table.

Name	Crystallization			
	Concentration	Sitting drop	Hanging drop	Synchrotron
Smc5 hinge S +	15 mg/ml	Clear Strategy, PACT, ProPlex, Structure Screen 1+2. 18ºC, with/without DNA 4nt		
	12 mg/ml and 30 mg/ml with 5% glycerol	JCSG, PACT, ProPlex, Structure Screen 1+2. 18 ºC		
Smc6 hinge S	20 mg/ml	Clear Strategy, JCSG, ProPlex, Structure Screen 1+2. Met/No Met, 18ºC and 4ºC		
304/376-722/803 Arm Smc5	9 mg/ml	Clear Strategy, JCSG, PACT, ProPlex. 18ºC		
	8 mg/ml at pH6	Clear Strategy, JCSG, ProPlex, Structure Screen 1+2. 18ºC	Optimization based on PDB:3HTK /	
Nse2	16 mg/ml at 200 mM NaCl concentration	Clear Strategy, JCSG, ProPlex. 4ºC	Optimization based on the one that diffracted	5 Å
304/344-722/803 Arm Smc5 Nse2	8 mg/ml and 25 mg/ml	HTSI, HTSII, Clear Strategy, PACT, Structure Screen. 4ºC	Optimization based on the one that diffracted	

Details of the crystallization conditions are detailed as follow:

-Smc5 hinges small + Smc6 hinges small

The Smc5 hinges small + Smc6 hinges small complex expression and purification was very good to set up several crystallization trays.

We tried almost 500 different crystallization conditions at 18°C and 4°C, and at different protein concentrations. In addition, we attempted to employ some optimization methods to improve the crystal formation, such as changing the buffer pH or adding some glycerol during the concentration process. Interestingly, we also tried the lysine methylation method (Walter *et al*., 2006), which gave us really good results, and we set up plates at different temperatures. Unfortunately, no crystal was obtained despite all these attempts and the good purification results.

$-^{304/376\text{-}722/803}$Arm/SMC5 + Nse2

The $^{304/376\text{-}722/803}$Arm/SMC5 + Nse2 complex was purified, and we obtained enough protein to set up plates and try several conditions at different temperatures and concentrations.

At 4°C, we found several crystals three weeks after setting up the plates. The crystals were taken to the ALBA synchrotron, Barcelona. We inspected them using the X-ray beam, and only one of them was constituted by protein and it diffracted up to 5 Å, as shown in Figure CI. 8.
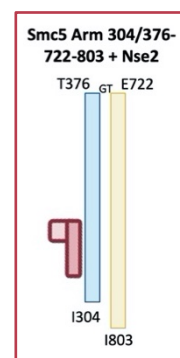
Due to the bad quality of this crystal, we were unable to collect the entire set of diffraction images required to solve the structure. In addition, the initial images showed low resolution, which also difficulted the process. However, since it was a promising result, we optimized the crystallization condition where this crystal grown by using several protocols. Unfortunately, no significant improvement has been achieved yet.
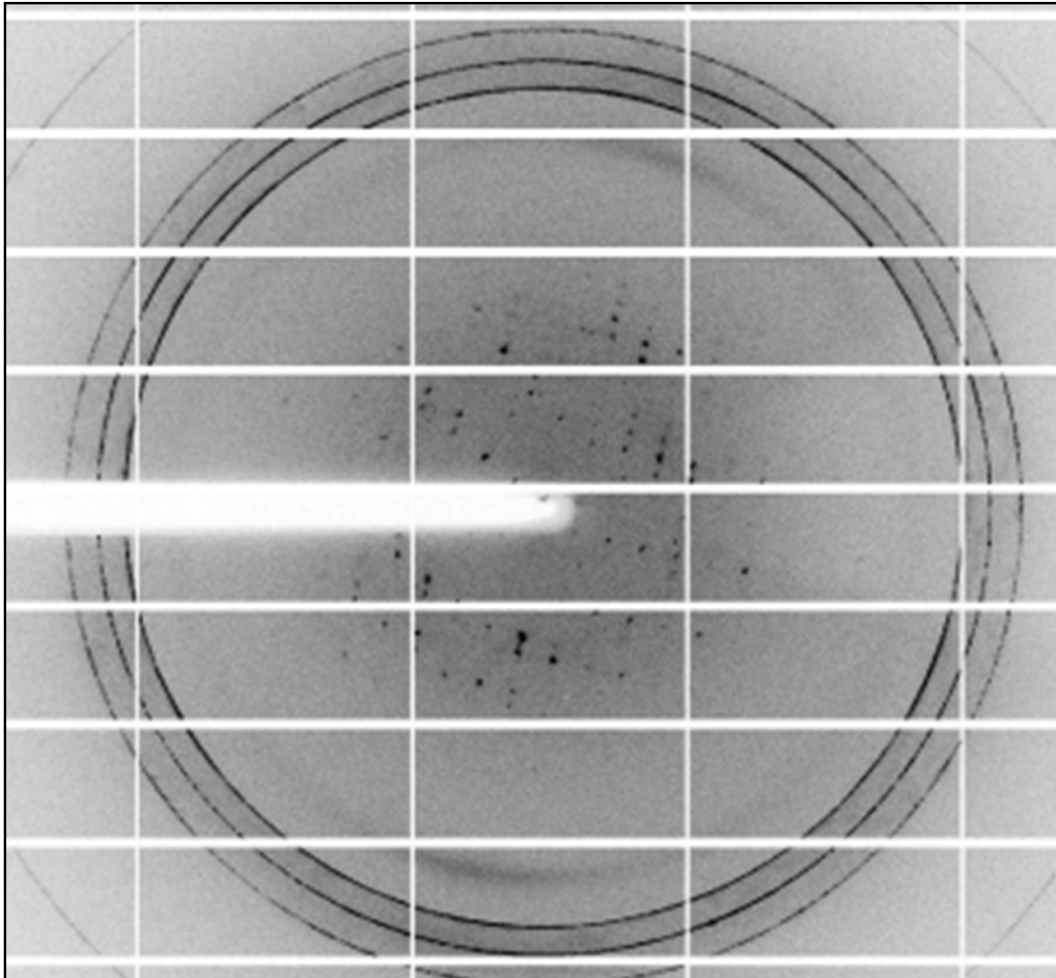
Figure CI. 8. Diffraction pattern from a native crystal of $^{303/377\text{-}719/802}$Arm/SMC5-Nse2.

A representative image collected from a native crystal of $^{303/377\text{-}719/802}$Arm/SMC5-Nse2 that diffracted about 5.0 Å resolution at a synchrotron X-ray source.

$^{-304/344\text{-}722/803}$Arm/SMC5 + Nse2

The purification of this construct was very good, and we were able to concentrate it up to 25 mg/ml in 300 µL. The volume and concentration were satisfactory and allowed us to set up sitting-drop plates for crystallization at ~500 conditions at 4°C. In addition, we also set up hanging drop plates optimizing the condition where we found crystals that diffracted from the previous $^{304/376\text{-}722/803}$Arm/SMC5 + Nse2 complex. Unfortunately, we did not obtain any crystal for this new construct yet.
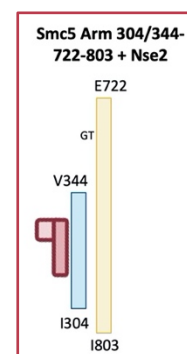
SUMO conjugation assays

Besides the structural studies, we also investigated whether the human Arm/Smc5-Nse2 constructs would be enzymatically active. For this purpose, SUMOylation studies were conducted with those Smc5/6 constructs that contained the Nse2 protein, forming a complex with the Smc5 *arm* domain. As a substrate, we used the C-terminal domain of Nse4 (cNse4 from Ile246 to Asp402), although SUMO conjugation can target internal lysine residues of Smc5 (coiled coil).

We compared the three purified *arm* constructs combined with Nse2: [268/376-722/830]Arm/Smc5, [304/376-722/803]Arm/Smc5, and [304/344-722/803]Arm/Smc5 (Figure CI. 6A). *In vitro* SUMOylation assays show the presence of several SUMO conjugation bands after 5 minutes in the reactions as shown in SDS-PAGE (Figure CI. 11A), where SUMO-conjugation bands labeled as *cNse4-S* and *cNse4-2S* stands for the *cNse4* substrate modified by one or two SUMO molecules, and *PolyS* stands for higher molecular species result of polySUMOylation. Quantification of all SUMOylated bands shows that all three complexes are very active, being [304/376-722/803]Arm/Smc5 ~40% less active than the other two after 15 minutes (Figure CI. 9B).
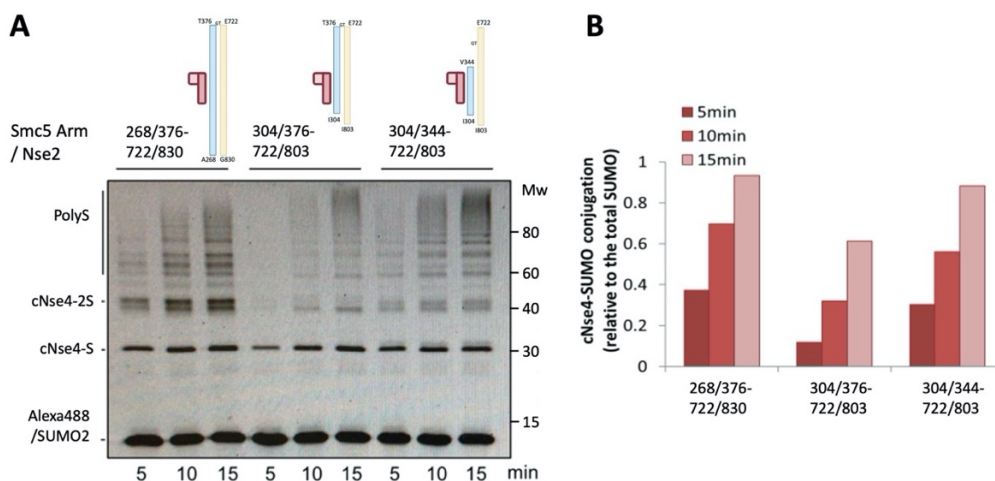
Figure CI. 9. Multiple turnover reactions of SUMO conjugation carried out by NSE2 E3-ligase bound to the different Arm/SMC5 constructs.

A) Time-course SUMO conjugation reaction using truncated Smc5 *arm* constructs in complex with full length Nse2 in the presence of 0.8μM ssDNA (50nt oligonucleotide). SUMO2-Alexa488 was used for conjugation. C-terminal domain of Nse4 (cNse4) was used as the substrate. Reactions were run at 30°C and stopped at indicated times by adding SDS-loading buffer (cNse4-S, cNse4-SUMO2; cNse4-2S, cNse4-2SUMO2; and polyS, poly-SUMO2).
B) Bar diagram representation of the relative SUMO conjugation activity of Nse2 in complex with truncated Smc5 *arm* constructs. Data values are the mean of 3 technical replicates. The boundaries of the Smc5 *arm* are shown in the figure.

These results opened the possibility to further study the regulation of this human E3. The SP-RING domain of the Nse2, crucial for the E3-ligase activity, is located in the C-terminal, from the 183-238 amino acid residues in *S. cerevisiae* and from the 154-236 in humans (Potts & Yu, 2005). Structural and sequence comparison between both Nse2 (Figure CI. 10A-B) showed that the SP-RING domain are highly conserved in both species. However, there is an important difference in the C-terminus, as the yeast protein contains an additional tail of ten residues, when compared to the human sequence. Moreover, due to studies associating the deletion of C-terminal of Nse2 to human severe dwarfism (Payne *et al.*, 2014), it seemed interesting to us to compare the enzymatic activity of the wild-type Nse2 with different C-terminal truncation mutants.
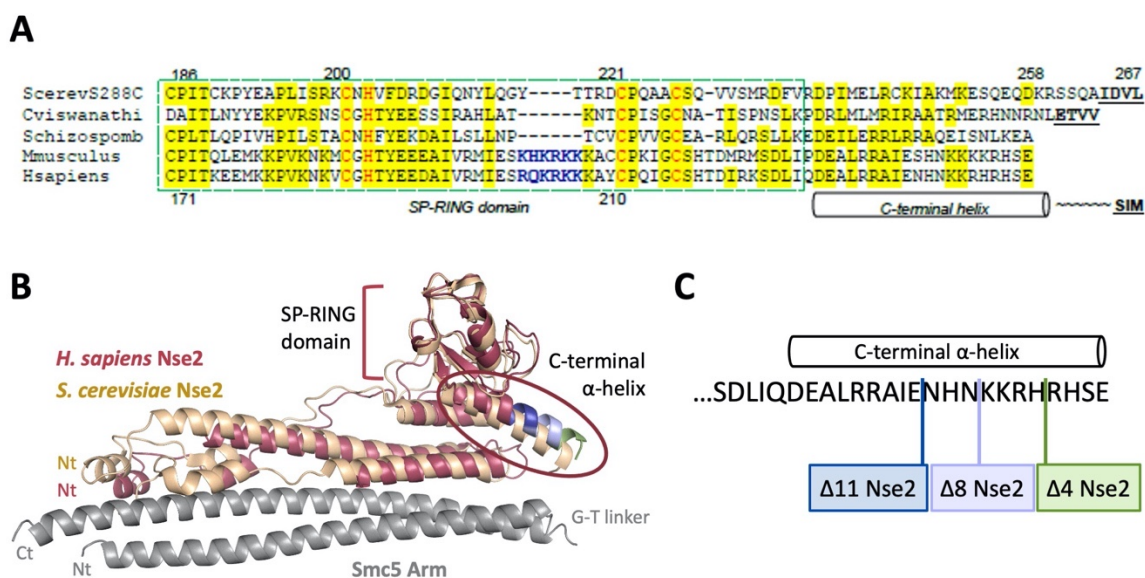
Figure CI. 10. Structural and sequential analysis of the C-terminal domains of Nse2 from different species.

A) Multiple sequence alignment of primary sequences of Nse2/Mms21 from yeast to human using PSI-coffee algorithm (score=852). Conserved residues are highlighted in yellow, SP-Ring domain is marked by green dashed box and zinc coordinating residues are shown in red, C-terminal alpha-helix is depicted by a cylindrical form and it ends up in the Lys258 and Glu247 using S. cerevisiae and H. sapiens sequences, respectively. Internal insertion exhibit on vertebrate species is colored by blue. Alignment made by T-COFFEE program tool.
B) Superposition of the crystal structure of the yeast Arm/Smc5-Nse2 (PDB: 3HTK) and the predicted structure of human Nse2. Structures are shown in cartoon representation, Smc5 *arm* domain (gray), yeast Nse2 (wheat), human SP-Ring domain (red). It is also detailed the residues corresponding to the different mutants designed, as Δ11Nse2 (dark blue), Δ8Nse2 (violet) and Δ4Nse2 (green). Picture was rendered using PyMol program.
C) Scheme representation of the C-terminal of *H. sapiens* Nse2, showing the amino acid mutated to perform the different mutants labeled as Δ11Nse2 (dark blue), Δ8Nse2 (violet) and Δ4Nse2 (green).

To test the role of C-terminal domain in human Nse2 activity, we designed several truncation mutants of Nse2: Δ4Nse2, Δ8Nse2 and Δ11Nse2 (deletion of four, eight and eleven last residues, respectively) (Figure CI. 10C). To do so, we added point mutations introducing a STOP codon at the desired position by mutagenesis PCR and then we co-transformed it with Smc5 *arm* (Construct A) and assessed their SUMO-ligase activity in comparison with WT complex.

After purification of the C-terminal truncation mutants, we conducted similar enzymatic assays as the ones showed above. As expected, Arm/Smc5-Nse2FL (full length) is very active, as observed by a progressive enrichment of SUMOylated bands from 5 to 15 min reaction (Figure CI. 11A). Interestingly, Arm/Smc5-Δ4Nse2 exhibited similar activity levels as the FL (Figure CI. 11B), suggesting that the C-terminal tail in the human Nse2 protein does not compromise its SUMO-ligase activity, in contrast with the results we are going to be presented in Chapter III when we analyze this effect on *S. cerevisiae* Nse2 complex. On the other hand, Arm/Smc5-Δ8Nse2 showed ~50% decreased activity levels after 15 minutes (Figure CI. 11A,B). Finally, Arm/Smc5-Δ11Nse2 showed a complete loss of the SUMOylation capacity, we could barely measure it (Figure CI. 11A,B).
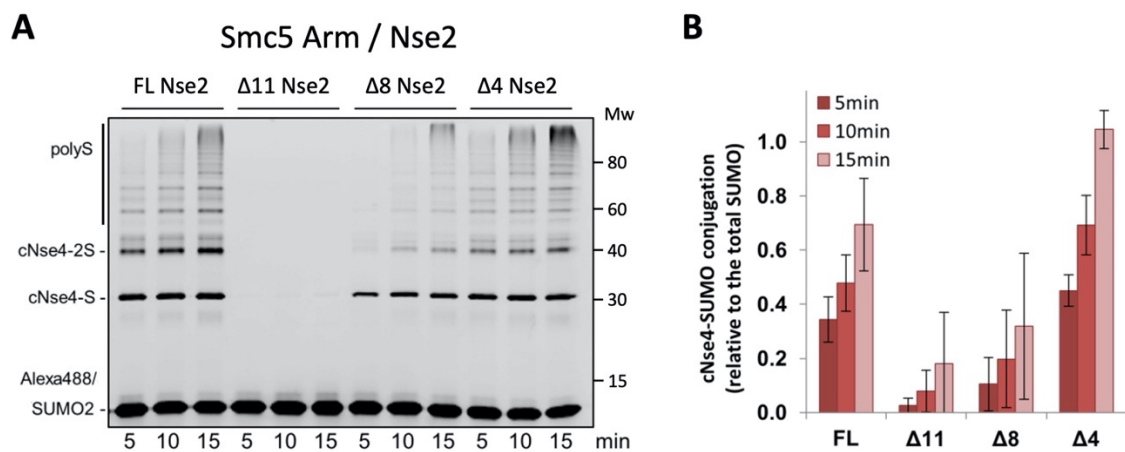
Figure CI. 11. Multiple turnover reactions of SUMO conjugation carried out by Smc5 arm with the different Nse2 C-terminal mutants.

A) Time-course SUMO conjugation reaction using Nse2 C-terminal mutants in complex with Smc5 *arm* in the presence of 0.8µM ssDNA (50nt oligonucleotide). SUMO2-Alexa488 was used for conjugation. C-terminal domain of Nse4 (cNse4) was the model substrate. Reactions were run at 30°C and stopped at indicated times by adding SDS-loading buffer (cNse4-S, cNse4-SUMO2; cNse4-2S, cNse4-2SUMO2; and polyS, poly-SUMO2).
B) Bar diagram representation of the relative SUMO conjugation activity of the different Nse2 mutants in complex with Smc5 *arm*.

By the analysis of a tridimensional model of human Nse2 generating by us (Figure CI. 10B), we became aware that by deleting those eight or eleven C-terminal residues we were entirely removing the C-terminal α-helix. In face of this observation, we believe those mutants are probably compromising the fold and stability of the adjacent SP-RING domain, which is in turn essential for the enzyme's normal activity.

Taken together, our data demonstrate that the human Nse2 is a *bona-fide* E3 ligase exhibiting SUMOylation activity when it is bound to a delimited coiled coil region of Smc5 encompassing Ile304-V344 and Glu722-Ile803. Moreover, we disclose that the impact of C-terminal deletions of Nse2 observed in human pathologies, seems to be more likely a result of the structural instability than a type of regulation of its SUMO-E3 ligase activity. These findings might be helpful for further structural and functional studies.

CHAPTER II:
DNA ACTIVATES THE NSE2 SUMO E3 LIGASE IN THE YEAST SMC5/6 COMPLEX
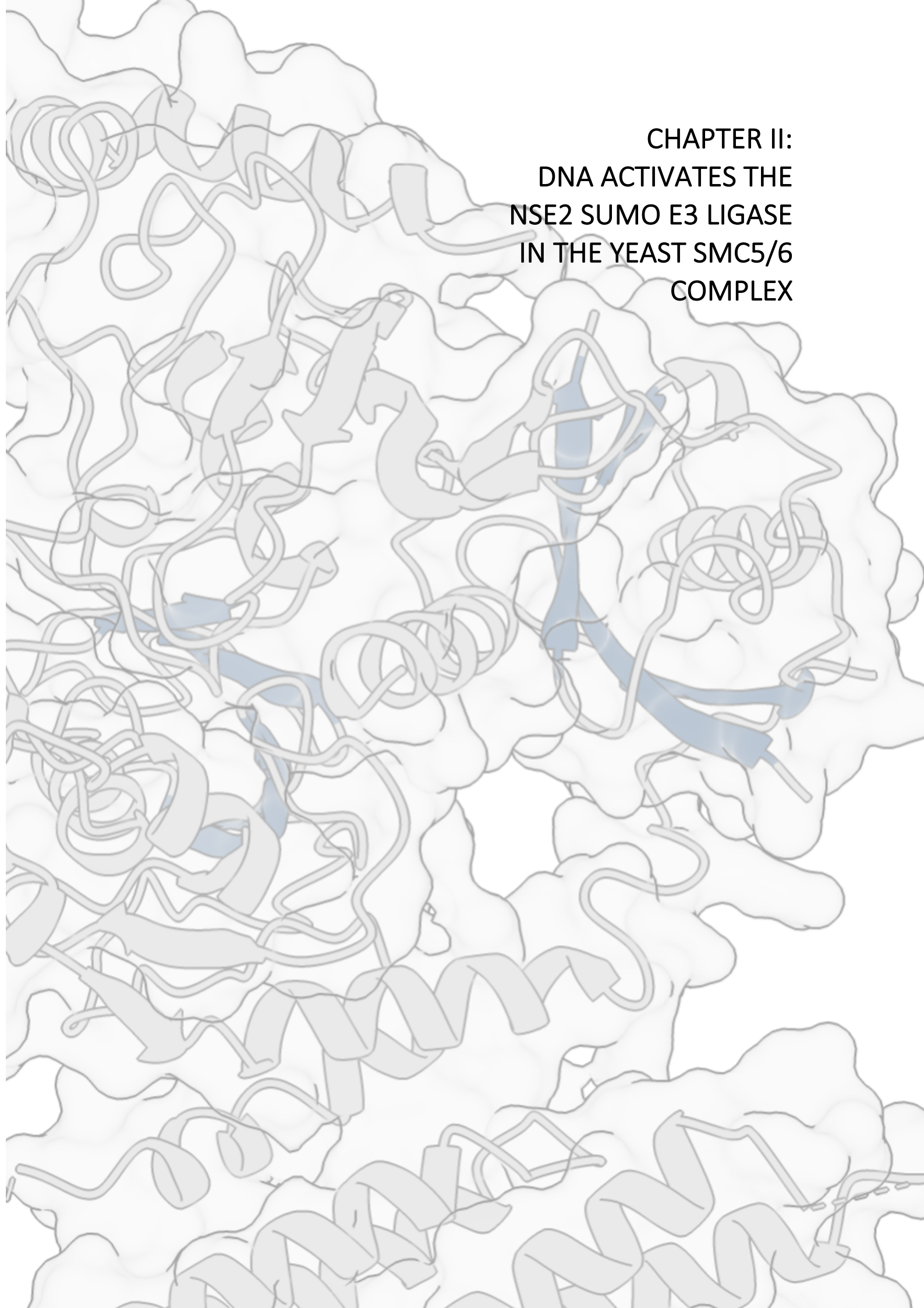
CII.1 Introduction

The recognition and association of the Smc5/6 complex with DNA is required for DNA repair processes (Bustard *et al.*, 2012; De Piccoli *et al.*, 2006; Lindroos *et al.*, 2006). Despite most known SUMO-targets of Nse2 are chromosomal proteins (Almedawar *et al.*, 2012; Andrews *et al.*, 2005; Potts & Yu, 2007; Yong-Gonzales *et al.*, 2012; Zhao & Blobel, 2005), it is currently unknown whether chromatin loading of Smc5/6 molecules modulates its E3 ligase activity.

Since Nse2 does not have DNA-binding domains, a stable docking between Nse2 and Smc5 is required for these DNA repair functions (Bermúdez-López *et al.*, 2015; Duan, Sarangi, *et al.*, 2009). The Nse2 interaction to the *arm* region of Smc5 is accomplished through a long N-terminal helical region (Duan, Sarangi, *et al.*, 2009). Whereas binding of the N-terminal region of Nse2 is essential in yeast (Bermúdez-López *et al.*, 2015; Duan, Sarangi, *et al.*, 2009), the lack of the C-terminal RING domain, where the E3 SUMO ligase activity is located, does not compromise yeast viability or even murine lifespan (Jacome *et al.*, 2015). Nevertheless, the relevance of the SUMO E3 ligase activity in genome maintenance is demonstrated since mutations in this domain make cells more sensitive to DNA damage (Andrews *et al.*, 2005; Branzei *et al.*, 2006; Potts & Yu, 2005).

In this chapter, we describe a new mechanism where the DNA binds an exposed positively charged patch on the *arm* region of Smc5 triggering a conformational change that activates the Nse2 SUMO E3 ligase enhancing the SUMOylation by the Smc5/6 complex in *Saccharomyces cerevisiae*. This work has been done in collaboration with the Cell cycle group of Dr Jordi Torres-Rosell from the Institut de Recerca Biomèdica at the Universitat de Lleida, who performed all *in vivo* experiments in *yeast cells*. We published these results in *The EMBO Journal* on May 2018 (doi.org/10.15252/embj.201798306).

CII. 2 Results

DNA binding enhances the SUMO conjugation activity of Nse2

We first investigated whether the presence of DNA could have any effect on Nse2 SUMO conjugation activity. Strikingly, our *in vitro* assays reveal that, in presence of single-stranded DNA, the full-length Smc5 in association with Nse2 presents a significant increase in SUMO conjugation. We have used the C-terminal domain of Nse4 (cNse4, from Ile246 to Asp402) as a substrate in our *in vitro* studies, even though SUMO conjugations can also occur internally on lysine residues of Smc5. After 30 minutes, we can observe in the presence of ssDNA a strong enhancement of the SUMO E3 ligase activity of Nse2 in either Smt3 (yeast SUMO), SUMO 1 or SUMO 2 (Figure CII. 1). These results clearly indicate that DNA promotes the E3 SUMO ligase activity of Nse2 by some unknown mechanism. It is important to remind here that E3 ligases not only help in target selectivity, but also optimize catalysis by orienting functional groups optimally for Ub/Ubl transfer to the target substrate (Buetow *et al.*, 2015; Deshaies & Joazeiro, 2009; Plechanovová *et al.*, 2012; Reverter & Lima, 2005; Streich & Lima, 2016).
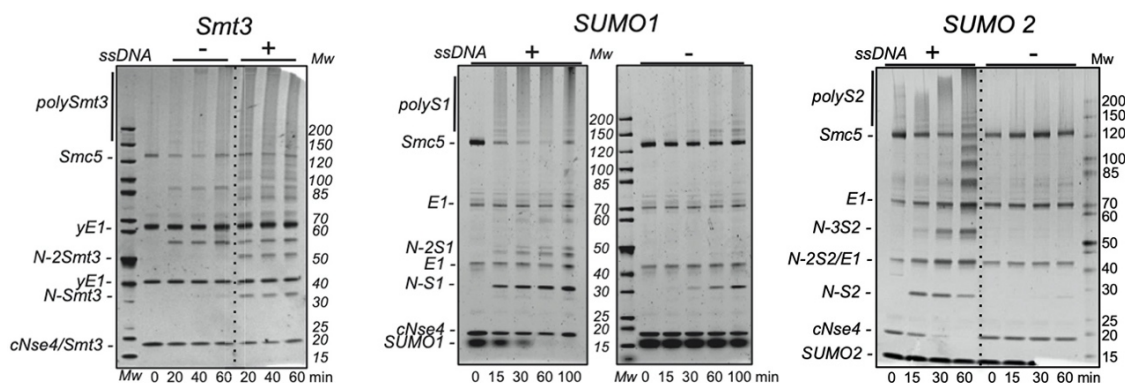
Figure CII. 1. Stimulation of the SUMO E3 ligase activity of the Smc5-Nse2 complex in presence of DNA.

Time-course conjugation reaction of Smt3 (left), SUMO1 (center) or SUMO2 (right) in the presence or absence of ssDNA (virion φx174) at 8 nM using full-length Smc5-Nse2 complex. The substrate used was the C-terminal kleisin domain of Nse4 (cNse4). Reactions using yeast or human E1 and E2 enzymes, for Smt3 or SUMO1/2 respectively, were run at 30°C and stopped at indicated minutes by adding SDS-loading buffer. Labels indicate the bands in the SDS–PAGE of the proteins in the reaction mixture.

Even though different types of DNA molecules can enhance SUMO conjugation, our *in vitro* assays suggest that single-stranded DNA (ssDNA, 5 kb virion φx174) produce a higher stimulation of SUMO conjugation than a double-stranded DNA plasmid of a similar length (Figure CII. 2). These results are in agreement with published articles that showed that ssDNA binds Smc5 and Smc6 molecules with more affinity than dsDNA using multiple binding sites, including parts of the coiled coil *arm* domain (Roy & D'Amours, 2011; Roy *et al.*, 2015, 2011).
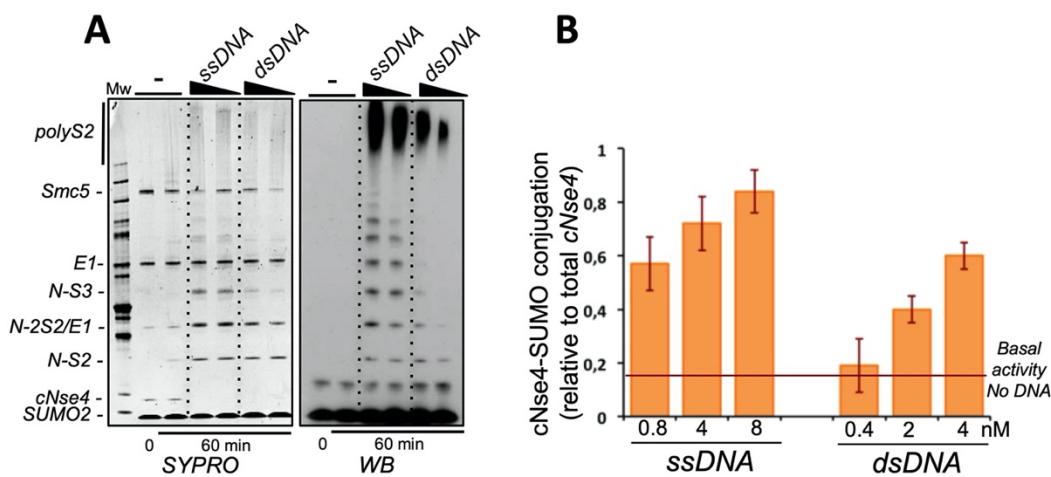
Figure CII. 2. Comparison of the enhancement of the SUMO E3 ligase activity of the Smc5-Nse2 complex between ssDNA or dsDNA.

A) SYPRO-stained and Western blot (anti-SUMO2) of the SUMO conjugation reaction by Smc5-Nse2 complex in the presence of ssDNA (virion φx174) and dsDNA (pET-DUET-1) at either 1 or 10 nM. Reactions were run at 30°C and stopped at 60 min by adding SDS-loading buffer.
B) Bar diagram comparison of the relative SUMO conjugated cNse4 substrate in the presence of either ssDNA (virion φx174) or dsDNA (pET-DUET-1) at indicated concentrations. Straight line shows the basal cNse4-SUMO conjugation in the absence of DNA. Data values are mean s.e.m. and n = 3 technical replicates. Bar diagrams calculation was generated using ImageJ software.

Moreover, we show that different random oligonucleotides shorter than the virion ssDNA used previously, of 20, 34 and 50 nucleotides, also improve SUMO conjugation in a dose-dependent manner, ranging from the nanomolar (nM) concentration of the virion plasmid to micromolar (μM) with the different oligonucleotides. The SUMOylation assays with different types of ssDNA molecules revealed a similar increase of the SUMO conjugation at equal nucleotide stoichiometry with short 50b nucleotides or long 5kb ssDNA molecules (Figure CII. 3A). Furthermore, we also observed that small oligonucleotides of 25b can stimulate SUMO conjugation used at higher concentrations

(Figure CII. 3B). Globally, these results indicate a non-specific dose-dependent binding of DNA to the complex, which stimulates the Nse2 SUMO E3 ligase activity.
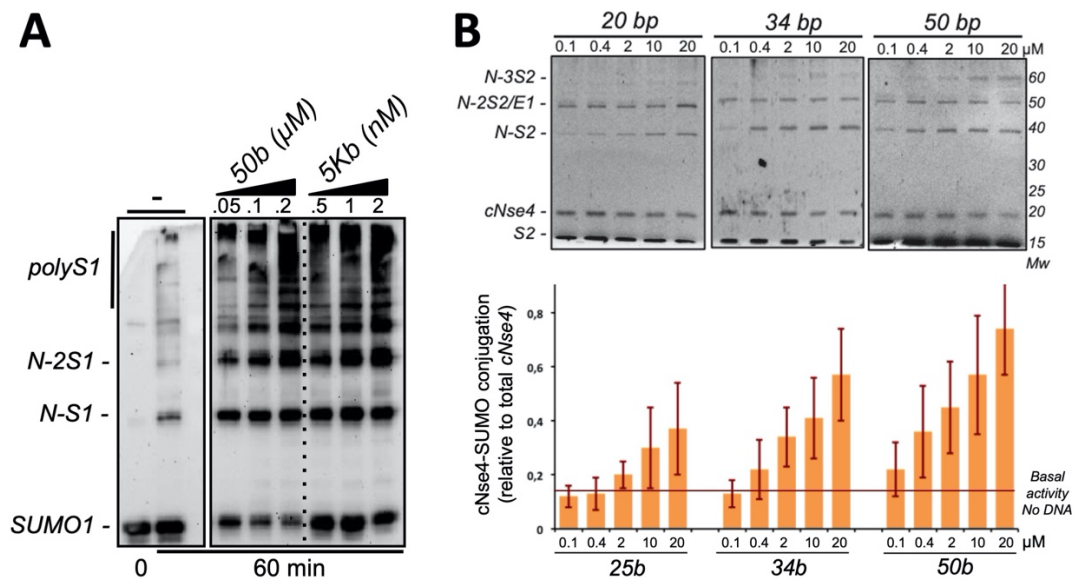
Figure CII. 3. Differences on the increasement of the Nse2 SUMO E3 ligase activity with DNA of different lengths.

A) Western blot of the SUMO conjugation reaction in the presence of 50b oligonucleotide and the 5 kb virion φx174 at the indicated concentrations. Reactions were run at 30°C and stopped after 60 min by adding SDS-loading buffer. **B)** Above, SYPRO-stained SDS–PAGE of one of the triplicate SUMO conjugation reactions used to calculate the oligonucleotide plot in below. The reactions were run for 60 min at 30°C and stopped by adding SDS-loading buffer. Below, bar diagram comparison of the relative SUMO conjugated cNse4 substrate in the presence of 25, 34, or 50 bases oligonucleotides at indicated concentrations. Straight line shows the basal cNse4-SUMO conjugation in the absence of DNA. Data values are mean s.e.m. and n = 3 technical replicates.

A minimal Smc5 domain is sufficient for the regulation of DNA-dependent SUMO conjugation

In the absence of Smc5, Nse2 has weaker SUMO conjugation activity, which barely results in an enhancement in the presence of ssDNA (Figure CII. 4C). This observation, together with the Smc5 binding to DNA through multiple binding sites (Roy & D'Amours, 2011; Roy *et al*., 2015, 2011), suggests that DNA binds to the Smc5 to increase SUMOylation. Therefore, we searched for the Smc5 regions involved for DNA sensing, which enhanced SUMO conjugation. We produced two truncations of Smc5 in complex with Nse2: one without the *hinge* domain (ΔHinge/Smc5), and another one without the *head* domain (ΔHead/Smc5) (Figure CII. 4A). All the designed constructs produce similar increasement in SUMO conjugation in the presence of DNA, although the ΔHinge/Smc5 presented a lower SUMOylation enhancement than full-length Smc5, most likely due to its higher

activity even in absence of DNA (Figure CII. 4B-C-D). We hypothesized that maybe the *hinge* domain was acting as an inhibitor of the Nse2-dependent SUMOylation.
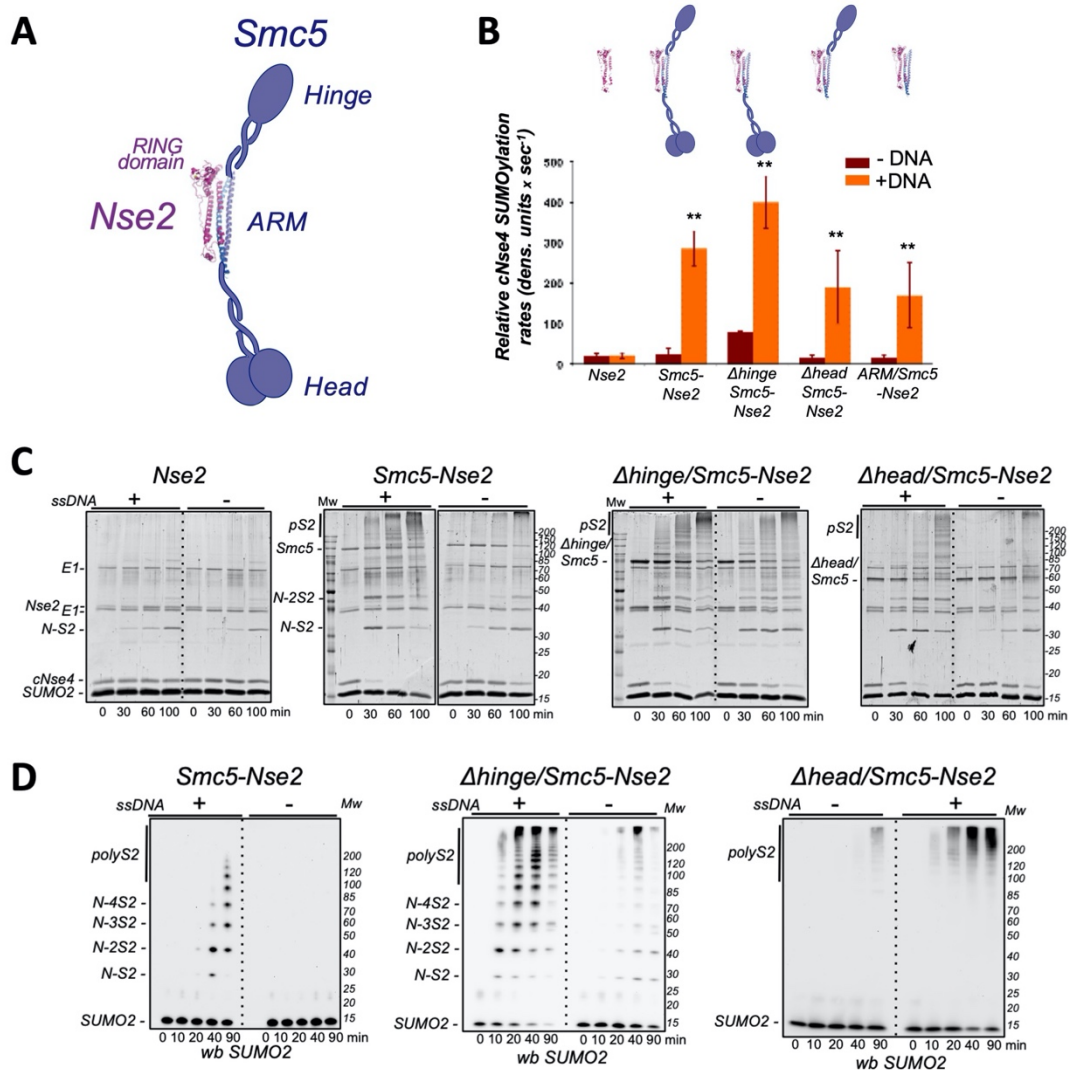
Figure CII. 4. Enhancement of the SUMO E3 ligase activity upon DNA binding by Smc5-Nse2 truncation complexes.

A) Schematic representation of the domain composition of the heterodimeric full-length Smc5-Nse2 complex and its different parts.
B) Bar diagram representation of the relative SUMO conjugation activity of Nse2, full-length Smc5-Nse2, ΔHinge/Smc5-Nse2, ΔHead/Smc5-Nse2, and Arm/Smc5-Nse2 truncation constructs (schematic representation above). Orange bars indicate the presence of ssDNA (virion φx 174), and red bars indicate absence of ssDNA. Reaction rates were performed at least in three different independent experiments. Data values are mean s.e.m.; and n=3 technical replicates. Significance was measured by a two-tailed unpaired t-test relative to wild-type. **P < 0.01.
C) SYPRO-stained SDS-PAGE of the time-course conjugation reactions of Nse2, full-length Smc5-Nse2, ΔHinge/Smc5-Nse2 and ΔHead/Smc5-Nse2 truncation constructs in the presence or absence of ssDNA (virion φx174) at 8 nM. The substrate utilized was the C-terminal kleisin domain of Nse4 (cNse4). Reactions were run at 30°C and stopped by adding SDS-loading buffer. Labels indicate the position of the proteins in the SDS-PAGE (N-S2, cNse4-SUMO2; N-2S2, cNse4-2SUMO2; pS2, polySUMO2 chains).
D) Western-blot of the SUMO conjugation reactions of FL/Smc5-Nse2, ΔHinge/Smc5-Nse2 and ΔHead/Smc5-Nse2 in the presence or absence of ssDNA (virion φx174) at 8 nM. The Nse4 C-terminal kleisin domain (cNse4) was used as a substrate in B and C. (N-S2, cNse4-SUMO2; N-2S2, cNse4-2SUMO2; N-3S2, cNse4-3SUMO2; N-4S2, cNse4-4SUMO2; polyS2, polySUMO2 chains).

In summary, the only common region in all these Smc5 constructs that improves the E3 ligase activity of Nse2 corresponds to the *arm* coiled coil region that binds Nse2 (Asp302-Thr366 and Arg737-Gln813). Therefore, we prepared this minimal Smc5 coiled coil *arm* region in complex with Nse2 (named Arm/Smc5), based on the boundaries of the published crystal structure of Nse2-Smc5 (PDB 3HTK; Duan *et al*., 2009). This minimal Arm/Nse2 is activated by DNA at similar levels than longer Smc5, indicating that it may contain a minimum DNA binding region or DNA sensor (Figure CII. 4). These results suggest that the DNA-binding patch implicated in E3 ligase enhancement is restricted to the Arm/Smc5 region in interaction with Nse2.

A positive-patch region of Smc5 *arm* domain interacts with DNA

In the minimal Arm/Smc5-Nse2 construct different ssDNA molecules can trigger SUMO conjugation in a dose-dependent manner, similar to the full-length Smc5-Nse2 complex (Figure CII. 5A).
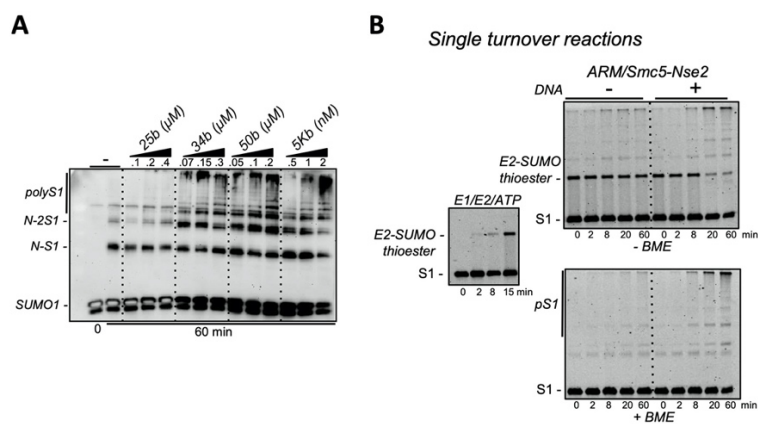
Figure CII. 5. Analysis of the SUMO E3 ligase activity of the Smc5-Nse2 mutants constructs upon binding to DNA

A) Western blot of the SUMO conjugation reaction in the presence of different oligonucleotides using the minimal Smc5/ARM-Nse2 construct. Reactions were run at 30°C and stopped after 60 min by adding SDS-loading buffer. 25b (μM), 34b (μM), and 50b (μM), stands for a 25, 34, and 50 bases oligonucleotides, respectively, and the indicated concentration is in μM units. 5 kb (nM) stands for the virion φx174, and the indicated concentration is in nM units (N-S1, cNse4-SUMO1; N-2S1, cNse4- 2SUMO1; and pS1, poly-SUMO1) (*overexposed chemiluminescent signal).
B) Left, Ubc9-thioester formation in the presence of E1, E2 enzymes, Alexa488-SUMO1, and ATP. Right, single turnover reaction of the SUMO conjugation reaction in the presence or absence of ssDNA (50b) using Arm/Smc5-Nse2 as E3. Samples were run in the presence (below) or absence of b-mercaptoethanol (above).

Moreover, single turnover reactions are used to understand the isolate events at the active site of the enzyme without catalytic cycling. In this case, we use this technique to understand the E2-SUMO thioester discharge, by using this minimal Arm/Smc5-Nse2 construct. The results of this single turnover reactions show a strong stimulation of the E2-SUMO thioester discharge, indicating the role of DNA binding in enhancing the isopeptidic bond formation by stimulation of the E3 ligase (Figure CII. 5B).

The next step was to define the DNA-binding regions on the surface of the minimal Smc5 Arm domain that activates SUMO conjugation. Interestingly, positive-charged patch regions in the Smc5 coiled coil surface of Arm/Smc5-Nse2 are observed in the crystal structure of the Smc5-Nse2 complex, which might fulfill non-specific interaction to DNA (Figure CII. 6A). In order to study these electrostatic interactions, we designed several Arm/Smc5-Nse2 constructs with different combinations of lysine to glutamic acid mutations to counter-charge binding to phosphate groups of DNA: the Arm/Smc5-Nse2 KE mutants.

In the absence of DNA, all tested Arm/Smc5-Nse2 KE mutants exhibit comparable activities (Figure CII. 6), demonstrating that the mutagenesis does not compromise either the structure or the catalytic properties of the enzyme. In the presence of DNA, however, all mutants reduce SUMO conjugation at different levels, regardless of whether the mutation of whether the mutation is single, double, or triple point, being the K743E/K745E mutant the one virtually losing all the enhancement (Figure CII. 6B). Surprisingly, the most relevant lysine residues are found in a region near the RING domain, and their influence diminishes as they move away from it. We believe that this decrease in the Nse2 SUMO E3 ligase activity may be attributed to an electrostatic disturbance in DNA binding. Moreover, as a positive control, the K743R/K745R double mutant enhances SUMO conjugation similarly to the wild-type form, in contrast to the KE mutants (Figure CII. 6B), demonstrating the role of the electrostatic nature of this interface in DNA binding.
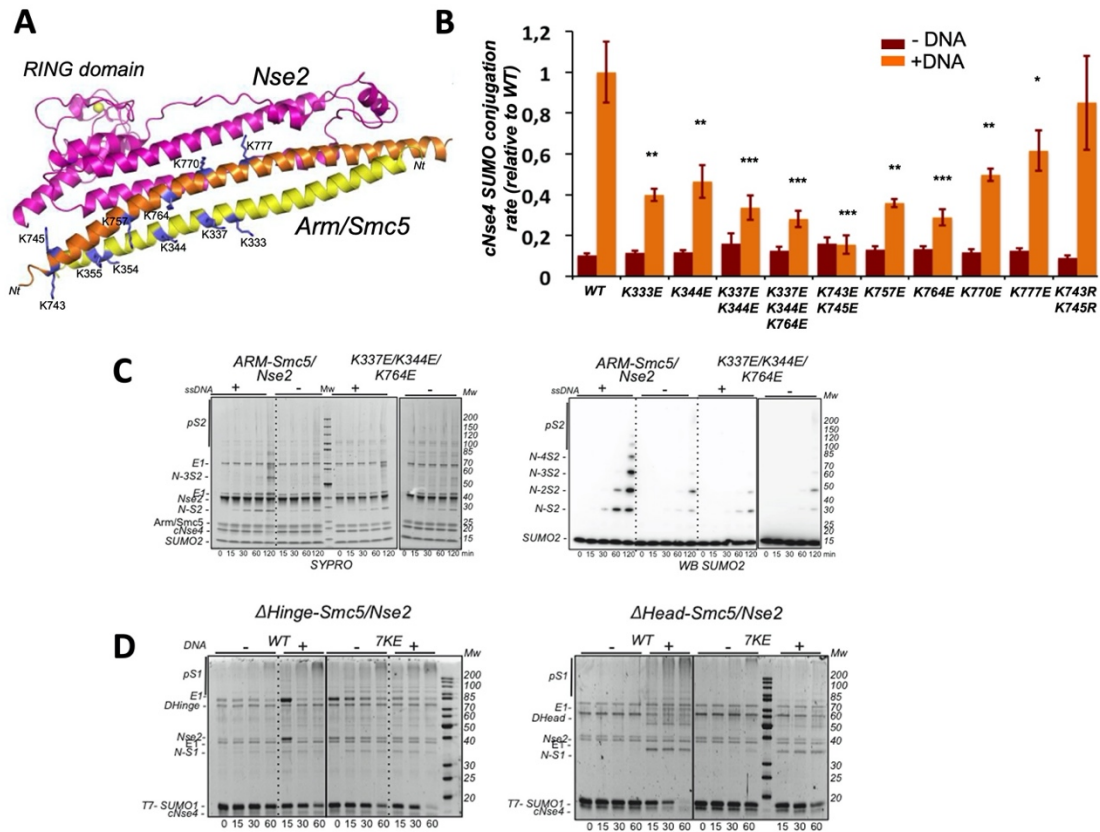
Figure CII. 6. A positive-patch region on the surface of Smc5 arm domain interacts with DNA.

A) Ribbon representation of the complex between the *arm* domain of Smc5 (yellow and orange) and Nse2 (pink) (PDB 3HTK; Duan *et al*, 2009). Lysine residues forming the positive-charged patch in the surface of the coiled coil Smc5 *arm* are labeled and shown in stick representation (blue). Zinc atom in the Nse2 RING domain is depicted as a yellow sphere.

B) Bar diagram representation of the SUMO conjugation rates of activity assays of Arm/Smc5-Nse2 KE mutants in the presence (orange bars) or absence (red bars) of ssDNA (virion φx174), relative to wild type (set to 1). Reaction rates were performed at least in three different independent experiments. Data values are mean s.e.m. and n = 3 technical replicates. Significance was measured by a two-tailed unpaired t-test relative to wild-type. *P < 0.05, **P < 0.01, ***P < 0.001.

C) SYPRO-stained (left) and Western blot (right) of the time-course reaction of SUMO conjugation in the presence or absence of ssDNA (virion φx174) at 8 nM, using either wild-type Arm/Smc5-Nse2 or K337E/K344E/K764E mutant. The reactions were run at 30°C in the presence of the C-terminal kleisin domain of Nse4 as a substrate. (N-S2, cNse4-SUMO2; N-2S2, cNse4-2SUMO2; N-3S2, cNse4-3SUMO2; and pS2, poly-SUMO2).

D) SYPRO-stained SDS–PAGE of SUMO conjugation reactions of wild-type and 7KE mutant of Δhinge/Smc5-Nse2 and Δhead/Smc5-Nse2 in the presence or absence of 50b ssDNA.

Furthermore, we conducted electrophoretic mobility shift assays (EMSA) using two Arm/Smc5-Nse2 KE mutants, K337E/K344E/K764E and K743E/K745E, which revealed a significant reduction in DNA binding compared to the wild-type form, demonstrating the disruption of DNA-Arm/Smc5-Nse2 complex binding (Figure CII. 7).
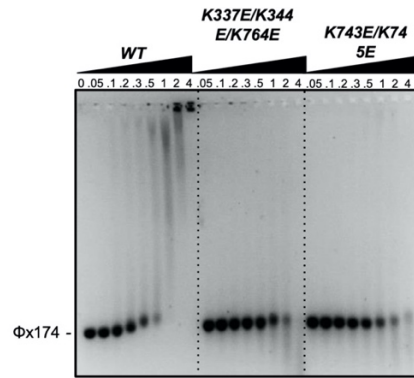
Figure CII. 7. Electrophoretic mobility shift assays (EMSA) with Arm/Smc5-Nse2 mutants.

DNA binding properties of wild-type, K337E/K344E/K764E and K743E/K745E Arm/Smc5-Nse2 mutants, were determined by electrophoretic mobility shift assays (EMSA) saturation experiments. Protein complexes were incubated for 30 min at 30°C before loading the agarose gel electrophoresis. Numbers above gel indicate the molar ratio (×103) of protein over ssDNA (virion φx174) in each lane.

DNA binding to Smc5-Nse2 triggers a conformational change

We believe that the enhancement of the SUMO conjugation activity is caused by a structural modification in the Nse2 E3 ligase upon binding to DNA. We used circular dichroism spectroscopy, which analyzes the differential absorption of circularly polarized light, to test this idea. This difference in the far ultraviolet region is mainly caused by changes in secondary structural elements and is highly sensitive to conformational changes of proteins (Kelly *et al*., 2005).

This analysis by circular dichroism of the Arm/Smc5-Nse2 complex reveals a well-folded α-helical rich protein, with two characteristic ellipticity minima at 210 and 222 nm, respectively (Figure CII. 8). Temperature denaturation after incubation at 100°C validated the structural stability of the complex, resulting in the complete loss of the circular dichroism signal (Figure CII. 8A). Interestingly, increasing DNA concentrations (φx174) resulted in a dose-dependent change in the circular dichroism spectra, which suggested a structural change mediated by DNA. Moreover, when four different types of Arm/Smc5-Nse2 KE mutants were used, the variation of ellipticity compared to the wild-type spectra was reduced dramatically at different levels (Figure CII. 8). Under similar experimental conditions, the Arm/Smc5-Nse2 KE mutants did not reach the saturation levels seen in the wild-type form, implying a loss affinity between DNA molecules and the KE mutants (Figure CII. 8A). In conclusion, all our circular dichroism assays show that when

Arm/Smc5-Nse2 binds to DNA, a structural change in the secondary structure elements might occur.
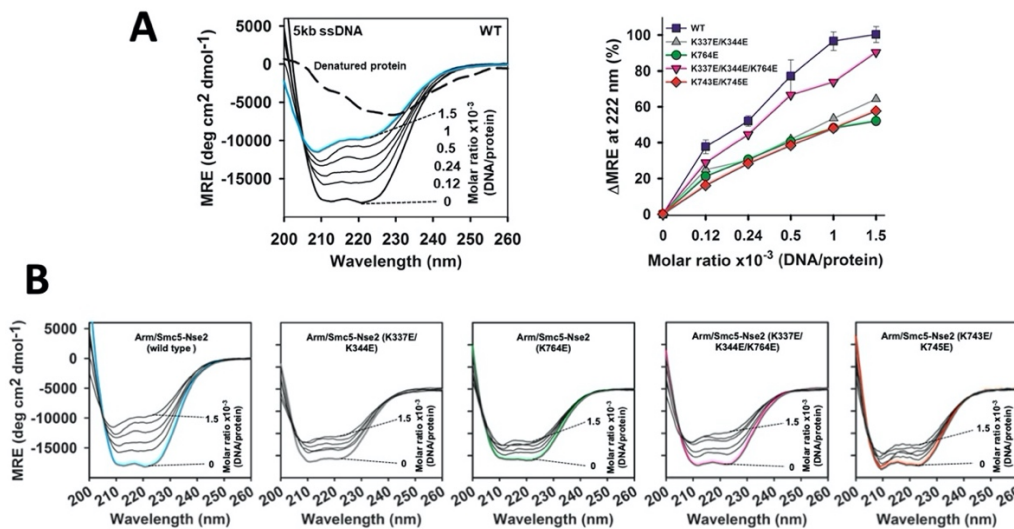
Figure CII. 8. Conformational changes in Arm/Smc5-Nse2 followed by far-UV circular dichroism.

A) Left, circular dichroism (CD) analysis of purified wild-type Arm/Smc5-Nse2. Black line, wild-type Arm/Smc5-Nse2 without bound ligand (no 5 kb ssDNA); dashed black line, denatured protein; blue line, ligand/Smc5-Nse2; numbers in graphs (dotted black lines), molar ratio of ligand/Smc5-Nse2. Right, conformational changes induced by 5 kb circular ssDNA quantified by ligand titration until signal change in mean residue ellipticity (MRE) at 222 nm achieved saturation. Blue squares Arm/Smc5- Nse2 (wild-type); gray triangles Arm/Smc5-Nse2 (K333E/K344E); green circles Arm/Smc5-Nse2 (K764E); pink triangles Arm/Smc5-Nse2 (K333E/K344E/K764E); red diamonds Arm/Smc5-Nse2 (K743E/K745E).
B) Raw data of circular Dichroism analysis of wild type; K333E/K344E; K764E; K333E/K344E/K764E and K743E/ K745E Arm/Smc5-Nse2 mutants. Colored thick lines, wild-type Arm/Smc5-Nse2 without bound ligand (no 5kb circular ssDNA); numbers in graphs (dotted black lines), ligand/Smc5-Nse2 (molar ratio).

The lack of tryptophan residues in the *arm* region of Smc5 makes possible to follow structural changes in Nse2 using Trp-intrinsic fluorescence by measuring a redshift in fluorescence emission upon DNA binding. Trp109 and Trp154, the two tryptophan residues of Nse2, are buried in the helical interface with the *arm* coiled coil structure at opposing ends of the Nse2 structure (Figure CII. 9A). Binding assays with different types of DNA molecules, such as circular ssDNA (5kb) and small ssDNA (25 and 50b), cause a similar significant red-shift of the Trp-fluorescence emission, indicating a conformational change. In titration experiments using increasing concentrations of DNA, a dose-dependent curve of fluorescence emission is observed for all DNAs (Figure CII. 9). Interestingly, the saturation curves of 50b oligonucleotide and long ssDNA had similar equilibrium constants (2.7-fold increase). These experiments are comparable to our *in vitro* activity assays with different types of DNA.
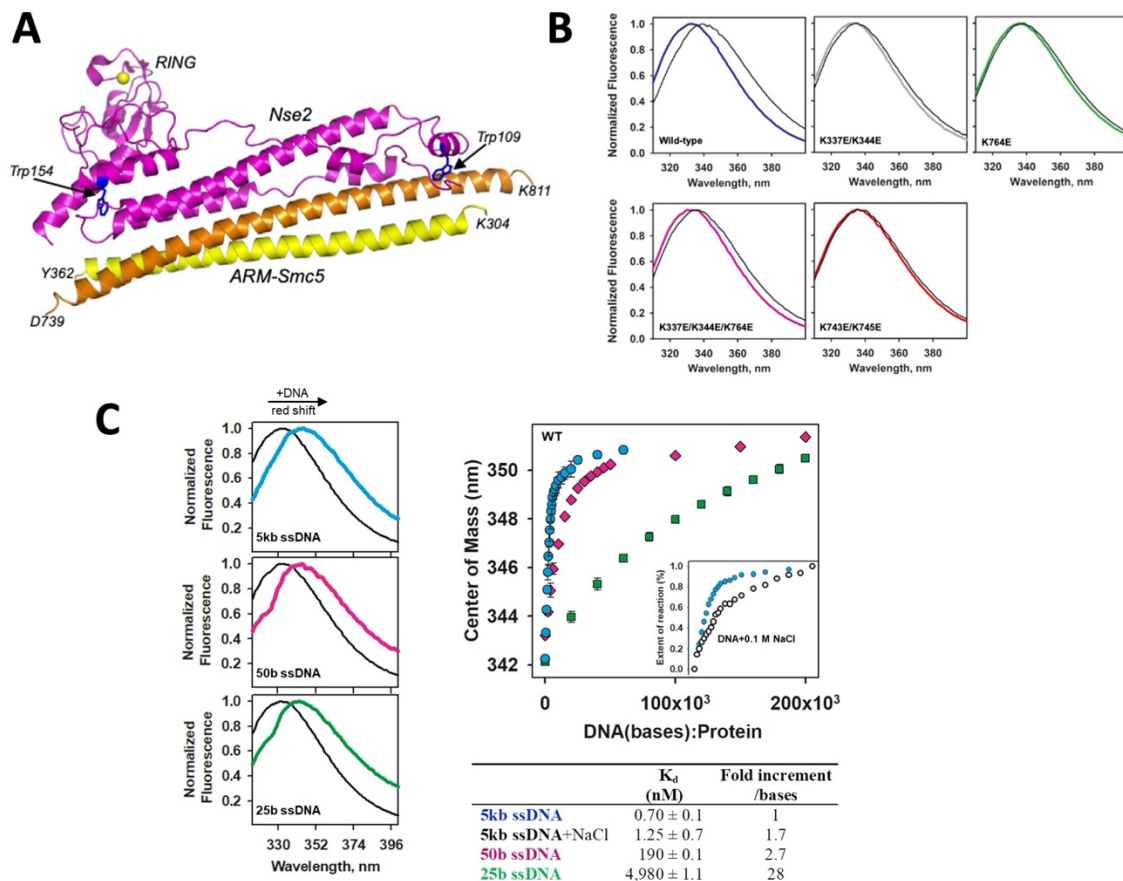
Figure CII. 9. Binding of DNA induces distinct conformational changes in Arm/Smc5-Nse2 wild type and mutants.

A) Ribbon representation of the complex between the *arm* domain of Smc5 (yellow and orange) and Nse2 (magenta) (PDB 3HTK). Tryptophan residues in Nse2 are labeled and shown in stick representation (blue). Zinc atom in the Nse2 RING domain is depicted as a yellow sphere.

B) Raw data of intrinsic Trp-emission spectra of wild-type Arm/Smc5-Nse2; K333E/K344E; K764E; K333E/K344E/K764E; and K743E/K745E mutants. Colored thick lines, native Arm/ Smc5-Nse2 without bound ligand (no 60b linear ssDNA); black lines, emission spectra after addition of DNA in a concentration able to induce the half of the maximal transition determined by titration experiments.

C) Left, tryptophan intrinsic fluorescence of wild-type Arm/Smc5-Nse2. Black line in each panel, native Arm/Smc5-Nse2 without bound DNA; blue line, 5 kb circular ssDNA/Smc5-Nse2; pink line, 50b linear ssDNA/Smc5-Nse2; and green line, 25b linear ssDNA/Smc5-Nse2. Right, conformational changes of wild-type Arm/Smc5-Nse2 induced by different types of DNA quantified by changes in center of mass (CM, redshift) of fluorescence spectra upon titration of the ligand until signal change achieved saturation. Blue circles, 5 kb circular ssDNA/Smc5-Nse2; pink diamonds and 50b linear ssDNA/Smc5-Nse2. Inset, titration curves of 5 kb circular ssDNA/Smc5- Nse2 reactions containing 0 or 100 mM NaCl (solid and hollow symbols). Below, table of the dissociation constants of the curves.

Furthermore, under similar experimental conditions, four distinct Arm/Smc5-Nse2 KE mutants can reduce significantly the Trp-fluorescence emission when compared to the wild-type form (Figure CII. 10A-B), demonstrating a loss of affinity between the DNA molecule and the complex. Interestingly, the Trp-fluorescence emission signal (Figure CII. 9C), as well as the SUMO conjugation assays (Figure CII. 10C), were both dependent on NaCl concentration, indicating the competition with electrostatic interaction.
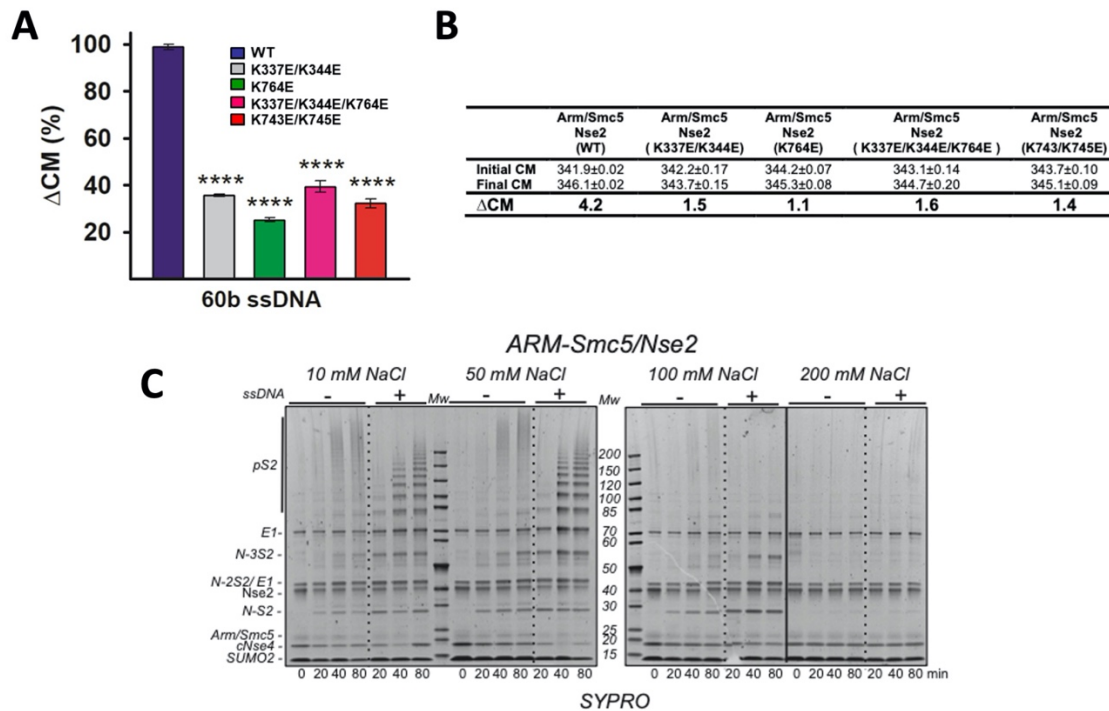
Figure CII. 10. DNA binding promotes conformational changes in Arm/Smc5-Nse2 complex.

A) Degree of conformational changes in CM induced by 60b linear ssDNA. Blue bar, Arm/Smc5-Nse2 (wild-type); gray bar, Arm/Smc5-Nse2 (K333E/K344E); green bar, Arm/ Smc5-Nse2 (K764E); pink bar, Arm/Smc5-Nse2 (K333E/K344E/K764E); red bar, Arm/Smc5-Nse2 (K743E/K745E). Reactions were performed at least in three different independent experiments. Data values are mean s.d. and n = 3 technical replicates. Significance was measured by a two-tailed unpaired t-test relative to wild- type. ****P < 0.0001.
B) Values of center of mass before and after DNA addition. These data were used to calculate the DCM presented in Fig CII.12A.
C) SYPRO-stained SDS–PAGE of SUMO conjugation reactions of wild-type Arm/Smc5-Nse2 at indicated NaCl concentrations in the presence or absence of ssDNA (virion φx174) at 8 nM (N-S2, cNse4-SUMO2; N-2S2, cNse4-2SUMO2; N-3S2, cNse4-3SUMO2; and pS2, poly-SUMO2).

All our biochemical and biophysical results suggest that the electrostatic interaction between the DNA and the *arm* domain (DNA sensor) results in a structural change that enhances the Nse2 E3 ligase SUMO conjugation activity, most likely through interactions between negatively charged phosphate groups of DNA and positively charged lysine residues of Smc5. Also, *in vitro* conjugation assays with a highly negatively charged small polymer such as enoxaparin, which resembles a non-specific DNA molecule, can also stimulate the SUMO E3 ligase activity of the Nse2/Smc5 complex (Figure CII. 11), imitating the non-specific charged-based interaction of the DNA molecules with the DNA sensor of Smc5.
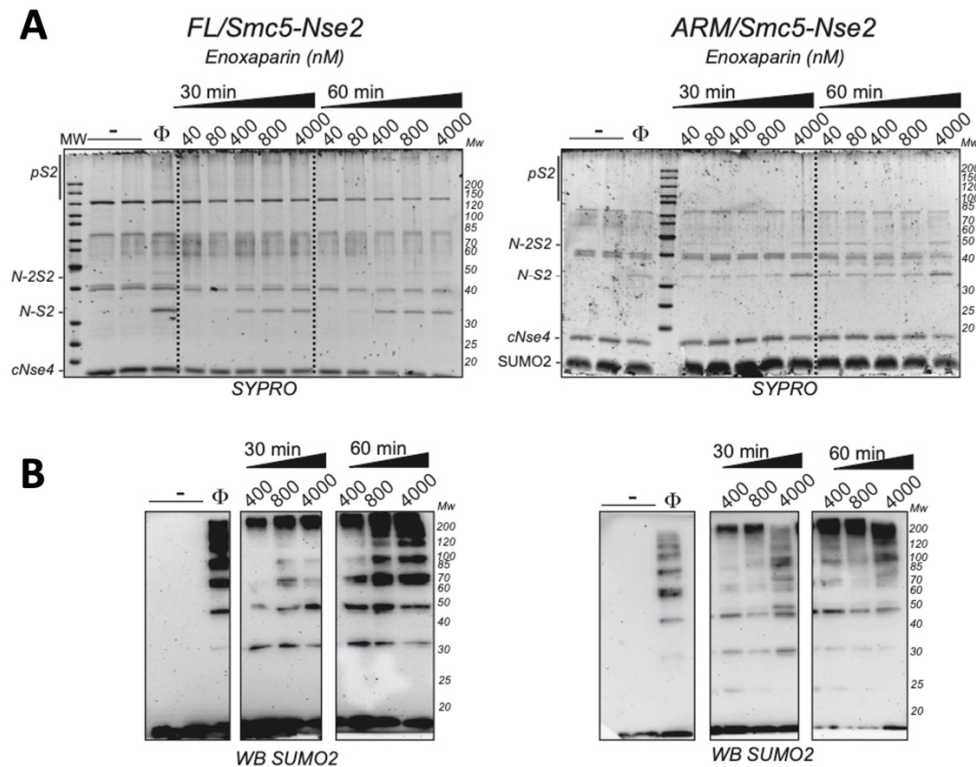
Figure CII. 11. Enhancement of the SUMO E3 ligase activity of Smc5-Nse2 upon binding to enoxaparin.

A) Time-course of the SUMO2 conjugation in the presence of increased concentration of enoxaparin using recombinant Full-length/Smc5-Nse2 or Arm/Smc5-Nse2 complex. The substrate utilized was the C-terminal kleisin domain of Nse4 (cNse4). Reaction was run at 30°C and stopped at indicated minutes by adding SDS- loading buffer. Φ stands for the 5 kb virion ssDNA (5 nM) used as positive control. Labels indicate the bands in the SDS–PAGE of the proteins in the reaction mixture. N-S2, cNse4-SUMO2; N-2S2, cNse4-2SUMO2; and pS2, polySUMOylation.
B) Western blot of the samples presented in panel (A). SUMOylated proteins were immunodetected by an anti-SUMO2 antibody.

In vivo experiments confirm the role of a positive patch in Smc5 as a DNA sensor

To prove the relevance of this DNA sensor *in vivo,* in collaboration with the Dr Jordi Torres-Rosell's group from Universitat de Lleida, we produced several SMC5 yeast plasmids with KE mutation. The different mutants are represented in Figure CII. 12A.

They performed some tests to analyze the influence of these mutations in yeast growth in the presence of MMS. The sensitivity of KE mutant cells to MMS is similar to that of Nse2 RING mutants (Andrews *et al.*, 2005; Zhao & Blobel, 2005), implying that lysine mutations in Smc5's DNA sensor affect the capacity of yeast cells to activate the Nse2 SUMO ligase. The results obtained (Figure CII. 12) suggest that MMS sensitivity in Smc5-KE cells is caused by counter-charge mutations, rather than a loss of lysine residues.

Interestingly, cells containing both the double mutant Smc5K743,745R and Smc5-7KR, which maintain the positive charge on the mutated residues, are not sensitive to MMS.

Their results *in vivo* confirm our *in vitro* results about the importance of the positive patch region, since the change to a negatively charged amino acid affects the DNA damage sensitivity more than mutation of lysines.

Figure CII. 12. A positively charged patch in Smc5 is required for DNA repair in vivo.

A) Ribbon representation of the complex between the ARM domain of Smc5 (yellow and orange) and Nse2 (red) (PDB 3HTK) (Duan *et al.*, 2009), showing positions of mutated lysine residues covered with black asterisks (3KE: K743E/K745E/K764E; 4KE: K337E/K344E/K354E/K355E; and 7KE: K337E/K344E/K354E/K355E/K743E/K745E/ K764E).
B) Growth test analysis of wild-type, nse2-CH, and the indicated smc5-KE mutants; 10-fold serial dilutions of the liquid cultures were spotted in YPD and pictures taken after 48 h.
C) Same as in (B) but using the nse2-CH, smc5-3KE, smc5-K743,745E, smc5-K743,745R, smc5-7KE, and smc5-7KR mutants.

Moreover, they performed some pull-down assays confirming that the DNA sensor is also required to increase SUMOylation of protein targets outside the Smc5/6 complex. They also found evidence that the loss of putative acceptor lysines in Smc5 could affect the interaction with DNA in the *arm* domain and compromised stability of the Smc5/6 complex (For more information about the *in vivo* results, see the publication on *The EMBO Journal*: Varejão, Ibars, Lascorz *et al.*, 2018).

Overall, the results obtained by *in vivo* assays complement those already obtained *in vitro*. They conclude that K743 and K745 represent a minimal positively charged patch in the Smc5 molecule, which acts as a DNA sensor in yeast, interacting with DNA and promoting the activity of the Nse2 SUMO ligase thus ensuing repair of MMS-induced DNA damage

CHAPTER III:
STRUCTURAL BASIS FOR
THE E3 LIGASE ACTIVITY
OF YEAST NSE2
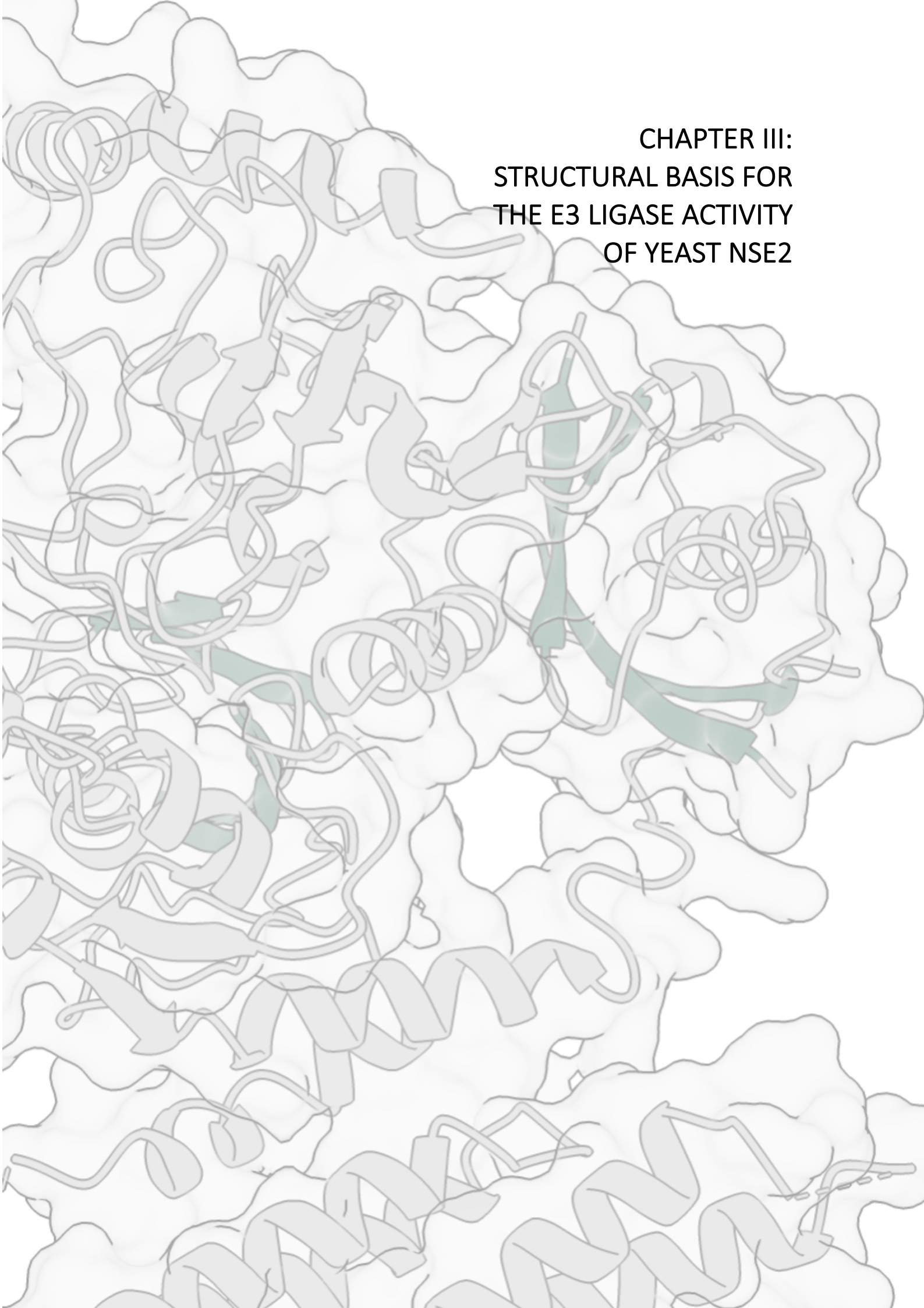
CIII.1 Introduction

The SUMO transfer from the E2 to the substrate can be enhanced by the action of E3 ligases, which in a few cases facilitate substrate binding, but which mostly increase the catalytic rate for the E2-SUMO discharge on the substrates (Berndsen & Wolberger, 2014; Pichler *et al.*, 2017). Such E3-dependent stimulation of the E2∼SUMO thioester discharge is mechanistically conducted by the stabilization of a "closed" or "active" conformation of the E2∼SUMO upon the binding to E3 ligase through SIM motifs and other regions (Varejão *et al.*, 2020).

To shed light on such interactions, in this chapter we present our solved crystal structure at 3.3 Å resolution of the *S. cerevisiae* Smc5/Nse2 E3 ligase in complex with an E2-SUMO$_D$ thioester mimetic and an additional SUMO$_B$ (SUMO$_D$ and SUMO$_B$ refer to donor and backside E2 SUMO), revealing the atomic details of this multiple interface enzyme-substrate complex. Using this structure, we were able to identify and analyze the combined action of two SIM motifs of Nse2. While SIM1 interacts with the thioester donor SUMO$_D$, SIM2 contributes to anchoring SUMO$_B$ at the E2 backside. Additionally, we could describe the interface between E2 and Nse2 SP-RING domain. Altogether, these E3 interactions contribute to the stabilization of the charged E2∼SUMO$_D$ thioester in an "optimal" catalytic orientation. Moreover, mutagenesis analysis, enzyme kinetics, and phenotypic experiments in yeast were used to confirm the importance of the interactions observed in the structure, which are essential in the conjugation activity of Nse2 and ultimately to cope with DNA damage. Again, all the *in vivo* experiments in *S. cerevisiae* were performed by the Cell cycle group of Dr. Jordi Torres-Rosell from the Institut de Recerca Biomèdica at the Universitat de Lleida. The results of this chapter have been published in *Nature Communications* in December 2021 (doi.org/10.1038/s41467-021-27301-9).

CIII.2 Results

Structure of Nse2/Smc5 in complex with the E2-SUMO thioester mimetics

To investigate the molecular mechanism of Nse2 SUMO E3 ligase, we reconstructed the complex between yeast Smc5/Nse2 and E2-SUMO thioester mimetic, which contains an inducible stable peptide bond between E2 and SUMO instead of the labile natural thioester bond. Throughout this chapter, we will use the abbreviations SUMO and E2 to refer to yeast Smt3 and yeast Ubc9. Based on previous studies (Streich & Lima, 2016, 2018), an E2-SUMO thioester mimic was created by changing Ala129 to lysine at a position close to the active site Cys93 in Ubc9, and Lys153 to arginine to prevent undesired E2 SUMOylation (Ho *et al*., 2011; Klug *et al*., 2013) . Under physiological pH conditions, Lys129 nucleophilically attacks the Cys93 E2 SUMO thioester, forming a stable isopeptidic bond in a position similar to the natural E2-SUMO$_D$.

According to previous studies and our findings, an SUMO$_B$ fused to the C-terminus of Nse2 can maintain the complex by interacting non-covalently with the E2 backside surface. Our first attempts to crystallize the Ubc9-SUMO thioester mimic in association with Smc5/Nse2 or fused Smc5/Nse2-SUMO$_B$ failed. To overcome this difficult, we created a shorter Nse2 containing the SP-RING domain that could still bind to a shorter Smc5/Arm coiled coil (Figure CIII. 1A). The E3 ligase activity of this Smc5Arm/Nse2$_{short}$ has not been altered, being similar to the WT Smc5Arm/Nse2 when the single cNse4 conjugation (cNse4-SUMO) is compared, only high molecular conjugates are reduced (Figure CIII. 1B). Smc5/Nse2$_{short}$-SUMO$_B$ fusion crystals in combination with E2-SUMO$_D$ thioester mimetics initially diffracted only to 5.5 Å. However, when non-fused Smc5/Nse2$_{short}$ was mixed with E2-SUMO$_D$ thioester mimetics and free SUMO$_B$ under similar conditions, the crystals diffracted up to 3.3 Å (Table CIII. 1).
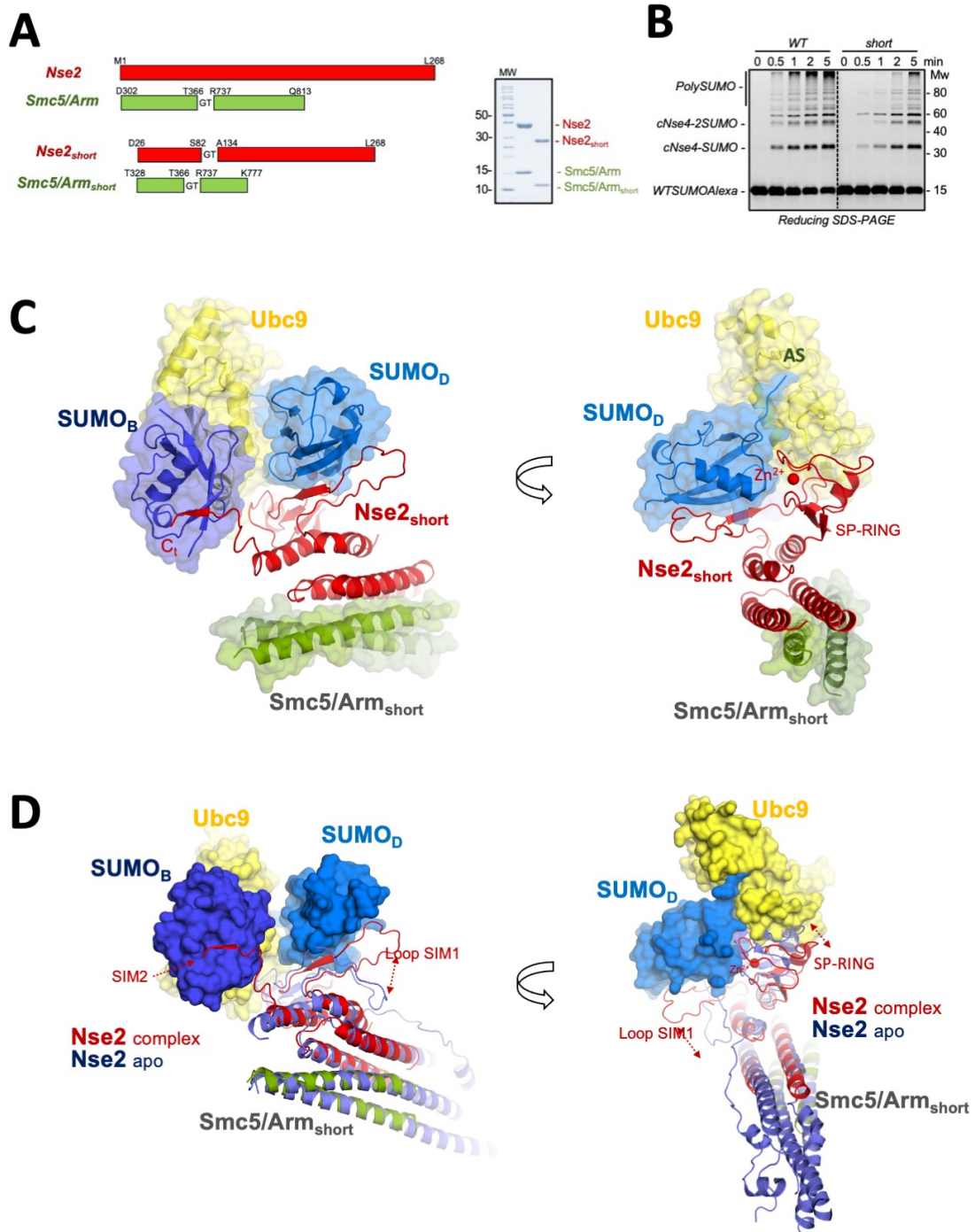
Figure CIII. 1. Structure of yeast Nse2/Smc5 in complex with the E2-SUMO thioester mimetics.

A) Schematic representation of the engineered short form of Nse2 and Arm/Smc5 coiled coil.

B) Multiple-turnover SUMOylation reactions using Nse2/Arm-Smc5 and $_{short}$Nse2/Arm-Smc5.

C) Side views of the $_{short}$Nse2/Arm-Smc5 E2-SUMO$_D$ SUMO$_B$ complex. Each subunit is color coded. The crystal asymmetric unit contained one complex composed of Smc5/Nse2$_{short}$, Ubc9-SUMO$_D$ thioester mimetic and SUMO$_B$.

D) Side views of the structural alignment of $_{short}$Nse2/Arm-Smc5 E2-SUMO$_D$ SUMO$_B$ complex with Nse2/Arm-Smc5 apo complex (PDB ID: 3HTK). Both structures were aligned using the Arm/Smc5 coiled coils domains. The superimposition reveals a major conformational change of loop SIM1 to interact with SUMO$_D$ and the C-terminal tail of Nse2 (named SIM2) to interact with SUMO$_B$.

The asymmetric unit contained one complex composed by Smc5/Nse2short, E2-SUMO$_D$ thioester mimetic, and SUMO$_B$ attached to the E2 backside (Figure CIII. 1C). The structure reveals a large interaction between the charged E2-SUMO$_D$ and the SP-RING domain of Nse2, which includes direct interactions with both E2 and SUMO$_D$. Moreover, SUMO$_D$ stablishes an extended interface with a long loop of Nse2 (called Loop SIM1), which undergoes a dramatic conformational change, establishing a β-like interaction with SUMO$_D$, resembling a SIM-like conformation (Figure CIII. 1C-D). Furthermore, the electron density maps shows that the C-terminal tail of Nse2 forms a second SIM-like interaction (named SIM2) with SUMO$_B$, which is attached to the Ubc9 backside. Hence, Nse2 clamps the SUMO$_B$-E2-SUMO$_D$ substrate complex via two SIM-like motifs, one of which binds the donor SUMO$_D$ and the other the backside SUMO$_B$.

Table CIII. 1. Crystallographic statistics of Smc5/Nse2 in complex with the E2-SUMO thioester mimetic and the backside SUMO$_B$.

Data collection	Nse2/Smc5 – Ubc9-Smt3$_D$ – Smt3$_B$
Beamline	ALBA-XALOC
Space group	P 2$_1$2$_1$2$_1$
Wavelength (Å)	0.9792
Resolution (Å)	47.14-3.31 (3.58-3.31)
a, b, c (Å)	71,14, 103.24, 115.61
α, β, γ (°)	α = β = γ = 90
Unique reflections	13097
Data redundancy	5.4 (5.5)
R_{merge}	0.13 (0.95)
CC (1/2)	0.99 (0.68)
I/σ	9.7 (2.0)
Completeness (%)	99.2 (96.7)
Refinement	
Resolution (Å)	47.13 - 3.31
Non-anomalous reflections	13056
R_{work}/R_{free}	0.235 / 0.293
Number of all atoms	4561
RMSD bond (Å)/Angle (°)	0.009 / 1.517
Ramachandran plot	
Favored (%)	87.77
Allowed (%)	10.40
Disallowed (%)	1.81

Therefore, this structure of the Smc5Arm/Nse2 in complex with the E2-SUMO$_D$ thioester mimetic displays some similarities with the Siz1 E3 ligase complex, particularly at the SP-RING interface with Ubc9. However, with SUMO$_B$-E2-SUMO$_D$, substantial changes that are unique to Nse2 emerge at the interface between SIM1 and SIM2 motifs. SIM-like elements, like the other SUMO E3 ligases Siz1, Nup358, or ZNF451, help to stabilize the "closed" conformation of the E2-SUMO thioester, enhancing SUMO discharge on the substrate.

Role of a C-terminal SIM motif (SIM2) in the catalytic activity of Nse2

In a previous published yeast Smc5/Nse2 structure (PDB: 3HTK) (Duan, Sarangi, *et al.*, 2009) the C-terminal tail of Nse2 could be not be observed, in spite of the presence of a hydrophobic stretch resembling a SIM motif **(Figure CIII. 2A)**. This kind of SIM-like motif is not found in humans or fission yeast, implying that it is associated with a specific function in the *S. cerevisiae* clade **(Figure CIII. 2A)**. The SP-RING domains of yeast and humans (PDB: 3HTK and 2YU4) can be superimposed (Cα rmsd 1.70 Å, identity 25.5 %), but the C-terminal α-helix lengths are different **(Figure CIII. 2B-C)**. The electron density of the C-terminal tail SIM motif (SIM2) in our structure of Smc5/Nse2 unequivocally shows SIM2 bound to the backside SUMO$_B$ in the E2-SUMO thioester mimetic **(Figure CIII. 1** and **Figure CIII. 3A)**.
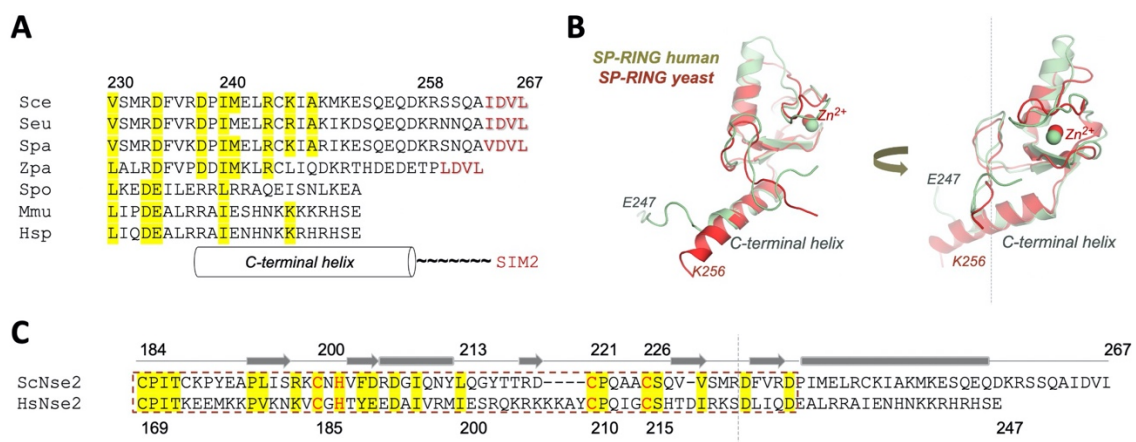
Figure CIII. 2. Comparisons between yeast and human Nse2.

A) Multiple alignment of Nse2 sequences from *Saccharomyces cerevisiae, S. eubayanus, S. paradoxus, Zygos. parabailli, Schizos. pombe, Mus musculus* and *Homo sapiens* (in red SIM2).
B) Superimposition of the yeast and human SP-RING domains (PDBs: 3HTK and 2YU4) revealing different lengths of the C-terminal α-helix, and absence of C-terminal tail on the human protein.
C) Pair-wise alignment of Nse2 sequences from *Saccharomyces cerevisiae* and *Homo sapiens,* revealing different lengths of the C-terminal α-helix.

SIM2 interacts with SUMO$_B$ in a canonical SIM-like conformation, in which the Ile264 and Val266 (positions 1 and 3 in SIM2) have their hydrophobic side chains buried in a SUMO surface cavity produced between the α-helix and the β-sheet **(Figure CIII. 3B)**. In the SUMO cavity, hydrophobic contacts are made with Phe37, Leu48, and Ala51, as well as electrostatic contacts with SUMO positive charges, such as between Asp265 (position 2

in SIM2) and His23, and, interestingly, between the C-terminal carboxylate group of Nse2 and Arg47 (Figure CIII. 3B). The structure reveals two main chain hydrogen bonds between SIM2 and the SUMO β-strand, forming a parallel SIM β conformation. The structure of the Nse2 SIM2 peptide superimposes very well with the structure of other SIM motifs, such as the C-terminal SIM2 of PIAS1 from the human SUMO1-SIM2 peptide structure (PDB: 6V7P) (Lussier-Price *et al.*, 2020) (Figure CIII. 3C). Despite the different orientations of the main chain, it is relevant to note similar positions for Ile264 and Val266 in the SUMO cavity (Figure CIII. 3C).
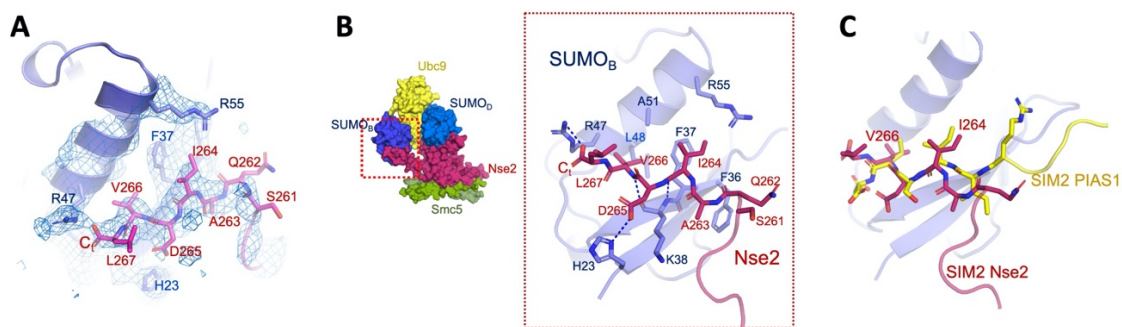
Figure CIII. 3. Interaction between the SUMO$_B$ and the SIM2 of Nse2.

A) Electron density maps of SIM2 Nse2 and SUMO$_B$.
B) Stick representation of the complex between SIM2 and SUMO$_B$.
C) Structural alignment of Nse2 SIM2 and SIM2 from PIAS1-peptide complex (PDB: 6V7P), evidencing similar locations of Ile264 and Val266 in the SUMO$_B$ cavity.

In order to analyze the role of the C-terminal tail of Nse2 (SIM2) in the SUMO E3 ligase activity, three-point mutations of SIM2 were produced: D265A/L267A (second and fourth positions of SIM2); I264P (first position of SIM2); and V266R (third position of SIM2). Also, C-terminal deletion mutants included: Δ4C-, Δ8C- and Δ16C-Nse2, the latter removes the last two turns of the α-helix (Figure CIII. 4).
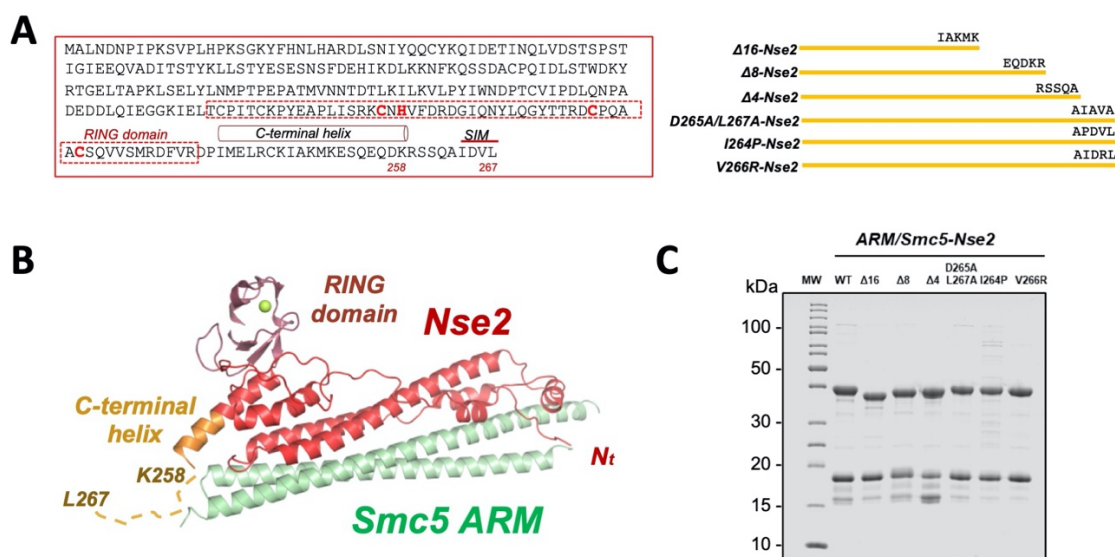
Figure CIII. 4. Analysis and design of the different C-terminal mutants of Nse2

A) Left, sequence of Nse2 from *Saccharomyces cerevisiae*, labeling SP-RING domain, C-terminal α-helix and SIM2. Right, schematic representation of C-terminal deletions and mutants.
B) Cartoon representation of the structure of wild-type Nse2/Smc5 (PDB 3HTK).
C) SDS-PAGE of the purified proteins.

To confirm the stability of the mutants, we solved the crystal structure of the Smc5/Δ16C-Nse2 deletion at 3.3Å resolution (Figure CIII. 5A), revealing a similar structure to the wild type (Cα rmsd between Δ16C and WT-Nse2 is 0.56 Å). Moreover, intrinsic Trp-fluorescence with the Smc5/Δ16C-Nse2 mutant revealed similar emission values and DNA-dependent red-shift as Smc5/WT Nse2 (Figure CIII. 5B). Through this biophysical analysis, we assured that even in the largest C-terminal deletion mutant, the stability and the structural integrity appears to be maintained.
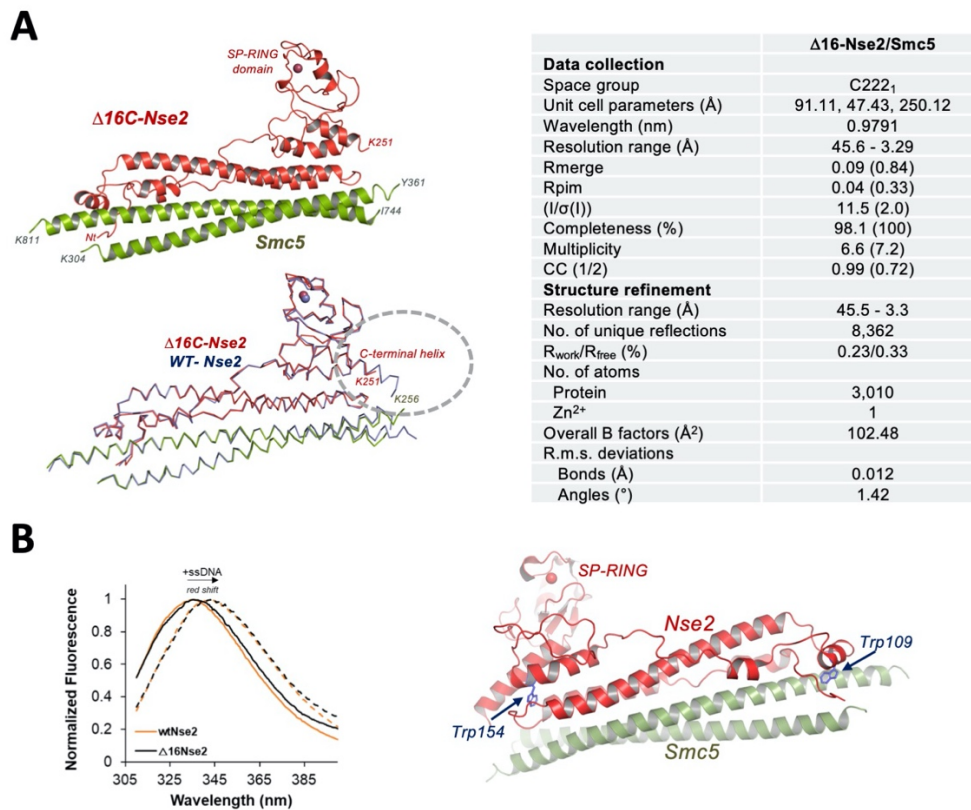
Figure CIII. 5. Structural and biophysical analysis of the truncated Δ16C-Nse2 in complex with Smc5 Arm.

A) Crystal structure of yeast Δ16-Nse2/Smc5 (cartoon representation) (left, above). Superimposition of the Δ16-Nse2/Smc5 and wild-type (PDB 3HTK) showing correct folding and assembly of the former (left, below). Table summarizing data-collection and refinement statistics (right).
B) Intrinsic Trp-fluorescence from Δ16-Nse2/Smc5 and wild-type spectra highlighting similar emission values and DNA-dependent red-shift (left). Cartoon representation of the Δ16-Nse2/Smc5, showing the position of the two tryptophan residues present in the complex (right).

In all Nse2 C-terminal mutants, *in vitro* SUMOylation assays using both human and yeast conjugation systems (SUMO, E1, E2 and ATP) reveal a clear decrease in SUMO conjugation (Figure CIII. 6A-B). Since we have already demonstrated that there were no stability problems, we attribute this reduction in conjugation activity to a role of SIM2 during the E3 ligase activity of Nse2. Interestingly, the yeast enzymes had a substantially higher conjugation rates than their human equivalents under similar conditions (Figure CIII. 6A-B). The SUMOylation assays was performed with three different SUMO substrates: the Nse4 C-terminal "Kleisin" domain (cNse4), the P53 C-terminal domain (cp53), and auto-conjugation on the Arm/Smc5, showing all of them a Nse2 E3-dependent activity (Figure CIII. 6C-E) and a reduction of the SUMO conjugation in all SIM2

mutants tested. The Δ4C-Nse2 (ΔSIM2) showed the highest reduction, around 80%, meanwhile I264P and V266R mutants showed around 30 to 50% decrease (Figure CIII. 6C-E). Overall, these results indicate a role for SIM2 in the SUMO E3 ligase activity of Nse2.
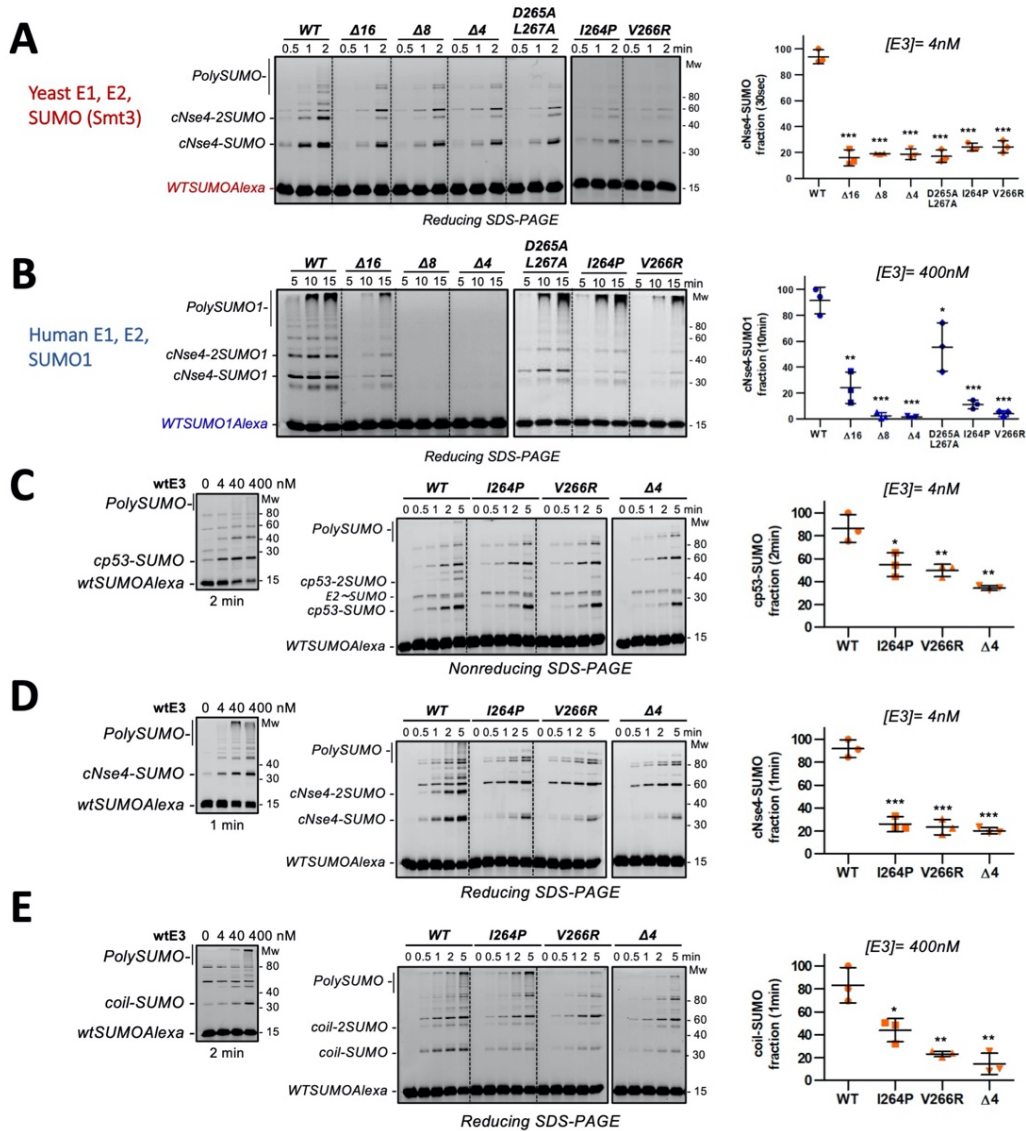
Figure CIII. 6. Multiple-turnover reactions with the different Nse2 constructions.

A-B) Multiple-turnover SUMOylation reactions of yeast Nse2/Smc5 complex (wild-type and mutants) using cNse4 substrate at 30ºC (left). **A** is performed using yeast conjugation system and **B** is using human system. Bar graphs showing that point mutations or deletion of SIM2 reduces E3 activity (right). The quantified rate data show mean ± s.d. (n = 3 technical replicates). All experiments were performed in the presence of 50nt ssDNA. Significance was measured by a two-tailed unpaired t-test relative to wild-type. *P < 0.05, **P < 0.01, ***P < 0.001.
C-E) Multiple-turnover SUMOylation reactions of yeast Nse2/Arm-Smc5 complex (wild type and mutants) using cP53, cNse4 and coil/Smc5 substrates. Enzyme concentration was chosen based on the concentration dependence assay (left). Error bars showing that point mutations or deletion of SIM2 reduce E3 activity (right). Data values represent standard deviation, n = 3 technical replicates. Significance was measured by a two-tailed unpaired t-test relative to wild-type. *P < 0.05, **P < 0.01, ***P < 0.001.

The SIM2 participates in DNA damage repair in yeast

Since the Nse2 SUMO ligase cooperates with the Smc5/6 complex in genome integrity, the inactivation oh the SIM2 is expected to decrease the efficiency of DNA repair in cells. To test the role of the SIM2 *in vivo*, we introduced a STOP codon just after Ala263 at the endogenous budding yeast NSE2 locus, thus preventing translation of the C-terminal IDVL SIM2 sequence (hereafter referred to as nse2-SIM2Δ for simplicity). Under normal conditions or after DNA damage, nse2-SIM2Δ cells did not have any apparent phenotype, showing that the SIM2 is not required for normal growth or DNA repair in otherwise wild-type yeast cells (Figure CIII. 7A). This could be due to compensatory mechanisms using other DNA repair pathways, for example, in yeast, SUMOylation of the Smc5 protein is not essential, but it cooperates with the Mms4-Mus81 and Slx4 structure-specific endonucleases, and the SUMO-like domain containing protein Esc2 for DNA alkylation damage repair. So, to test our hypothesis, the Torres-Rosell's group combined the nse2-SIM2Δ mutants with deletions in the *MMS4*, *SLX4*, and *ESC2* genes. As shown in Figure CIII. 7A, truncation of the Nse2 protein just before the SIM2 motif reduces the growth of *slx4Δ* and *esc2Δ* cells and aggravates the sensitivity to MMS of the *mms4Δ*, *esc2Δ*, and *slx4Δ* mutant cells. This indicates that the SIM2 in Nse2 promotes DNA repair in budding yeast in combination with genes involved in DNA recombination intermediate processing.

Probably due to the diminished Smc5/6 function, many Smc5/6 mutants are also hypomorphic for Nse2-dependent SUMOylation (Bermúdez-López *et al*., 2015). We attributed that truncation of SIM2 would potentiate the effects of mutations in other complex subunits, compromising Smc5/6 function even more. To study this hypothesis, they crossed nse2-SIM2Δ cells with thermosensitive mutants affected in the NSE1, NSE3, NSE4, NSE5, or NSE6 subunits of the Smc5/6 complex. After selection of double mutants and compared their growth to wild-type and single mutant cells we observe that the deletion of the SIM2 in combination with smc5/6 mutants reduced cell growth at the permissive temperature and increased the thermosensitivity of cells (Figure CIII. 7B). Overall, these results suggest that the SIM2 in Nse2 cooperates with other Smc5/6 subunits and DNA repair pathways to promote repair of DNA damage and normal cell growth.
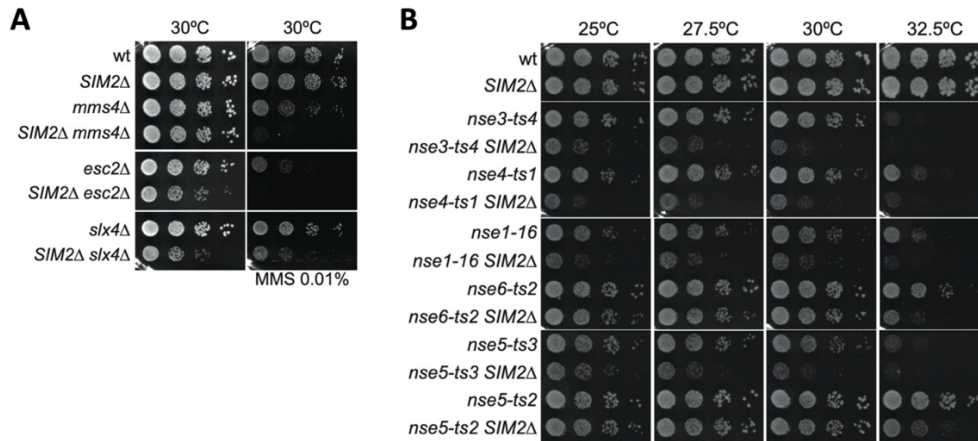
Figure CIII. 7. Analysis of nse2-SIM2Δ mutants in yeast.

A) Growth test analysis of nse2-SIM2Δ (SIM2Δ) cells in combination with mms4Δ, esc2Δ and slx4Δ; 10-fold serial dilutions of liquid cultures were spotted in YPD in the presence or not of MMS 0.01% and incubated at 30ºC for 48h. **B)** Growth test analysis of nse2-SIM2Δ (SIM2Δ) cells in combination with the indicated Smc5/6 complex alleles; 10-fold serial dilutions of liquid cultures were spotted in YPD and incubated at the indicated temperatures for 48h.

The C-terminal SIM2 of Nse2 fixes SUMO$_B$ to the E2 backside

Our complex structure reveals the presence of a second SUMO$_B$ bound to the backside of Ubc9. In our case, SUMO$_B$ was added during the complex preparation, in contrast to the E3-SUMO$_B$ fusion used in the Siz1 complex (Streich & Lima, 2016). In our structure, SUMO$_B$ displays two different interfaces, one side faces the backside of Ubc9, and the opposite side engages contacts with the C-terminal SIM2 of Nse2 (Figure CIII. 1C). Different studies have observed non-covalent SUMO binding to the E2 backside that was initially associated to the formation of SUMO chains, but it now appears to be necessary in the E3-dependent discharge reaction (Capili & Lima, 2007; Cappadocia, Pichler, & Lima, 2015; Eisenhardt *et al.*, 2015; Knipscheer *et al.*, 2007; Koidl *et al.*, 2016; Streich & Lima, 2016). Like other reported E2-SUMO structures, SUMO$_B$ binds Ubc9 through an interface rich in electrostatic interactions: Asp68 interacts with Arg13 and Arg17 from the α-helix of Ubc9; and Glu90 interacts with His20 and the mainchain oxygen of Gly23 (Figure CIII. 8A). E2 overlapping in the Nse2 and Siz1 complexes exhibits around 2Å SUMO$_B$ displacement, resulting in a contact loss between Asp68 and arginine in the Siz1 complex (more than 5Å apart) (Figure CIII. 8B). Our hypothesis points to the role of SIM2 to anchor SUMO$_B$ to the E2 backside and to contribute to the formation of a full-contact interface.
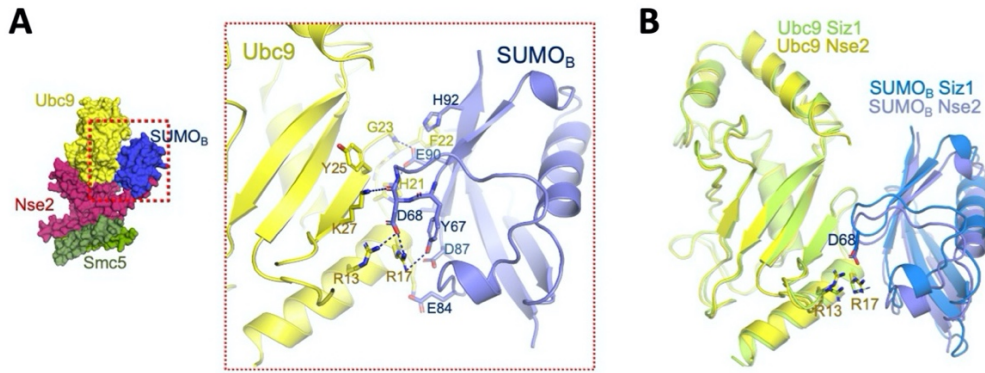
Figure CIII. 8. Interaction between the SUMO_B and the Ubc9.

A) Cartoon representation of the interaction between Ubc9 and SUMO_B (Asp68 SUMO makes electrostatic contacts with Ubc9's Arg13 and Arg17).
B) Structural alignment of Ubc9 in Nse2 and Siz1 complexes (PDB: 5JNE), revealing a displacement of the backside SUMO_B.

E3 Nse2	Added SUMO	K_M (µM)	k_{cat} (s^{-1})	k_{cat}/K_M (µM^{-1}/s^{-1})
WT	WT	2.35 ± 1.1	0.059 ± 0.011	0.025 ± 0.005
Δ4	WT	2.98 ± 1.3	0.017 ± 0.003	0.007 ± 0.0011
Δ4	D68R	3.82 ± 1.7	0.015 ± 0.003	0.005 ± 0.0007
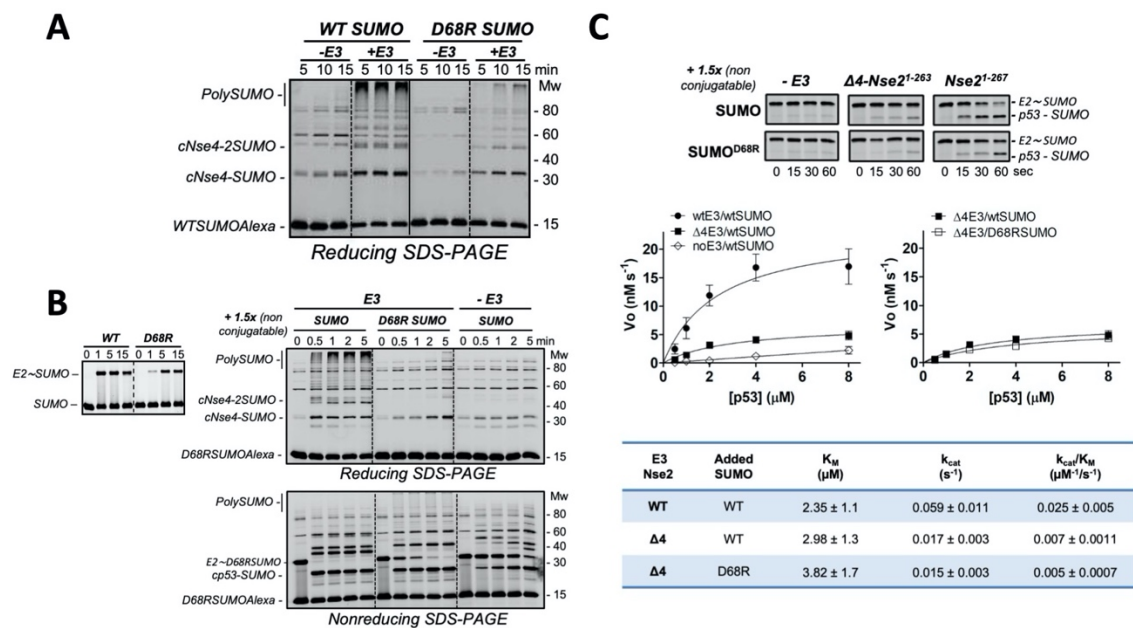
Figure CIII. 9. The SUMO_B backside is fixed by the C-terminal SIM2 of Nse2.

A) Multiple-turnover SUMOylation reactions using of wild type or D68R SUMO in the absence or presence of yeast Nse2/Arm-Smc5 E3 complex at 30 ºC.
B) Single-turnover SUMOylation reactions stopped by EDTA using [D68R]SUMO_D~E2 thioester by yeast Nse2/Arm-Smc5 E3 complex in the presence of 1.5-fold excess non-conjugatable SUMO (WT or D68R) at 30 ºC. [D68R]SUMO is activated by E1 and transferred to the E2 at lower rates as the wild type (left). WTSUMO triggers the E2 discharge on cNse4 or cp53 compared to [D68R]SUMO.
C) Kinetics of discharge reactions of [D68R]SUMO_D~E2 thioester by WT-Nse2 and Δ4C-Nse2 (ΔSIM2) in the presence of non-conjugatable SUMO (WT or D68R) using increasing concentrations of cp53 substrate, (0.5 to 8 µM) at 2 ºC. Representative SDS–PAGE of reactions at 2 µM of cp53. The quantified rate data show mean ± s.d. (n = 3 technical replicates). Kinetics parameters obtained from the curves upon fitting using M-Menten equation in Prism (GraphPad) are shown (bottom).

The E2-SUMO$_B$ interaction can be disrupted by a point mutation in Smt3, D68R, in the E2-interface (Knipscheer *et al.*, 2007). *In vitro* conjugation reactions with Smt3 D68R reveal a significant decrease in conjugation rates, especially for polySUMO chains, either in presence or absence of the E3 ligase **(Figure CIII. 9Figure CIII. 8A)**. Despite the slow rate formation of E2~SUMO thioester with Smt3 D68R **(Figure CIII. 9B, left)**, single turnover discharge reactions with extra WT or Smt3 D68R were performed after stopping the E1 activation with EDTA. End-point reactions show that extra WT Smt3 increases E2 discharge on $_c$Nse4 compared to Smt3-D68R addition, which present comparable conjugation rates in the absence of E3 **(Figure CIII. 9B, upper)**. A similar pattern was seen with $_c$p53, although with WT Smt3 the E2 discharge is faster and completes after 30 seconds, as opposed to the slower rates seen with Smt3-D68R **(Figure CIII. 9B)**. These findings support the idea that the non-covalent E2-SUMO$_B$ interaction improves the discharge reaction.

We next compared the kinetics of WT Nse2 and Δ4C-Nse2 (ΔSIM2) in single turnover SUMO conjugation on $_c$p53 substrate to see if there is a relationship between the C-terminal SIM2 and the SUMO$_B$-E2 interaction. When SIM2 was eliminated, the Nse2 catalytic characteristics were reduced by 4-fold, with K_{cat}/K_M values of 0.025 and 0.007 for WT and ΔSIM2, respectively **(Figure CIII. 9C, left)**. In the absence of E3 did we could not retrieve any detectable metrics. Interestingly, Nse2-ΔSIM2 reactions with extra WT or Smt3D68R gave equal kinetic values **(Figure CIII. 9C, right)**, demonstrating that the addition of SUMO does not improve the discharge reaction in the absence of SIM2. These findings reveal a connection between SIM2 deletion (Δ4-Nse2) and SUMO$_B$ E2 interface disruption (Smt3-D68R), shedding light on the role of SIM2 to anchor SUMO$_B$ to the E2 backside.

SUMO$_B$ in the kinetics of the E2-SUMO discharge reaction

We next carried out a more detailed kinetic analysis by performing single-turnover reactions using this time purified E2~SUMO$_D$ thioester labeled with a fluorophore (Alexafluor488) as substrate, in which the only components are the E2~Smt3 thioester

donor, the Smc5/Nse2 E3 ligase, and the $_c$p53 substrate acceptor **(Figure CIII. 10A)**. The results suggest that the presence of SUMO$_B$ enhances the catalytic constant (K$_{cat}$) by three times while does not affects affinity constants (K$_M$) **(Figure CIII. 10B-C)**. The "optimal" stability of the E2~SUMO thioester is likely achieved upon SUMO$_B$ interaction. Interestingly, the curves of initial velocities vs substrate could only be plotted to a sigmoidal equation (Hill equation), which is characteristic of cooperative behavior in multi-interfaced enzyme kinetics **(Figure CIII. 10B-C)**.

Moreover, this kinetic analysis also shed light at the role of ssDNA, which we have shown in Chapter II to enhance the E3 activity of Nse2 by binding to the Smc5/Arm subunit. In the absence of ssDNA, the curve is shifted to the right **(Figure CIII. 10B)**, resulting in a 4-fold increase in the K$_M$, from 2.7 to 8.5 µM **(Figure CIII. 10C)**. This shift in the curve suggests a positive cooperativity, confirming the stabilization and/or E3 rearrangement upon ssDNA binding (Varejão *et al.*, 2018). Taken together, the kinetic study of the discharge reaction suggests that the SIM2-SUMO$_B$-E2 interaction improves catalysis, while ssDNA binding increases substrate affinity.

Nse2	Add SUMO	DNA	K$_M$' (µM)	K$_{cat}$ (s^{-1})	K$_{cat}$/K$_M$' (µM^{-1}/s^{-1})
1-267	+	+	3.57± 0.40	0.039 ± 0.002	0.011 ± 0.0007
1-267	-	+	2.81 ± 0.51	0.013 ± 0.001	0.004 ± 0.0004
1-267	-	-	8.52 ± 2.77	0.014 ± 0.005	0.001 ± 0.0001
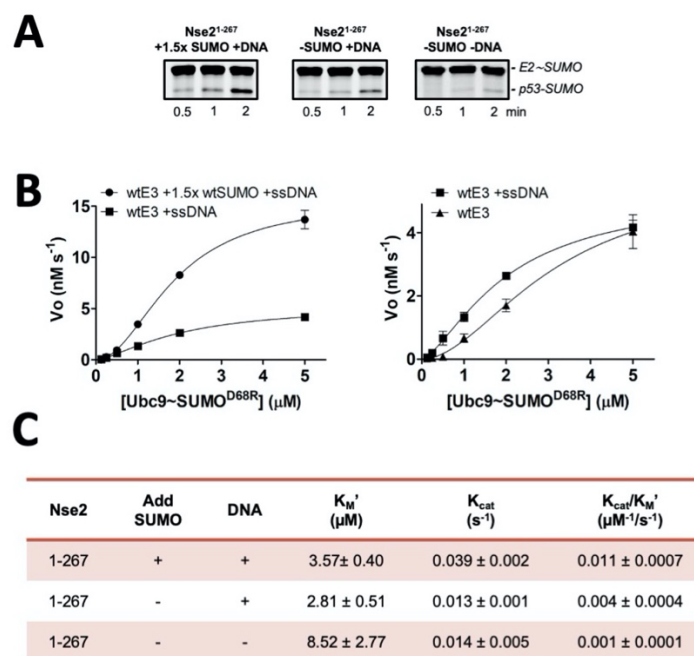
Figure CIII. 10. Effect of SUMO$_B$ backside and ssDNA on E3 activity of Nse2-Arm/Smc5.

A) Representative SDS–PAGE reactions at 1 µM Ubc9~SUMOD68R–Alexa488 thioester.
B) Kinetics of single-turnover reactions using purified E2Ubc9~SUMOD68R–Alexa488 thioester, ± 1.5-fold excess of non-conjugatable SUMOB, ± 50nt ssDNA, cp53, and non-fusion E3 (400 nM) at 30ºC.

C) Kinetics parameters were obtained using Hilll's sigmoidal equation in Prism (GraphPad). The quantified rate data show mean ± s.d. (n = 3 technical replicates).

At last, a fusion between C-terminal tail of Nse2 and $SUMO_B$ was created to explore the effect of a constitutive $SUMO_B$ present at the E2 backside. Gel filtration chromatography revealed that the complex formed between the E2-SUMO mimetic and the fused Nse2-$SUMO_B$ was more stable than WT-Nse2, which did not elute as a single peak (Figure CIII. 11).
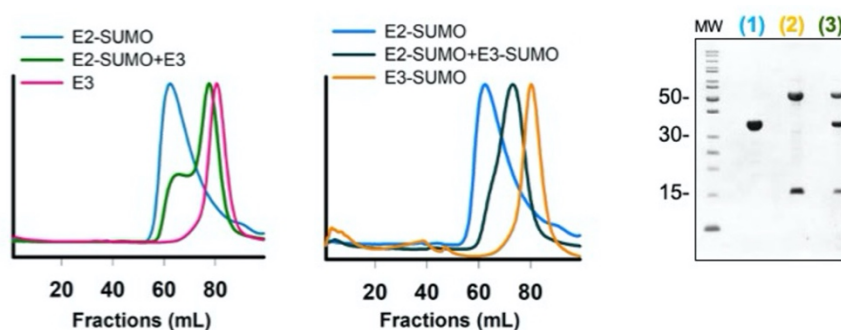
Figure CIII. 11. Purifications of the different elements of the complex in the presence or absence of the fusion Nse2.

Gel filtration chromatography and SDS-PAGE of Nse2 and Nse2-SUMO fused in complex with Ubc9-$SUMO_D$ thioester mimetic.

Nse2-fusion	Add ssDNA	K_M (μM)	K_{cat} (s^{-1})	K_{cat}/K_M (μM^{-1}/s^{-1})
1-267-FLSUMO^{WT}	+	0.92 ± 0.2	1.30 ± 0.13	1.42 ± 0.14
1-267-FLSUMO^{WT}	-	2.33 ± 2.4	0.38 ± 0.26	0.16 ± 0.03
1-267-FLSUMO^{D68R}	+	*ambiguous*	*ambiguous*	*ambiguous*
1-267-Δ18SUMO^{WT}	+	1.65 ± 0.6	1.20 ± 0.26	0.72 ± 0.08
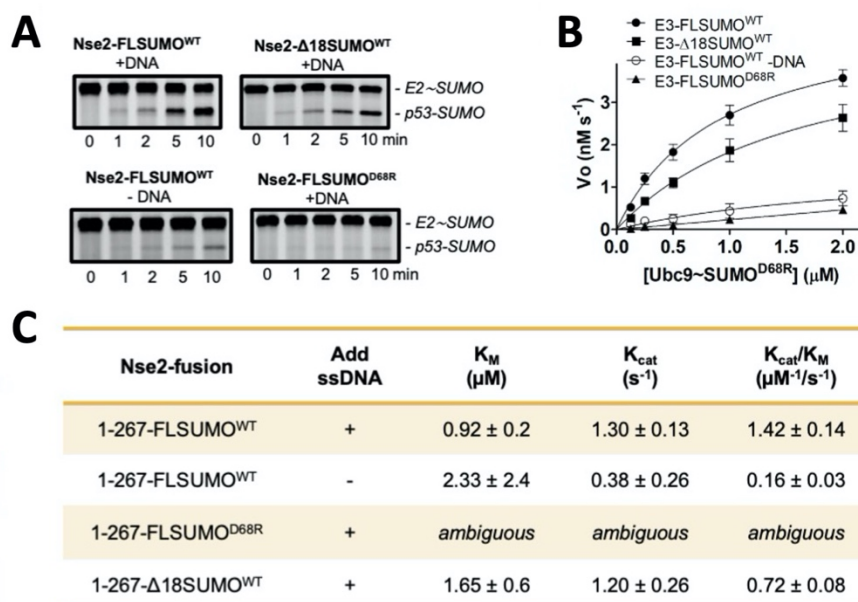
Figure CIII. 12. Analysis of the interaction of Nse2-Smt3 fusion and ssDNA on E3 activity

A) Representative SDS–PAGE reactions at 1 μM Ubc9~SUMO^{D68R}–Alexa488 thioester.
B) Kinetics of single-turnover reactions using purified Ubc9~Smt3^{D68R}–Alexa488 thioester, ± 50nt ssDNA, cp53, and indicated fusion E3-SUMO (4 nM) at 30ºC.

C) Kinetic parameters were obtained using M-Menten's equation in Prism (GraphPad) are shown. The quantified rate data show mean ± s.d. (n = 3 technical replicates).

Single-turnover discharge reactions with the E2~SUMO$_B$ fluorophore substrate displayed a remarkable rate increase with the Nse2-SUMO$_B$ fusion, highlighting the entropic benefit of increasing the local concentration of SUMO$_B$ at the E2 backside. Interestingly, a single D68R point mutation in the fused SUMO$_B$ reduced the rate constants substantially **(Figure CIII. 12)**, emphasizing the importance of the SUMO$_B$ E2 interface in the process. Moreover, SUMO$_B$ flexibility was further restricted by shortening the N-terminal extension (Δ18-Smt3), which also reduced the catalysis **(Figure CIII. 12B-C)**. Finally, the absence of ssDNA reduced catalytic efficiency by 9-fold while raising up the K_M value, as shown in reactions with non-fused Nse2. Interestingly, in contrast to the sigmoidal curves for WT Nse2, all kinetic curves with the Nse2-SUMO$_B$ fusion were fitted to a hyperbolic equation, possibly indicating a loss of cooperativity when the SIM2-SUMO$_B$ interaction is removed from the complex.

Conformational change of Loop-SIM1 upon binding to the E2-SUMO$_D$ donor

Our complex structure reveals a direct interaction between SUMO$_D$ and some elements outside the SP-RING, called the Loop SIM1, which undergoes a significant conformational change (18Å movement of Cα Asp169) **(Figure CIII. 1** and **Figure CIII. 13A)**. In contact with SUMO$_D$, Nse2 SIM1 adopts a SIM-like β-conformation, creating an extended antiparallel β-strand with multiple main chain hydrogen bonds **(Figure CIII. 13B)**. Commonly, in SIM motifs two hydrophobic residues are buried in a SUMO cavity between the α-helix and the edged β-strand. In yeast Nse2 SIM1 polar residues, Asp172 and Gln174, occupy these sites making them unsuitable for SIM binding. However, the presence of additional electrostatic interactions with SUMO$_D$ residues surrounding the SIM1 cavity compensates the binding affinity of Loop SIM1. In particular, Glu170 and Asp171 are engaged with Arg47 and His23, respectively; and SUMO$_D$ Arg55 makes polar interactions with the main chain oxygen of Ile161 and the side chain of Gln174 **(Figure CIII. 13B)**. The poor sequence conservation of Loop SIM1 in Nse2 orthologs **(Figure CIII. 13C)** highlights the role of main chain hydrogen bonding in the SUMO$_D$ interface. Only the acidic region around the SIM1

motif, which interacts with $SUMO_D$, displays some sequence conservation (Figure CIII. 13C).
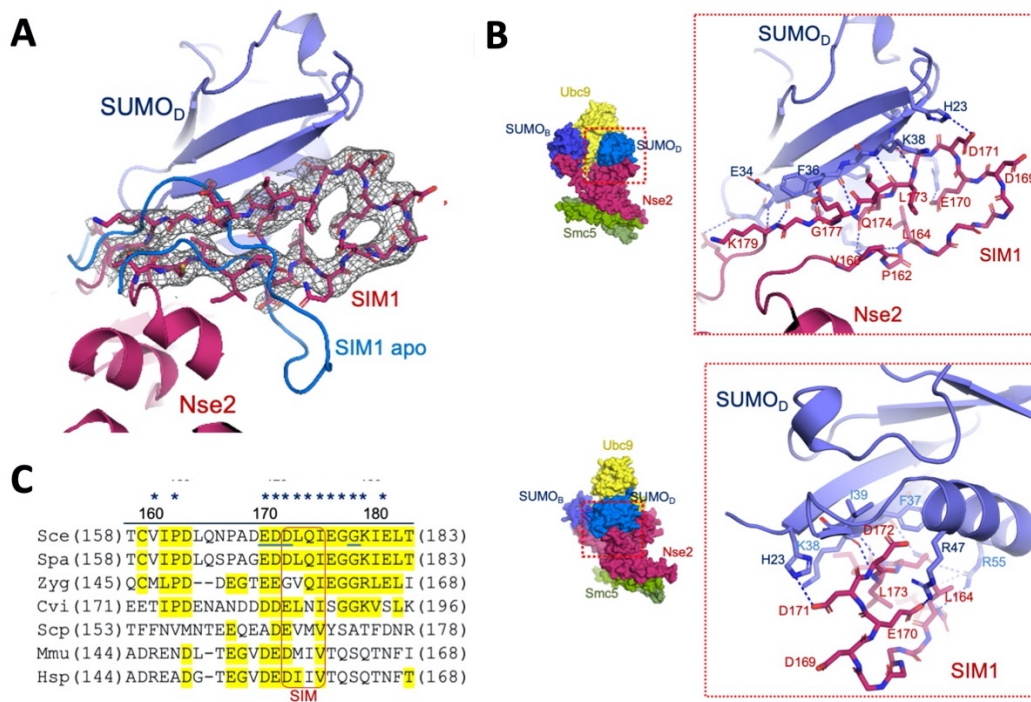
Figure CIII. 13. Conformational change of Loop-SIM1 upon binding to the E2-SUMO$_D$ donor.

A) Structure and electron density maps of Loop SIM1.
B) Cartoon representation of the complex between Loop SIM1 Nse2 (V160 to K179) and SUMO$_D$.
C) Multiple alignment of SIM1 sequences from *Saccharomyces cerevisiae, S. eubayanus, S. paradoxus, Zygos. parabailli, Schizos. pombe, Mus musculus* and *Homo sapiens* (poor conservation except for the acidic region).

To check the importance of those observations, we produced three Nse2 Loop SIM1 mutants: Nse2 ΔLoop1-SIM1 (deletion from Val160 to Gly176), Nse2 G177P point mutant, and Nse2 E170R/D171R/D172R triple mutant. *In vitro* conjugation analysis showed in all cases a strong decrease in SUMO conjugation compared to WT-Nse2, up to 90% reduction for the ΔLoop1-SIM1 deletion mutant (Figure CIII. 14A). These findings indicate the critical role of E3 interfaces outside the SP-RING to fix the E2~SUMO$_D$ thioester in an optimal catalytic orientation, in this case through direct contact of SIM1 with SUMO$_D$ after a significant conformational change.

Also, Torres-Rosell's group introduced SIM1 mutations at the endogenous *NSE2* locus to investigate the role of SIM1 *in vivo*. Thus, they created *nse2* mutants bearing a ΔLoop1-

SIM1 deletion (*nse2-Δ160-176*), a substitution of three conserved negatively charged residues in this loop (Glu170, Asp171, and Asp172) to positively charged Arg residues (*nse2-EDD-RRR*) and a G177P mutation (*nse2-G177P*). All three mutants were sensitive to MMS, as shown in (Figure CIII. 14B), demonstrating that the SIM1 is required for the repair of alkylation damage in budding yeast.
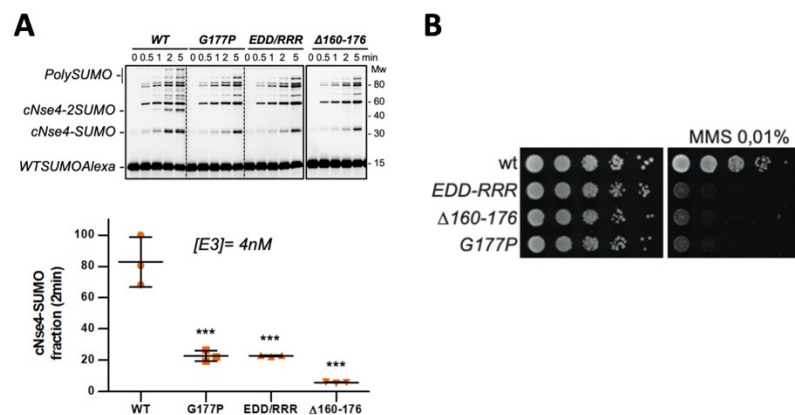
Figure CIII. 14. Activity and viability effects of the different Loop-SIM1 mutation

A) Multiple-turnover SUMOylation reactions of yeast Nse2-Arm/Smc5 complex (wild type and mutants) using cNse4 at 30ºC. Error bars showing that point mutations or deletion of SIM2 reduce E3 activity. Data values represent standard deviation, n = 3 technical replicates. Significance was measured by a two-tailed unpaired t-test relative to wild-type. ***P < 0.001.
B) Growth test analysis of wild type, nse2-EDD-RRR, nse2-Δ160-176 and nse2-G177P cells; 10-fold serial dilutions of liquid cultures were spotted in YPD in the presence or not of MMS 0.01% and incubated at 30 ºC for 60h.

Extensive SP-RING interaction in Nse2 to bind the E2-SUMO$_D$ thioester

We can observe a large interface between the SP-RING domain and Ubc9-SUMO$_D$ in our complex structure. The Ubc9 interface is similar to the canonical interaction of RING-like E3 ligases with E2 enzymes from the SUMO or ubiquitin families. In Ubc9 the interface includes hydrophobic and polar contacts from the α1-helix and two-loop/coil regions, such as Leu4, Gln7, and Arg8 from α1-helix; Pro69 and Ser70 from the β3-β4 loop; and Glu99, Arg104 and Pro105 from a coil after α2-helix (Figure CIII. 15A).

The electrostatic bonds formed between Ubc9's Glu99 and Arg104 with Arg219 and Asp220 from the SP-RING of Nse2, respectively, are noteworthy. On the SP-RING side, the contact is formed by two regions: the loop around Ile186, which is mostly conserved

in E3 RING domains, and the residues near the Zn^{2+} site, Tyr212, Arg219, and Asp220 (Figure CIII. 15A-C).
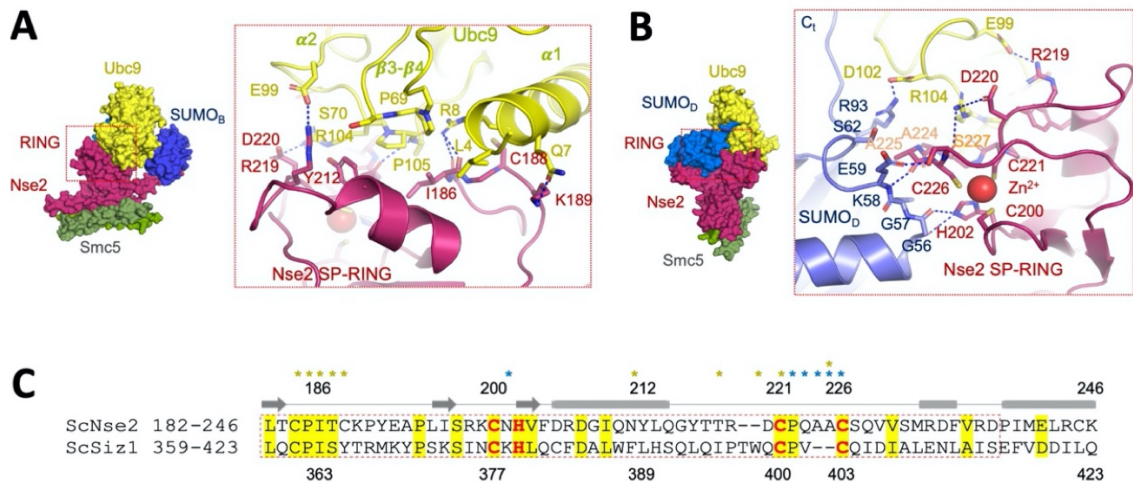
Figure CIII. 15. Extensive SP-RING interaction with the E2-SUMO$_D$ thioester mimetic.

A) Cartoon representation of the complex between SP-RING Nse2 (Ile186 to Ser227) and Ubc9.
B) Cartoon representation of the complex between SP-RING Nse2 (Ile186 to Ser227) and SUMO$_D$ (Gly53 to Arg93).
C) Sequence alignment of SP-RING domains of yeast Nse2 and Siz1. Asterisks indicate residues that make interactions with Ubc9 (yellow) and SUMO$_D$ (blue). Secondary structure elements are depicted above (middle).

In contrast to the contacts observed in Siz1, in Nse2 the SP-RING contacts with SUMO$_D$ through His202 (Zn^{2+} ligand), forming two hydrogen bonds with main chain oxygens of Gly57 and Gln56; and through the loop from Gln223 to Ser227 with SUMO$_D$ surface residues from Lys58 to Ser62 (Figure CIII. 15B and Figure CIII. 16B). The insertion of two alanines (Ala224-Ala225) between the Zn^{2+} ligands Cys221 and Cys226 (Figure CIII. 15B and Figure CIII. 16B). and the hydrogen bonds formed by His202 (Zn^{2+} ligand), are responsible for the various contacts engaged by the Nse2 SP-RING, which is not present in the Siz1 complex but is found in ubiquitin RING domains (Plechanovová et al., 2012; Streich & Lima, 2016). Structural alignment between SP-RING domains (rmsd 1.89 Å, 20% identity) shows an extensive SUMO$_D$ interface area in Nse2, 234 Å^2, compared to Siz1, 168 Å^2 (Figure CIII. 15C and Figure CIII. 16A), which does not engage any hydrogen bond with SUMO$_D$. Globally, Nse2 and Siz1 have developed different interfaces to fix the donor SUMO$_D$ in a "closed" conformation for the E3-dependent discharge reaction, either outside the SP-RING domain (SIM1 and SIM2 interfaces) or by different contacts between

SP-RING and the donor SUMO$_D$ as it is shown in different figures along this chapter (Figure CIII. 1C-D, Figure CIII. 3B, Figure CIII. 13B, Figure CIII. 15A-B).
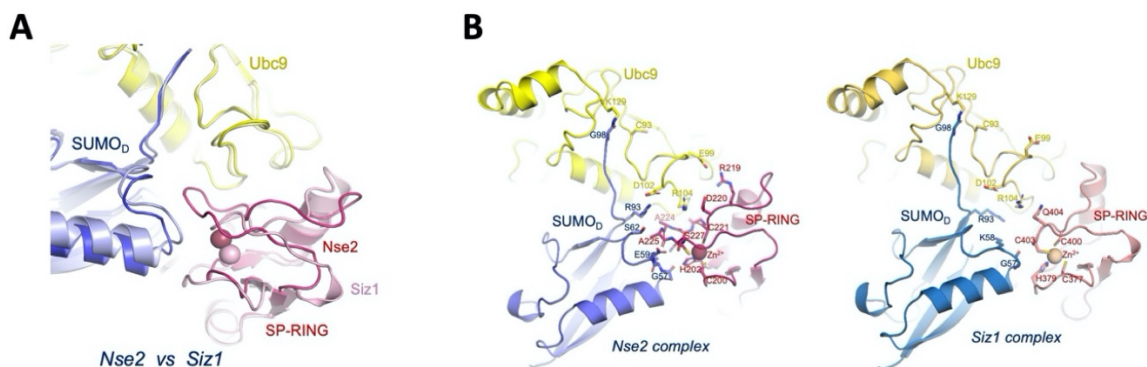
Figure CIII. 16. Comparison between SP-RING domains of Nse2 and Siz1.

A) Structural alignment comparison of SP-RING domains in Nse2 and Siz1 complexes.
B) Binding interfaces of Smt3~Ubc9 and SP-RING domains of yeast Nse2 and Siz1. Side-views of the structures of Nse2/Smc5 (above) and Siz1 (below) in complex with Ubc9~Smt3 thioester mimetic (PDBs 7P47 and 5JNE), revealing that the SP-RING in Nse2 uses similar contacts as ubiquitin RING E3s to bind SUMO$_D$, such interaction is not observed in the SP-RING of Siz1.

Taken together, our findings describe an advance in the understanding of how different SUMO ligases organize the E2~SUMO thioester to enhance the SUMO conjugation efficiency. Finally, the success of our purification and crystallization approach expands the possibility to solve this complex structure in the presence of DNA.
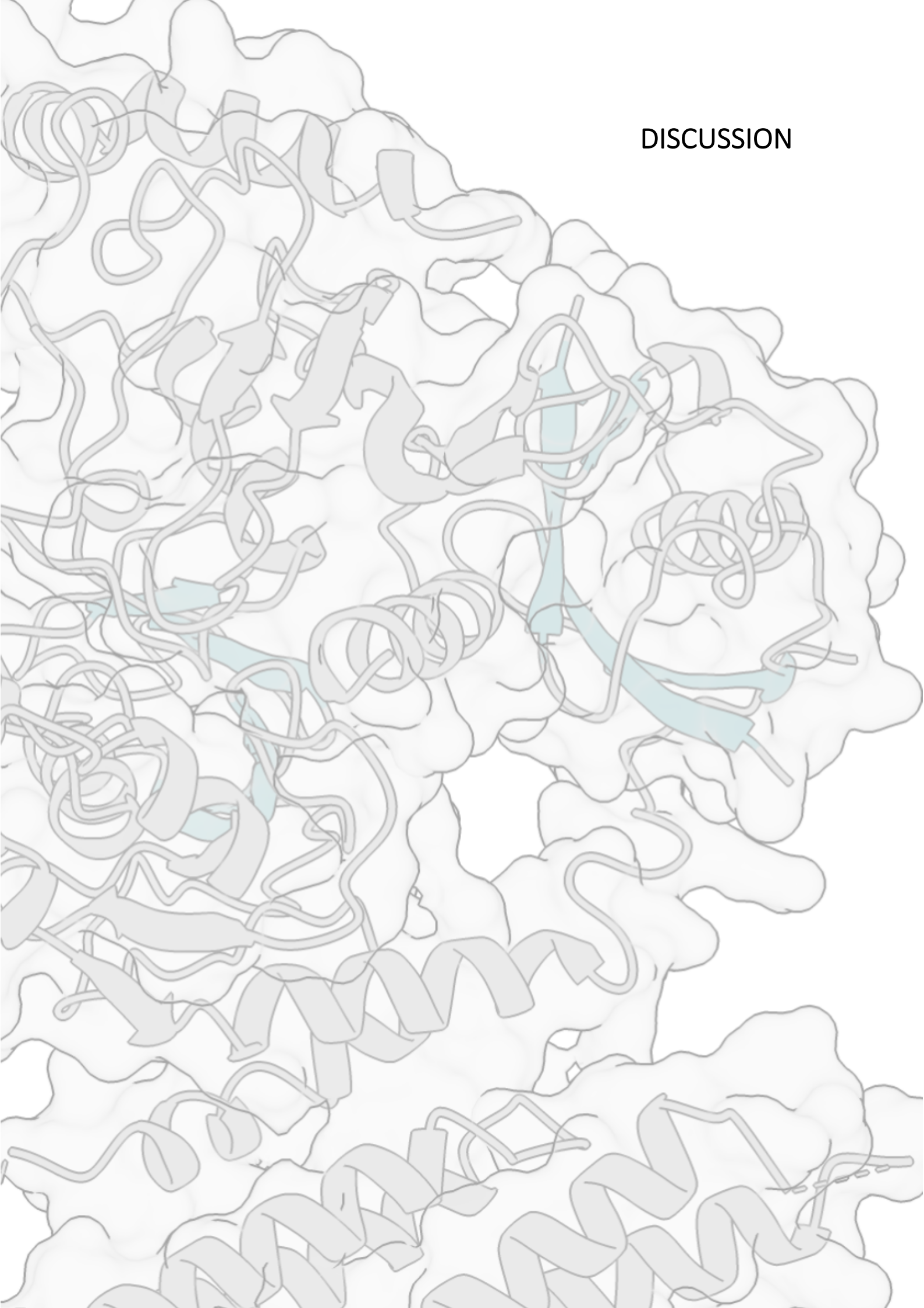
Discussion

The results described in the previous three chapters presented different approaches to the study of the Smc5/6 complex. The work in **Chapter I** provides some structural and functional insights to the human Smc5/6 complex. **Chapter II** demonstrated the activation of E3 ligase of the yeast Smc5/6 complex upon DNA binding. Finally, **Chapter III** revealed structural details of the molecular mechanism of the SUMO E3 ligase of the yeast Smc5/6 complex. Thus, the common thread of all these studies is the analysis of the Smc5/6 complex from the structural and functional aspects, by recombinant Smc5/6 subcomplex reconstruction and by the analysis of the SUMO E3 ligase of Nse2 subunit.

The human Smc5/6 complex has been less studied than the yeast complex. From a structural point of view, less is known about its subunit's organization, only the Nse1 and Nse3 subunits have been crystallized. Thus, our major goal was to study the atomic details of substructures formed by Smc5, Smc6 and Nse2 proteins. Although we have not been able to obtain any structure for the human complex so far, we have been able to produce and purify several constructs that might provide structural results in the future.

The acquired experience prompts us to consider future new construct designs and purification procedures. For the Smc5 and Smc6 constructs that could not be purified, the first approach to be employed would be to design new versions based now on the recent and highly accurate AlphaFold predictor (Jumper *et al.*, 2021). Moreover, recent published papers on Smc5/Smc6 (Adamus *et al.*, 2020; Taschner *et al.*, 2021; Yu *et al.*, 2021) contain crosslinking studies performed between Smc5 and Smc6 proteins that may provide more hints on the interaction points between the coiled coils of both proteins. This will facilitate the design of new protein constructs more stable when forming complexes with other subunits. Interestingly, disruptions in the coiled coil structure are conserved in other SMC proteins, and could have important implications in the structure and functions of the complex (Beasley *et al.*, 2002). On the other hand, combinations with other subunits that we have not been yet obtained, such as Nse1 or Nse3, might also contribute to increase the stability of the different subcomplexes of Smc5/6. Finally,

considering its human source, new expression systems such as the mammalian expression system might be a good option.

In the case of those constructs that have been successfully purified but no good quality crystals have emerged, different purifications protocols could be explored, by changing buffer components such as pH, salt concentration, reduction agents, or even adding glycerol to improve the stability of the protein. It is worth to consider that small changes in the purification of the protein sometimes can cause changes in the crystal packing, resulting in the formation of crystals whose internal interactions are more stable. In addition, the lysine methylation method (Walter *et al.*, 2006), which has been described in **Chapter I**, could enhance the formation of crystals after optimization of the purification.

Besides, to improve the diffraction of crystals, different crystallographic techniques, such as dehydration (Heras & Martin, 2005), can be used. Another example is the use of additive screens in the crystallization buffer, which consists of small compounds added into the buffer condition in which crystals have previously emerged to improve their diffraction quality.

From a functional point of view, we have obtained satisfactory results with the human complex, which also has SUMO E3 ligase activity and functions in a similar manner to its yeast counterpart (described in **Chapter II**). Since SUMO2 conjugation levels increase under stress conditions (Liang *et al.*, 2016; Saitoh & Hinchey, 2000; Wei *et al.*, 2008), it would be interesting in the future to check if human Nse2 has more preference for SUMO2 over SUMO 1 paralog. However, based on a work that relates different mutations on the Nse2 C-terminal with the development of some human pathologies, such as primordial dwarfism, extreme insulin resistance, or gonadal failure (Payne *et al.*, 2014), we tested the effects of amino acid deletion in the C-terminal may have on the SUMO E3 ligase activity. We discovered that while the loss of the last four amino acid residues did not reduce human Nse2 activity, longer deletions of eight and eleven amino acids in the human protein almost abolished its SUMO-E3 ligase activity. Comparing these results with those obtained in **Chapter III**, it appears that human and yeast Nse2 may have a different regulation. In human Nse2, the C-terminal deletion of Nse2 would not be

directly linked to the interaction with SUMO backside but seems instead to be related to structural instability in the C-terminal α-helix of SP-RING domain. It is important to mention that in difference to yeast E3, the C-terminal tail of human Nse2 is populated with several positively charged residues, suggesting the absence of a second SIM2 in this region.

In **Chapter II** we have explored the influence of DNA binding in the Nse2 SUMOylation activity of the Smc5/6 complex from *S. cerevisiae*. Our results revealed the presence of a positively charged patch in the minimal coiled coil region of Smc5 (DNA sensor) that is capable to binding DNA triggering a conformational change of the complex that stimulates of the Nse2 SUMO ligase. The *in vitro* results obtained have been contrasted *in vivo* in the Cell Cycle group of the Universitat de Lleida. Their experiments have confirmed that the positively charged region that recognizes DNA participates in SUMOylation *in vivo* and that this region is necessary for cell viability, consistent with our *in vitro* results.

Based on those results, we propose a new mechanism for the activation of a SUMO ligase *in situ*, which is not simply based on the recruitment of E3 to DNA but such a binding regulates E3 local activity upon the structural rearrangement of the enzyme. Our findings have been broadly accepted by peers in the field, receiving a *News & Views* commenting article on EMBO Journal (Pichler, 2018) and counting 21 Scopus citations so far (Varejão *et al.*, 2018).

Many aspects of chromosome replication, repair, and segregation require post-translational modification by SUMO to maintain the integrity of the genome (Bergink & Jentsch, 2009). Different proteomic studies have identified a large number of SUMO-targeted chromosome-associated proteins, many of them involved in nucleic acid metabolism (Lamoliatte *et al.*, 2014; Tatham *et al.*, 2011). In our case, although it is formally unproven that Smc5/6-Nse2 SUMOylation occurs on chromatin, there are several studies relating Smc5/6-Nse2 binding to different parts of chromosomes where accumulations of ssDNA are observed (Bustard *et al.*, 2012; De Piccoli *et al.*, 2006; Jeppsson *et al.*, 2014; Lindroos *et al.*, 2006; Torres-Rosell *et al.*, 2005). Those findings, together with the results showing a higher affinity of the complex for ssDNA than dsDNA

(Roy *et al*., 2015), suggest that probably chromatin is one of the targets of this SUMO E3 ligase activity. Our results also show that ssDNA has a stronger effect on SUMOylation activation than dsDNA, although both can potentiate it. This predilection to the ssDNA may lead to consider a role Nse2 E3 activity in DNA repair, since DNA damage normally induces the accumulation of ssDNA.

Since Nse2 is not active in the absence of DNA and does not have any DNA binding region indicate that docking to the Smc5/6 complex is essential and has a direct influence on Nse2-dependent SUMOylation. In particular, our analyses demonstrate that a small region at *arm* of Smc5 is sufficient to cause DNA dependence *in vitro*, although we cannot discard that some other parts of the Smc5/6 complex participate in modulating the effect of DNA on E3 ligase activity.

In addition to being required for DNA binding, Smc5 has been described as one intrinsically target of Nse2 SUMOylation (Zhao & Blobel, 2005). Thus, we have employed two different types of substrates throughout this study: the internal lysines of Smc5 and also the C-terminal domain of Nse4 (cNse4), which can be considered an external substrate since it does not interact directly with Smc5 or Nse2. Both substrates showed enhanced SUMOylation levels in the presence of ssDNA or dsDNA binding.

From a structural point of view, we reasoned that the proximity of the DNA sensor in Smc5 to the RING domain of Nse2 should facilitate the activation of SUMO E3 ligase. The results of Trp-intrinsic fluorescence and circular dichroism confirm this idea, indicating a structural remodeling of the Smc5-Nse2 complex upon DNA binding.

Moreover, from a functional perspective, our *in vivo* results in yeast confirm the importance of strategic sites, such as Smc5 residues interacting with DNA (e.g. K743 and K745) and the RING domain of Nse2. Therefore, *in vivo* experiments point that KE and RING mutants compromise the enzymatic activity of the Nse2 SUMO E3 ligase, either by preventing the interaction with the E2 enzyme (in the case RING domain mutants) or by perturbing the association of DNA with the Smc5 DNA sensor (in DNA sensor patch mutants). These mutations could have consequences on the regulation of some Nse2 targets, such as cohesin, the Sgs1-Top3-Rmi1 complex, or the Smc5/6 complex itself.

Despite the exciting results we have discussed, a criticism raised up the possibility of DNA is functioning as a scaffold on which the substrates are bringing closer and more susceptible to the Smc5-Nse2. However, we have reasoned that: (a) even short DNA molecules, structurally impaired from binding to more than one protein at a time, are capable to stimulate Smc5-Nse2; and (b) negatively charged enoxaparin can also elicit SUMOylation and conformational changes, suggesting that electrostatic interactions are the activators of SUMOylation.

The dependence on the ATPase activity is probably twofold: binding to ATP promotes a conformational change in the Smc5-Nse2 molecule that stimulates its SUMO ligase activity (Bermúdez-López *et al.*, 2015); additionally, binding to ATP regulates the association of the Smc5/6 holocomplex with DNA (Kanno *et al.*, 2015), what, according to the results presented here, further enhances its SUMO ligase activity. Therefore, we speculate that the Smc5/6 complex can be first activated by ATP-dependent remodeling of the molecule and loaded onto DNA; this would facilitate contacts between DNA and the DNA sensor patch in Smc5, which would subsequently activate the SUMO E3 ligase activity of Nse2 only in the vicinity of DNA (Figure D. 1).
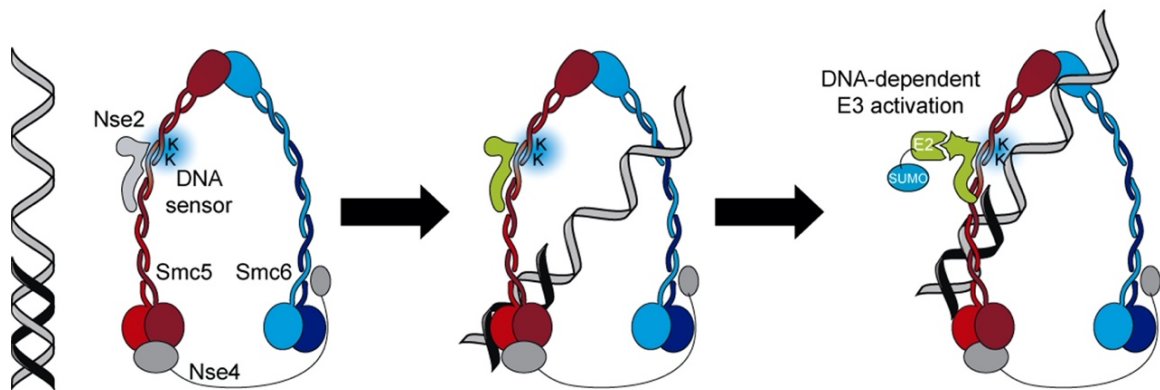
Figure D. 1. Model for ssDNA-dependent activation of the SUMO E3 ligase Nse2.

Scheme of the Smc5/6 complex and its Nse2 and Nse4 subunits, where the Nse1, Nse3, Nse5 and Nse6 subunits are not shown. The ATPase activity of the Smc5/6 complex is initially used to interact with DNA. Upon this interaction, the positively charged patch (DNA sensor) in the Smc5 *arm* domain activates the Nse2 SUMO E3 ligase.

Hence, in **Chapter II** we have revealed a novel mechanism regulating a SUMO E3 ligase activity both by localization, occurring only upon association with DNA, and by the structural rearrangement of the E3 ligase. The enhancement of SUMO E3 ligase activity

only upon direct DNA binding seems to restrict SUMOylation in the vicinity of those Smc5/6-Nse2 molecules engaged on DNA.

Chapter III represents a great advance in the understanding the structural basis of the findings presented in the previous chapter, as it sheds light on the structural reorientations that occur in Nse2 upon binding to the E2 enzyme and to SUMO. Mainly we examine the crystal structure of the Nse2/Arm-Smc5 E2-SUMO$_D$ SUMO$_B$ complex, which we have solved at 3.3 Å.

Moreover, in this study we show the conformational changes that occur in Nse2 upon binding to E2 and the implication of two SUMOs in SUMO ligase activity. Different experiments provide us an expanded perspective of the regulation of SUMO E3 ligase activity of Nse2, which belongs to the SP-RING family of SUMO E3 ligases, from a structural, functional, and *in vivo* aspects.

In the crystal structure, we mainly found four relevant aspects: (I) the interaction of E2 (Ubc9) with SUMO$_B$ located at the E2 backside; (II) the binding between SUMO$_D$ (SUMO donor), Ubc9 and the SP-RING domain of Nse2; and the interactions of the two SIMs, (III) SIM1 interacting with SUMO$_D$ and (IV) SIM2 with SUMO$_B$, as illustrated in Figure D. 2.
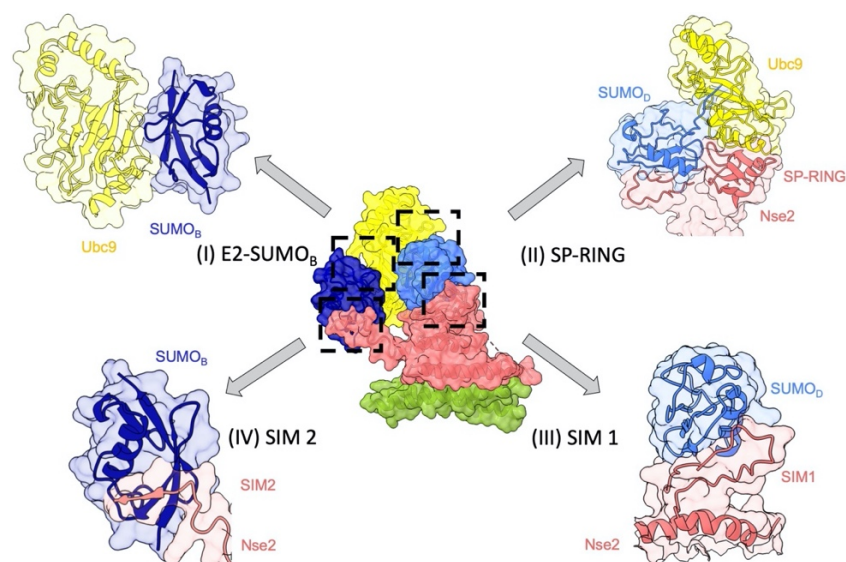
Figure D. 2. Scheme of the multifaced interactions points of the $_{short}$Nse2/Arm-Smc5 E2-SUMO$_D$ SUMO$_B$ complex.

Cartoon representation showing the analyzed points of the complex structure: the E2(Ubc9)-SUMO$_B$ junction, the interaction between Ubc9, SUMO$_D$ and the SP-RING domain of Nse2, and the binding of the two SIMs of Nse2 with their respective SUMOs.

The presence of the backside SUMO$_B$ influences the stability of the E2-E3 complex, particularly by contributing to fix the E2~SUMO$_D$ thioester (Figure D. 2). In the complex structure of the ZNF451 E3 ligase, a second SIM motif binds SUMO$_B$ at the Ubc9 backside and is essential for the E3 ligase activity (Cappadocia *et al*., 2015). In the Siz1 structure, SUMO$_B$ was also observed bound to the E2 backside. But in this instance, the binding was prompted by the use of the Siz1-SUMO$_B$ fusion engineered protein, although biochemical data showed a role of a C-terminal SIM motif in Siz1 to anchor SUMO$_B$ at the E2 backside (Streich & Lima, 2016). In contrast, the complex structure with the IR1-M fragment of RanBP2, tethering to the E2 backside seems to be conducted directly by a short α-helix of the RanBP2 E3 ligase, which binds Ubc9 in a similar location as the backside SUMO$_B$ (Reverter & Lima, 2005), shown in Figure I1. 4. In our primed complex structure with the Nse2 E3 ligase, the electron density maps clearly show a direct interaction of the C-terminal SIM motif of Nse2 (SIM2) at the backside SUMO$_B$ (Figure D. 2-IV).

Interestingly, analysis of our enzymatic experiments using a purified E2~SUMO$_D$ thioester suggest a cooperative mechanism of the discharge reaction (Figure CIII. 10) by the action of several interfaces (Figure D. 2). However, when the interaction with SIM2 is not present, as occurs using the fused Nse2-SUMO$_B$ protein in the enzymatic reactions, the cooperativity in the discharge reaction is lost (Figure CIII. 10). In the future, it would be interesting to check whether the cooperative behavior shown in the kinetics of the discharge reaction, where SIM2 plays a role, has a mechanistic explanation in terms of structural remodeling.

Additionally, our complex structure shows a more extensive interface between the SP-RING domain and Ubc9-SUMO$_D$ than those observed in ubiquitin RING E3 ligases, but we noticed that both share similar contacts, such as the hydrogen bonds between His202 (Zn^{2+} ligand) and the donor SUMO$_D$, (Dou *et al.*, 2012; Plechanovová *et al.*, 2012). Intriguingly such interaction was not observed in the SP-RING of Siz1 (Streich & Lima, 2016).

On the other hand, the interaction of SIM1 with the donor SUMO$_D$ is characteristic of all three types of SUMO E3 ligases, where the closed E2~SUMO conformation is anchored by contacts with the donor SUMO$_D$ utilizing SIM motifs located outside the SP-RING

domain (SIM1). This interaction was first described in RanBP2, and later reported in ZNF451 and Siz1 (Cappadocia *et al.*, 2015; Reverter & Lima, 2005; Streich & Lima, 2016), and in all cases, a SIM-like motif interacts with the same cavity in the SUMO surface. *In vitro* conjugation analysis with the different Nse2 loop-SIM1 mutants demonstrated a significant decrease in SUMO conjugation compared to WT-Nse2. These observations remark the importance of the major conformational change suffered by loop-SIM1 to bind $SUMO_D$ clearly evidenced our primed structure, and its fundamental role in to set the correct orientation of the E2~$SUMO_D$ thioester.

As pointed out in a recent review (Pichler *et al.*, 2017), therefore before our study, the understanding if the hydrophobic patch observed at the C-terminal tail of yeast Nse2 would represent a functional SIM-like motif used by this E3 to fix $SUMO_B$ was unclear. Moreover, back then, in the only available apo structure of Smc5Arm/Nse2 (PDB: 3HTK, (Duan *et al.*, 2009)) this C-terminal seem to be unstructured as it could not be observed in the electron density of that crystal structure. The first evidence that prompted us to investigate this important question was that we observed in our initial *in vitro* experiments that deletion of residues of C-terminal Nse2 drastically diminished the SUMOylation activity. After several efforts, we finally solved our E3-E2-SUMO complex, the electron density maps clearly show a direct interaction of the C-terminal SIM motif of Nse2 (SIM2) with the backside $SUMO_B$, a mechanism comparable to the ones recently reported by other SP-RING E3 ligases (PIAS and Siz1) to fix a second SUMO at the E2 backside (Lussier-Price *et al.*, 2020; Streich & Lima, 2016).

Our structure revealed that the affinity between $SUMO_B$ and SIM2 is achieved by the β-backbone hydrogen bonds and, also by two conserved hydrophobic residues buried in the $SUMO_B$ cavity, as well as by an electrostatic contact between the SIM C-terminal carboxylate and the $SUMO_B$ Arg47. This SIM2-$SUMO_B$ interaction is similar to the structures of SUMO with SIM peptides (Anamika & Spyracopoulos, 2016; Chang *et al.*, 2011; Namanja *et al.*, 2012), such as the structure of SUMO1 bound to a peptide of the C-terminal human PIAS1 (Lussier-Price *et al.*, 2020) displaying a similar location for the hydrophobic side chains of positions 1 and 3 of the SIM motif, but with a different C-terminal carboxylate engagement with a SUMO arginine.

Since the C-terminal SIM2 is absent in human Nse2, the effect of the deletion of C-terminal tail on human Nse2 observed in a human syndrome, mentioned in **Chapter I**, seems to rely on the impact in the structural stability of the complex instead of its SUMOylation activity (Payne *et al.*, 2014), raising the question on how Nse2 is regulated in humans.

Recent low-resolution cryoEM structures and MS analysis revealed the presence of different structural conformations of the Smc5/6 complex, one exhibiting a rod shape stabilized by the interaction between two *arm* domains of Smc5 and Smc6, and another exhibiting a O-ring shape, probably caused by the action of DNA-binding that modulates ATP hydrolysis, which leads both coiled coils to become apart (Gutierrez-Escribano *et al.*, 2020; Serrano *et al.*, 2020; Taschner *et al.*, 2021). In such scenario, other possible regulatory mechanisms for the SUMO E3 ligase activity of Nse2 could be envisaged, in which, after remodeling, other subunits within the complex might communicate with Nse2 to regulate the E3 activity (Bermúdez-López *et al.*, 2015). Yeast two hybrid experiments have shown that the Nse5 subunit in the Smc5/6 complex interacts, through SIM-like motifs, with several members of the SUMO pathway, including the PIAS family Siz1 and Siz2 E3 SUMO ligases, the Ubc9 E2-conjugating enzyme, and SUMO (Bustard *et al.*, 2016, 2012). Additionally, it has been recently reported that dimer formed by Nse5/Nse6 also interacts Nse2 subunit, which might regulate the SUMO E3 ligase activity (Yu *et al.*, 2021). In a different scenario, another possible regulatory mechanism within the Smc5/6 complex might involve binding of SUMOylated subunits of the Smc5/6 complex to the E2 backside of the E2~$SUMO_D$ thioester, resembling the $SUMO_B$ backside interaction observed in the present structure.

Moreover, the deep kinetic analysis realized on **Chapter III** shed some light on the results presented in **Chapter II** in relation to the enhancement of the SUMO E3 ligase activity of Nse2 by binding to DNA through the Smc5 *arm*, published on Varejão *et al.*, 2018. The experiments showed that ssDNA enhances the affinity either for the fusion Nse2-$SUMO_B$ or WT-Nse2 for the E2~$SUMO_D$ thioester, increasing SUMOylation activity.

In summary, we perceive both **Chapters II** and **III** as an important advance in the understanding of the mechanism of this SUMO E3 ligase. **Chapter II** demonstrates that

Nse2 SUMOylation activation is DNA binding dependent, and **Chapter III** reveals the essential role of two SIMs rearrangements on Nse2 activity (Figure D. 3). It would be very interesting in the future to expand the research presented in **Chapter I** with the human complex, in which the C-terminal SIM2 is not present in Nse2 and other mechanisms of regulation might be present to fix SUMO$_B$ to the E2 backside.
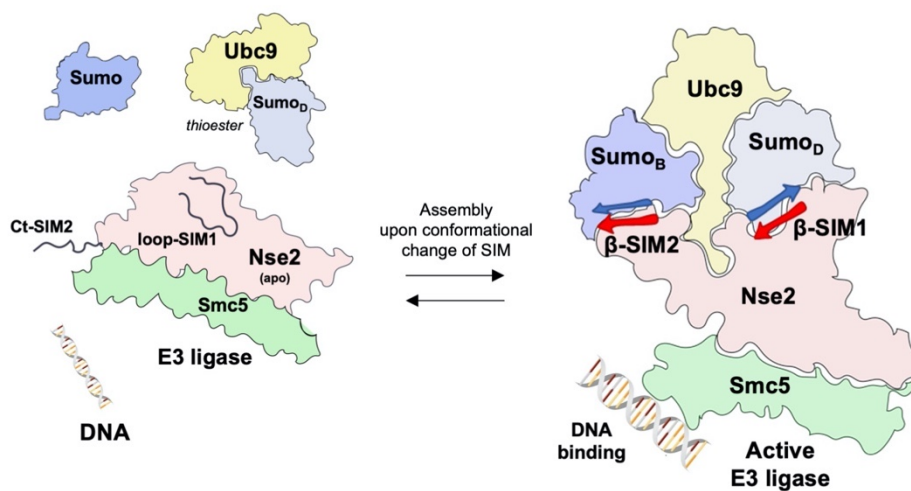
Figure D. 3. Model of Arm-Smc5/Nse2 interaction with E2-SUMO$_D$ thioester and SUMO$_B$ backside.

DNA associates with Smc5 leading to conformational changes of Nse2 SIM1 and SIM2 which clamps E2~SUMO thioester and SUMO backside into the "closed" and active conformation.

Chapter I: Structural approaches into the human Smc5/6 complex

- A good design of the constructs using different prediction software is key to obtain a good result in the purifications.

- Achieving optimal purification results, such as those obtained in the construction of Smc5/6 hinges small or the different Smc5 *arm* constructions with Nse2, to facilitate the formation of crystals.

- Production of a minimal Smc5 Arm-Nse2 human complex that maintains the SUMO E3-ligase activity.

- Longer deletions of eight and eleven amino acids in the C-terminal compromise its SUMO-E3 ligase activity, contrary to the loss of the last four amino acid residues that does not affect the SUMOylation activity.

Chapter II: DNA activates the Nse2/Mms21 SUMO E2 ligase in the Smc5/6 complex

- Nse2 SUMO E3 ligase activity is enhanced by the binding of DNA to a minimal part of Smc5 named *arm*.

- ssDNA has a stronger effect on SUMOylation activation than dsDNA, but there is not significant difference between a short ssDNA (50bp) than a longer ssDNA (5kb).

- A positive patch region of the Smc5 *arm* surface is the responsible of DNA binding.

- The DNA binding to Smc5 *arm* might produce a conformational change of the Nse2 E3 ligase.

- The *in vivo* results obtained by yeast complementation corroborates our *in vitro* experiments with the DNA sensor.

Chapter III: Insights into the structure and mechanism of the Nse2 E3 SUMO ligase

- The crystal structure of Nse2/Smc5 in complex with the E2-SUMO thioester mimetics reveals important structural information about the function of this SUMO E3 ligase.

- The Nse2 C-terminal SIM motif (SIM2) has a fundamental role in the catalytic activity of Nse2, by fixing the $SUMO_B$ to the E2 backside.

- One of the most significant changes in Nse2 in this complex is the conformational change that occurs on the Loop-SIM1, adopting a SIM-like β-conformation to bind $SUMO_D$.

- Structural and functional analysis of this $_{short}$Nse2/Arm-Smc5 E2-$SUMO_D$ $SUMO_B$ complex confirms its behavior as a multi-face enzyme complex.

MOLECULAR BIOLOGY

Oligonucleotides design

Vector culture

ON at 37ºC

DNA extraction by Miniprep Kit

Cloning PCR

Agarose gel+ purification

Double restriction enzyme digestion   1 h 37ºC

1 h 37ºC   Double restriction enzyme digestion

Agarose gel + purification

Agarose gel + purification

CiP (alkaline phosphatase)

30 min 37ºC
5 min 75ºC

T4L ligation

Check concentrations

ON at 16ºC

Transformation to XL1B

Colony PCR

5 ml culture
Glycerol stock
DNA extraction by Miniprep Kit

DNA sequencing

EP 1. Molecular biology

Primer design

For the design of the different constructions of chapter I, we used the prediction program PCOILS (Biegert *et al.*, 2006; Lupas *et al.*, 1991; Zimmermann *et al.*, 2018). This program calculates the probability of an amino acid to be forming a coiled coil structure according to the amino acid it is and according to the amino acids it presents in its vicinity on which it could interact. After determining the positions of the amino acids that form coiled coil structures, we studied the possibility of making several constructions of the same protein, trying to do not disturb the stability and the structure of the complex, in order to obtain stable fragments with high probabilities of crystallization. Once we have decided which constructions we wanted to create, we designed the oligonucleotides for each of them.

All the oligonucleotides used on the three chapters throughout this thesis, are resumed on Table EP.1, Table EP. 2 and Table EP. 3, respectively.

Amplification PCR

To obtain the different constructions, a PCR with the appropriate primers on commercial plasmids with the full-length cDNA sequences of our proteins were carried out. To perform the PCR, the Phusion High-Fidelity DNA Polymerase (Thermo Scientific) was used, and the elongation time and Tm were determined for each fragment and oligonucleotides. Finally, the PCR results was confirmed on an 1% agarose gel (w/v).

Mutagenesis PCR

For the obtention of the different mutants, we used an adaptation of QuikChange Site-Directed Mutagenesis protocol. We elongated the DNA template with the proper mutation we have designed. We used the Phusion High-Fidelity DNA Polymerase (Thermo Scientific), and we checked the result of the mutagenesis by 1% agarose gel (w/v). The result of the PCR has been treated with 1 µL of DpnI to digest the methylated DNA meaning the template DNA will be eliminated. It will continue with a regular *E. coli* transformation.

Table EP. 1. Table of the different oligonucleotides used on Chapter I.

Name	Characteristics	Sequence (5'-3')
H. sapiens Smc5		
Smc5 FL	Forward (BamHI)	CGCGGGATCCGCGACTCCGAGCAAGAAGACGTC
	Reverse (NotI)	GCAGCGGCCGCTCAAGAAGGTTGAGTGAATGTAATACG
Smc5 Hinges small	Forward (BamHI)	CGCGGGATCCCAGAGGAGAATAGGTAATACC
	Reverse (NotI)	GCAGCGGCCGCTCAGGTTTTTCTCTCAAGAAGCTCC
Smc5 Hinges large	Forward (BamHI)	CGCGGGATCCGCAAAAAGGCCATGGGTGG
	Reverse (NotI)	GCAGCGGCCGCTCAACCCAGGTTACATACTTGCC
Smc5 Heads small	Forward (KpnI)	GCCTGGTACCTGCTTCACGGGACTGAATCC
	Reverse (KpnI)	GCCTGGTACCTCGCTTCCGTTCATAGAACC
Smc5 Heads large	Forward (KpnI)	GCCTGGTACCGAACAGGATACTTGCAATCTTG
	Reverse (KpnI)	GCCTGGTACCGCGGGTATTACCTATTCTCCTC
Smc5 Arm	FW (Hinges large)	CGCGGGATCCGCAAAAAGGCCATGGGTGG
	RV (Hinges large)	GCAGCGGCCGCTCAACCCAGGTTACATACTTGCC
	FW (Heads large)	GCCTGGTACCGAACAGGATACTTGCAATCTTG
	RV (Heads large)	GCCTGGTACCGCGGGTATTACCTATTCTCCTC
Smc5 Arm B	Forward I304 (BamHI)	CGCGGGATCCATTCCTATAACATGTCGAATTG
	Reverse V344 (KpnI)	GCCTGGTACCAACATCTTGCTTCTGTTTGC
	Forward T761 (KpnI)	GCCTGGTACCACTTCTTTGCATATACAAAAAGTAG
	Reverse I803 (NotI)	GCAGCGGCCGCTCAGAAATGTTGCTCTGTAAGACG
H. sapiens Smc6		
Smc6 FL	Forward (SalI)	GCCTGTCGACGCCAAAAGAAAGGAAGAAAATTTTTCC
	Reverse (NotI)	GCAGCGGCCGCTTACCTTTGGTCATCATCTTCTTCTTGAG
Smc6 Hinges small	Forward (SalI)	GCCTGTCGACGAACCTGAACGGTTGG
	Reverse (NotI)	GCAGCGGCCGCTTAATAATGTAGTTGGCACC
Smc6 Hinges large	Forward (SalI)	GCCTGTCGACTACATTATGGAAACGAAAG
	Reverse (NotI)	GCAGCGGCCGCTTAGTGCTCCATGATTTCTCC
Smc6 Heads small	Forward (KpnI)	GCCTGGTACCGGAGATCGAGAGGAAATAATG
	Reverse (KpnI)	GCCTGGTACCACCAGCAATACTTTGAAAACG
Smc6 Heads large	Forward (KpnI)	GCCTGGTACCACAAGACCTAAGTTCC
	Reverse (KpnI)	GCCTGGTACCGCCATGTTCTTCTTTGTCC
H. sapiens Nse2		
Nse2 FL	Forward (NdeI)	CGCGCCATATGCCAGGACGTTCCAGTTCAAATTC
	Reverse (BamHI)	CGCGGGATCCTTACTCGGAATGACGATGTCTTTTCTTG
Nse2 Δ11	Forward	GAAGGGCAATTGAGTAACATAACAAGAAAAG
	Reverse	CTTTTCTTGTTATGTTACTCAATTGCCCTTC
Nse2 Δ8	Forward	GAGAACCATAACTAGAAAAGACATCG
	Reverse	CGATGTCTTTTCTAGTTATGGTTCTC
Nse2 Δ4	Forward	CAAGAAAAGACATTGACATTCCGAGTAG
	Reverse	CTACTCGGAATGTCAATGTCTTTTCTTG

Table EP. 2. Table of the different oligonucleotides used on Chapter II.

Primers Chapter II

Name	Characteristics	Sequence (5'-3')
Smc5		
Smc5 △Hinge	Forward	CTAGGTACCTCTCAAAAGATTAAAGATATTGATGATC
	Reverse	ACGCGGATCCTCCTCTATAATATTCGTTCTGG
Smc5 △Head	Forward	CGCGGGATCCAAGAAGACTTTGGAAAATCAGGTG
	Reverse	GCCTGTCGACAGGAGTGTCTCTCATTTCTTTTACG
Smc5 Arm	Forward	CGCGGGATCCGATAAAAAACCATTTGC
	Reverse	GCCTGTCGACTTATTGGCTCTTCAAATCAGCTTC
Smc5 Arm K333E	Forward	GAGTTCCTGGAAGCAAAAG
	Reverse	CTTTTGCTTCCAGGAACTC
Smc5 Arm K337E	Forward	GCAAAAGAAGAGATCAACG
	Reverse	CGTTGATCTCTTCTTTTGC
Smc5 Arm K344E	Forward	CGAAATCTTCGAAGAATTAAATACTATTAGGG
	Reverse	CCCTAATAGTATTTAATTCTTCGAAGATTTCG
Smc5 Arm K743E K745E	Forward	CGTATCTCAAGAGATTGAAGATATTGATG
	Reverse	CATCAATATCTTCAATCTCTTGAGATACG
Smc5 Arm K757E	Forward	CAACTATTACTCGAGCAAAGACATTTGC
	Reverse	GCAAATGTCTTTGCTCGAGTAATAGTTG
Smc5 Arm K764E	Forward	CATTTGCTGTCTGAAATGGCCTCTTC
	Reverse	GAAGAGGCCATTTCAGACAGCAAATG
Smc5 Arm K770E	Forward	GGCCTCTTCAATGGAGAGTTTAAAG
	Reverse	CTTTAAACTCTCCATTGAAGAGGCC
Smc5 Arm K777E	Forward	GAATTGTCAGGAGGAGTTAATAAG
	Reverse	CTTATTAACTCCTCCTGACAATTC
Smc5 Arm K743R K745R	Forward	CGTATCTCAAAGGATTAGAGATATTGATG
	Reverse	CATCAATATCTCTAATCCTTTGAGATACG

Name	Characteristics	Sequence (5'-3')
Nse2		
Nse2	Forward	CAGTCTCGAGGCCTTGAACGATAATCCTATACC
	Reverse	GCTGGGATCCTTATAAAACATCGATGGCTTGAC

Name	Characteristics	Sequence (5'-3')
Nse4		
C-term (Ile 246-Asp402)	Forward	GACGGATCCATAGAAAAGAAGCCACG
	Reverse	GCGGCCGCTTAGTCTAAGAATGGTGAAG

Table EP. 3. Table of the different oligonucleotides used on Chapter III.

Name	Characteristics	Sequence (5'-3')
Smc5		
Smc5 Arm	Forward	CGCGGGATCCGATAAAAAACCATTTGC
	Reverse	GCCTGTCGACTTATTGGCTCTTCAAATCAGCTTC
Smc5 Arm T328-K777	Forward	GGACCCATGGGCACTGATGAGTTCCTGAAAGC
	Reverse	GGACCTCGAGTTACTTCTGACAATTCTTTAAAC
Nse2		
Nse2	Forward	CAGTCTCGAGGCCTTGAACGATAATCCTATACC
	Reverse	GCTGGGATCCTTATAAAACATCGATGGCTTGAC
Nse2 △16	Forward	GATCGCCAAGATGAAATAATCTCAGGAACAGG
	Reverse	CCTGTTCCTGAGATTATTTCATCTTGGCGATC
Nse2 △8	Forward	GAACAGGATAAAAGATGAAGTCAAGCCATC
	Reverse	GATGGCTTGACTTCATCTTTTATCCTGTTC
Nse2 △4	Forward	AGTAGTCAAGCCTAGGATGTTTTATGA
	Reverse	TCATAAAACATCCTAGGCTTGACTACT
Nse2 I264A V266A	Forward	AGTAGTCAAGCCGCCGATGCTTTATGACTCGAGCGC
	Reverse	GCGCTCGAGTCATAAAGCATCCGGGGCTTGACTACT
Nse2 I264P	Forward	AGTAGTCAAGCCCCGATGTTTTATGA
	Reverse	TCATAAAACATCGGGGGCTTGACTACT
Nse2 V266R	Forward	CAAGCCATCGATCGTTTATGACTCGAG
	Reverse	CTCGAGTCATAAACGATCGATGGCTTG
Nse2 M250P	Forward	TGTAAGATCGCCAAGCCGAAAGAATCTCAGGAACAG
	Reverse	CTGTTCCTGAGATTCTTTCGGCTTGGCGATCTTACA
△26 Nse2	Forward	GCTGCTCGAGGCCCGAGACTTATCAAATATATATC
Nse2 △83-134	Forward	GGACGGTACCGCAACCATGGTTAATAACACAGATAC
	Reverse	ACGCGGTACCTGAGTTGGATTCCGATTCG
Nse2 S260E	Forward	GAACAGGATAAAAGAGAGAGTCAAGCCATCGAT
	Reverse	ATCGATGGCTTGACTCTCTCTTTTATCCTGTTC
Nse2 S261E	Forward	CAGGATAAAAGAAGTGAGCAAGCCATCGATGTT
	Reverse	AACATCGATGGCTTGCTCACTTCTTTTATCCTG
Nse2 S260E/S261E	Forward	CAGGATAAAAGAGAAGAGCAAGCCATCGATGTT
	Reverse	AACATCGATGGCTTGCTCTTCTCTTTTATCCTG
Nse2-△18Smt3	Reverse (Nse2)	GCTGGGATCCTAAAACATCGATGGCTTGAC
	Forward (Smt3)	GCTGGGATCCCCTGAGACTCACATCAATTTAAAGG
	Reverse (Smt3)	GCTGGGATCCTTAAATCTGTTCTCTGTGAGCCTC
Nse2 △160-176	Forward	GCCTGGTACCGGTGGTAAAATTGAATTGACTTGTCC
	Reverse	GCCTGGTACCTACACAAGTTGGATCATTCCA
Nse2 G177P	Forward	CTACAAATAGAACCCGGGAAAATTGAATTG
	Reverse	CAATTCAATTTTCCCGGGTTCTATTTGTAG
Nse2 E170R/D171R/D172R	Forward	CTGCAAAACCCCGCAGACAGAAGAAGACTGCAGATAGAAGGTGG
	Reverse	CCACCTTCTATCTGCAGTCTTCTTCTGTCTGCGGGGTTTTGCAG
Ubc9		
Ubc9 A129K	Forward	AATCCAAATTCCCCTAAGCAAGAGCCTGCATGG
	Reverse	CCATGCAGGCTCTTGCTTAGGGGAATTTGGATT
Ubc9 K153R	Forward	GTTTTGCTTCAAGCTAGACAGTACTCTAAA
	Reverse	TTTAGAGTACTGTCTAGCTTGAAGCAAAAC
Smt3		
Smt3 K11C	Forward	GTCAATCAAGAAGCTTGCCCAGAGGTCAAGCCAG
	Reverse	CTGGCTTGACCTCTGGGCAAGCTTCTTGATTGAC
Smt3 D68R	Forward	CCTTAAGATTCTTGTACCGCGGTATTAGAATTCAAGC
	Reverse	GCTTGAATTCTAATACCGCGGTACAAGAATCTTAAGG

DNA restriction and ligation

The samples were purified from the agarose gel with the Purification Kit (Thermo Scientific). Then, the DNA fragments have been digested using selected FastDigest[TM] restriction enzymes (Thermo Scientific), following the manufacturer's instructions. The digestion was checked by 1% agarose gel (w/v).

The DNA fragments were ligated with previously digested plasmid by T4 DNA ligase (Thermo Scientific) which was incubated ON at 18°C. The plasmids selected to clone the different parts of the Smc5/6 complex throughout this work were pET28a, pET15b or pCDFDuet, with different antibiotic resistance. The ligation result will be the vector with the insert, forming a plasmid that can be transformed to *E. coli* cells.

Transformation in *Escherichia coli* XL1B strain

The resulting plasmid will be transformed to *Escherichia coli* XL1Blue strain, that is specifically designed for cloning methods. Transformation will be performed using the heat shock protocol, which involves putting 5 µL of plasmid for every 50 µL of cells for 30 minutes on ice. A thermal shock will be performed by incubating one minute at 42°C, and then the cells will be placed on ice for another 3 minutes. After this, 1 ml of LB medium has been added, and incubated for 1 hour at 37°C and 250 rpm for cell growing. We centrifugated for 6 minutes at 6000 x g at 4°C, and then seed an agar plate of LB with the bacteria remaining in the pellet. This plate will have been previously prepared with the necessary antibiotic or antibiotics for resistance selection. Finally, the plate seeded with the cells will be ON at 37°C.

Clone selection and DNA sequencing

To select which colonies are the ones that have our clone of interest, we performed a colony PCR with Thermo Taq polymerase using the T7 oligonucleotides, since all the plasmids used has the T7 tag. A 1% agarose gel (w/v) will be used to check the positive colonies, that will be selected to be confirmed by DNA sequencing.

The positive colonies were incubated ON in a 5ml LB medium at 37°C and 250 rpm. The extraction of plasmid DNA was carried out with the GeneJET Miniprep Kit (Thermo Scientific), following the instructions of the manufacturer. The results were sending to the Servei de Genòmica I Bioinformàtica (UAB) to check the DNA sequence by Sanger sequencing reactions.

PROTEIN EXPRESSION AND PURIFICATION

Transformation to R2 or BL21

Co-transformation to R2 or BL21

5 ml LB preculture

ON at 37ºC

Glicerol stock → 300 ml LB preculture

20 ml culture

ON at 37ºC

2h at 37ºC until $OD_{600} = 0.6$

4 l or 6 l culture

IPTG induction

Expression ON at 20ºC or 3 h at 30ºC
Keep the cell pellet

2h at 37ºC until $OD_{600} = 0.6$

EXPRESSION TEST

Confirmed by 12.5% SDS-PAGE

IPTG induction

Expression ON at 20ºC or 3 h at 30ºC

Keep the cell pellet

PURIFICATION

Metal-Affinity

Size-Exclusion

CHROMATOGRAPHY

Ion-Exchange

Confirmed by 12.5% SDS-PAGE

Protein concentration

CRYSTALLIZATION

EP 2. Protein expression and purification

Transformation in *Escherichia coli* Rosetta 2 strain and expression

The protein expression of all the recombinant proteins were made with His6-tag in *Escherichia coli* Rosetta 2 (DE3) cells (Novagen), and the protocol for transformation is the same heat shock protocol. Rosetta 2 is designed to increase the expression of eukaryotic proteins with codons that aren't often used in *E. coli*, and moreover, it has an additional chloramphenicol resistant that allows to add one additional control to the resistance selection. Co-expression of protein complexes were done by transforming the vector into a R2 cell already containing a vector encoding for another protein. In this way, the same Rosetta 2 cell will contain two vectors for the two proteins with different antibiotic resistances.

Bacterial cultures were grown at 37°C to OD_{600}=0.6, before 0.5 mM IPTG addition. Cultures were then incubated for 4 h at 30°C or for 16 h at 20°C and harvested by centrifugation. The same protocol was followed for expression tests as for large-scale expression.

Expression test

Expression tests are designed to prove and optimize expression conditions, such as time and temperature of the expression, before attempting to do the protein expression and purification on a large scale.

After the induced culture centrifugation, which is normally 20 ml, the remaining pellet is resuspended with 1 mL of 20% Sacarose + 50mM Tris pH8 or 20mM Hepes pH7, depending on the conditions to be tested. Then, 150 µl of 5M NaCl, 1µL of a 10% solution of β-mercaptoethanol 14M, 7.5 µl of 2M Imidazole and 15 µl of 10% IGEPAL (lysis buffer). The cells were disrupted by sonication at 30% amplitude for 40 seconds at 4°C, and a sample of 20 µl is taken which is the Total Extract sample (ET). The remaining sample is centrifuged at 10,000 x g 15 min at 4°C and from the resulting supernatant another 20 µl is obtained to have a sample for the protein gel (Supernatant = SN). Since all the proteins we worked with are soluble proteins, the rest of the supernatant is passed through a

Nickel-Sepharose resin (GEHealthcare) which will be equilibrated with a binding buffer (usually, 20mM Tris pH 8, 0.35 M NaCl, 10 mM Imidazole, 1mM β-mercaptoethanol), where the protein will be bound due to the histidine tag. After successive washes with the ligation buffer, to elute the protein from the nickel resin we will add a similar buffer to the previous one but increasing the Imidazole concentration up to 0.3M. Since Imidazole has a higher affinity for Nickel than His-tags, it will compete with them for binding to the column, causing the proteins to elute. At this point we take the last sample, corresponding to the peak (PK) where the protein is found in higher concentration and partially purified. The three samples obtained (Total Extract or ET, Supernatant or SN and Peak or PK) are tested on a 12.5% SDS-PAGE gel to analyze the results.

Protein expression and purification

In large-scale expression, the amount of culture is adapted to the grade of protein expression assessed in the expression test. After IPTG induction and centrifugation, cell pellets were equilibrated in Lysis Buffer (usually, 20% sucrose, 50 mM Tris pH 8.0, 1 mM 2-mercaptoethanol, 350 mM NaCl, 20 mM imidazole, 0.1% IGEPAL), and cells were disrupted by sonication 40% amplitude for 6 min at 4°C. Cell debris was removed by centrifugation (40,000 g for 15 min at 4°C). Hexa-histidine tagged proteins were purified by metal affinity chromatography using Chelating Sepharose Fast Flow resin (GE Healthcare) and eluted with 20 mM Tris pH 8.0, 350 mM NaCl, 1 mM β-mercaptoethanol, and 280 mM imidazole. Fractions containing the protein were filtered with 0.22μM membrane and further purified by Gel-Filtration or Size Exclusion chromatography (Superdex 200 or Superdex 75 HiLoad; GE Healthcare) followed by ion-exchange chromatography (Resource Q, or S; GE Healthcare), if necessary. The elution fractions were analyzed by 12.5% SDS-PAGE, using *Unstained Protein Ladder* (Thermo Scientific) as a molecular weight marker and stained with Coomasie solution (0.1% Coomassie (w/v), 10% acetic acid (v/v), 40% methanol (v/v)).

A challenging purification was to obtain the crystallized complex in Chapter III. [A129K/K153R]Ubc9-[FL]Smt3 thioester mimetic was prepared according to Streich & Lima, 2016 in a buffer containing 20 mM BIS-TRIS propane (pH 9.5), 50 mM NaCl, 10 mM MgCl2, 0.1% Tween-20, 2 mM ATP, 0.5 μM E1, 100 μM Ubc9[A129K/K153R], and 200 μM Smt3 for 1 h

at 30 °C and purified by Superdex75 equilibrated in 20 mM Tris pH 8.0, 350 mM NaCl and 1 mM BME. Purified sample was dialyzed to decrease salt concentration up to 10 mM. Finally, sample was additionally purified by Resource Q equilibrate in the same buffer without salt, Ubc9-thioester mimetic was eluted using a 0-400 mM NaCl gradient. In parallel, purification of the $_{short}$Nse2/Arm-Smc5 and the additional $^{\Delta N18}$Smt3 were conducted in a standard way, by metal affinity chromatography, Gel-Filtration chromatography and ion-exchange chromatography. Purified $_{short}$Nse2/Arm-Smc5, $^{\Delta N18}$Smt3, and $^{A129K/K153R}$Ubc9-^{FL}Smt3 thioester mimetic were mixed in equimolar concentrations (~7 μM of each protein) in 20 mM Tris-HCl (pH 8.0) containing 100 mM NaCl and 1 mM BME and concentrated until a suitable concentration for crystallization. The results were confirmed by 12.5% SDS-PAGE at each step of the process.

Another challenging purification of Chapter III was the Ubc9^{K153R}~Smt3$^{K11C/D68R}$-Alexa488 thioester purification. Ubc9^{K153R}~Smt3$^{K11C/D68R}$-Alexa488 thioester was formed and purified as described by Streich & Lima, 2016. Briefly, the reaction mixture contained 20 mM HEPES (pH 7.5), 50 mM NaCl, 10 mM MgCl2, 0.1% Tween-20, 2 mM ATP, 0.4 mM DTT, 11 μM E1, 220 μM Ubc9^{K153R}, and 100 μM Smt3$^{K11C/D68R}$-Alexa488 was incubated for 5 min at 30°C and purified by Superdex75 equilibrated in 50 mM NaCitrate pH 5.5, 200 mM NaCl, 5% glycerol, concentrated up to 30 μM and stored at −80°C before use.

Protein concentration

Protein concentration is a key step to achieve a good result in crystallography, as well as an important variable to take into consideration for the improvement of a result. The samples have been concentrated with different Centricon (Millipore) adapted to the size and volume of the sample are used. The sample concentration has been determined with Coomassie Brilliant Blue using the Bradford assay at OD$_{595}$.

EP 3. Proteomic assays and crystallization

Crystallization

Crystallization experiments has been conducted using two main techniques with two different types of plates: the sitting-drop method and the hanging drop method.

The sitting-drop method was used to perform the condition screening, using 96-wells plates with different commercial conditions suitable for protein crystallization. The screen conditions tested throughout this work in the different crystallization experiments were Clear Strategy^{TM}, JCSG-*plus*^{TM}, PACT *premier*^{TM}, ProPlex^{TM} and Structure Screen 1+2 from Molecular Dimensions. 96-wells plates were prepared using the automated robotic Phoenix nano-dispenser (RIGAKU) system, stored at two different temperatures (4°C and 18°C) and checked two times a week to follow crystal formation.

The hanging-drop method has been used to optimize the crystals and increase their size once they have appeared in the sitting drop plates, using a 24-well plate that allows to increase the volume of the crystallization drops. In this plate the conditions in which the crystals have been obtained in the sitting plate are replicated, being able to add small modifications in its components (such as varying pH or salt concentration) to try to obtain better crystals and improve its diffraction. After its preparation, the 24-well plates were stored at two different temperatures (4°C and 18°C) and checked two times a week to follow crystal formation.

To obtain the crystals of the $_{short}$Nse2/Arm-Smc5 E2-SUMO$_D$ SUMO$_B$ complex in Chapter III, the complex was concentrated up to 9 mg/ml (120 μM) and mixed 1:1 ratio with 12% PEG 8000, 0.1 M MES pH 6.5, 0.2 M dimethyl-2-hydroxyethylammoniumpropane sulfonate (NDSB 211), 8% ethylene glycol. Crystals appeared after 3 days using the hanging-drop vapor diffusion method at 18°C. Crystals were cryo-protected in a reservoir buffer containing 20% ethylene glycol and flash frozen in liquid nitrogen prior to diffraction analysis.

Data collection and structure determination

Diffraction data were recorded from cryo-cooled crystals (100°K) at the ALBA synchrotron in Barcelona (BL13-XALOC beamline) (Juanhuix *et al*., 2014). Data were integrated and merged using XDS (Kabsch, 2010) and scaled, reduced, and further analyzed using CCP4 (Winn *et al*., 2011). The crystal from $_{short}$Nse2/Arm-Smc5 E2- SUMO$_D$ SUMO$_B$ complex grown belongs to the P 2_1 2_1 2_1 space group. Phasing and model-building were obtained by molecular replacement using Phaser-MR from PHENIX (Adams *et al*., 2010). Refinements and model rebuilding were performed using PHENIX (Adams *et al*., 2010) and Coot (Emsley, Lohkamp, Scott, & Cowtan, 2010). Figures were generated using PyMOL (http://www.pymol.org). The data-collection and refinement statistics are summarized in Table CIII. 1.

Lysine methylation

The lysine methylation is a method to try to reduce the mobility of flexible parts of the proteins that we want to crystallize. In the case of Smc5/6 hinges small in Chapter I, the method used was Walter *et al*., 2006. The reaction was done using the protein at low concentration (~1 g/L) in HEPES 50mM pH 7.5 with NaCl 250mM and TCEP 1mM. Thus, 20μL of a freshly prepared solution of 1M ABC (dimethylamine-borane complex, Fluka) + 40μL of 1M formaldehyde were added per 1mL of the protein sample, and the reaction was incubated by gently agitating at 4°C for two hours. Then another 20μL of ABC + 40μL of formaldehyde was added and incubated for two hours. Finally, a further 10μL of ABC per milliliter of protein was added and incubates by agitating at 4 °C overnight. As a protocol suggestion, the sample was centrifuged and repurified by Gel-Filtration in Superdex200 equilibrated in 20mM Tris pH 8 with 100mM NaCl and 1mM TCEP, in the case of Smc5/6 hinges small. This sample was also subjected to the crystallization process.

Western blot

For western blotting, samples were loaded onto an 12.5% SDS-PAGE gel. In this case, *PageRuler^TM Plus Prestained Protein Ladder* (Thermo Scientific) was the selected ladder to identify the size of the bands detected in the membrane. After running the SDS-PAGE gel, the proteins were transferred to a PVDF membrane (GH Healthcare) previously

activated with methanol and equilibrated in transfer buffer following manufacturer's instructions. The SDS-PAGE gel was also equilibrated in the transfer buffer. The protein transfer was carried out by a Trans-Blot Semi-Dry transfer cell (BioRad) at 17 V for 30 min for one membrane. Then, membranes were incubated 1 h at room temperature (RT) with Blocking Buffer (PBS + 0.05 % (v/v) Tween20 + 3% (w/v) dry milk). After the blocking time, incubation with the primary antibody is carried out with anti-Sumo1, anti-Sumo2 or anti-T7 antibodies diluted at the indicated concentration in Blocking Buffer for 2 hours at RT or ON at 4°C. Secondary antibodies (anti-IgG, diluted 1:5000 in Blocking Buffer) were incubated during 45 min at RT and used to reveal the membrane by a bioluminescence reaction catalyzed in the presence of a substrate (Luminata Forte, Millipore). Bioluminescence reactions were detected using VersaDoc (BioRad) and analyzed with QuantityOne software (BioRad).

Smt3 labeling with Alexa Fluor488

Mature ^{K11C}Smt3 (wild type and D68R) were fluorescent labeled using Alexa Fluor488 Maleimide C5 according to the manufacturer's instructions (Invitrogen). Protein was diluted in 20 mM HEPES pH 7.2, 50 mM NaCl, 0.5 mM TCEP up to 40 µM. Alexa Fluor488 stock solution was added gently to reach a 20:1 ratio. Mixtures were kept at 4°C by 16 hours. Free probe molecules were removed using PD-10 desalting column (Cytiva), followed by 10x times volume washing by Centricon (MerckMillipore) centrifugation equilibrate on the same HEPES buffer. Proteins were concentrated up to 2 mg/mL and flash frozen prior use.

Multiple-turnover SUMOylation assays

SUMOylation reactions described in Chapter I, II and III were usually performed in a reaction mix containing 40 mM HEPES (pH 7.5), 10 mM $MgCl_2$, 0.2% Tween-20, 50 mM NaCl, 4 mM dithiothreitol, 2 mM ATP, 32 µM SUMO1, SUMO2 or Smt3, 2 µM substrate (as cNse4 C-terminal kleisin domain, Ile246-Asp402), 300 nM Sae1- Sae2 (E1), 200 nM Ubc9 (E2), and the E3.

In Chapter II, the same reactions were also performed in parallel with the addition of DNA substrates (5 kb circular ssDNA, 5 kb circular dsDNA-, 60b-, 50b-, 34b-, and 20b-

oligonucleotides) or enoxaparin at indicated concentrations. The DNA substrates sequences were randomly selected: 25b (ACCGCGCGCTTATTCAACAATGTTG), 34b (GACAGGATCCATGTCTAGTACAGTAATATCAAGG), 50b (TGCCATATTGACAAGACGGCAAAGATGTCCTAGCAATCCATTGGTGATCA), and 60b (CGCGGTCGACGGTTACCCATACGATGTTCCTGACTATGCGGCCTTGAACGATAATCCTAT). Circular single-strand DNA, ΦX174 (5 kb), was purchased from New England Biolabs. pET28a (5 kbp) and pET-DUET-1 (5 kbp) circular double-stranded DNA were purchased from Novagen. Samples were taken in different time intervals and stopped with SDS-Sample loading buffer (0.25 M Tris–HCl buffer pH 6.8, 10% (w/v) SDS, 30% (v/v) glycerol, 0.7 M β-mercaptoethanol, and 0.05% bromophenol blue). For dose-dependent experiments (as in Figure CII. 3), increased DNA amounts were added to reaction tubes and aliquots were taken after 60 min and stopped with SDS-Sample loading buffer. Products were verified by SDS-PAGE and visualized after SYPRO Ruby (Invitrogen) staining or by Western blotting with anti-SUMO1 or anti-SUMO2 (Sigma-Aldrich), or anti-T7 (Novagen).

In Chapter III, reactions were performed in a similar way with some modifications. 25 μL of a reaction mix containing 40 mM HEPES pH 7.5, 10 mM $MgCl_2$, 0.2% Tween-20, 25 mM NaCl, 4 mM dithiothreitol, 0.8 μM of ssDNA 50nt, 2 μM mature Smt3[K11C]-Alexa488, 6 μM substrate (cNse4 or cp53), 0.3 μM yeast E1 (Aos1:Uba2ΔC-term1–554), 0.2 μM yeast E2 (WTUbc9) were incubated with 25 μL of filtered purified water plus 4 or 400 nM yeast of the different E3. The reaction was immediately initiated by the addition of 2 mM ATP and conducted at 30°C. Samples were taken at the indicated time points and stopped with a 4X Laemmeli sample buffer with or without BME (BioRad). Reactions using human E1 (Sae1:Sae2), E2 (Ubc9) and mature SUMO1[S9C/C52A]-Alexa488 were also carried out under similar conditions.

Single-turnover SUMOylation assays

Single turnover experiment was performed as described (Yunus & Lima, 2005) with minor changes. In Chapter II, the E2-thioester was formed in a reaction mix that includes 20 mM HEPES (pH 7.5), 50 mM NaCl, 10 mM $MgCl_2$, 0.1% Tween-20, 400 nM DTT, 100 nM Sae1-Sae2 (E1), 1 μM Ubc9 (E2), and 500 nM of (Alexa488)-labeled SUMO1 or SUMO2. The

reaction was initiated by the addition of 1 µM ATP and was incubated at 30°C for up to 15 min. In Chapter III, the reaction was performed with similar changes. The E2-thioester was formed in a reaction mix that includes 20 mM HEPES (pH 7.5), 50 mM NaCl, 10 mM MgCl2, 0.1% Tween-20, 0.1 mM DTT, 0.2 µM yeast E1, 2 µM yeast E2 (Ubc9^{K153R}), and 2 µM Smt3$^{K11C/D68R}$-Alexa488. The reaction was initiated by the addition of 0.5 mM ATP and was incubated at 30°C for up to 5 min. In both cases, the reaction was quenched with the addition of 5 mM EDTA.

To follow the thioester transfer mediated by the E3, we added to the reactions 1.25 µM of the E3 and 2 µM of substrate in the absence or presence of 0.8 µM of 50b oligonucleotide, in the experiments of Chapter II. On the single turnover SUMOylations assays of Chapter III, to follow the thioester transfer mediated by the E3, 25 µl of formed Ubc9^{K153R}~Smt3$^{K11C/D68R}$-Alexa488 thioester solution were diluted with 25 µl water, and supplemented with, 0.8 µM ssDNA 50nt, 1.5 µM extra non-labeled Smt3 (wild type or D68R), 8 µM of cNse4 or cp53, and 400 nM wild type E3 ($^{1-267}$Nse2/Arm-Smc5$^{309-815}$). Reactions were incubated at 30°C and samples were taken at indicated time points after the addition of the E3. Additionally, to follow the kinetics of thioester discharge induced by the E3 (wild type and Δ4), 15 µL of formed Ubc9^{K153R}~Smt3$^{K11C/D68R}$-Alexa488 thioester solution were diluted with 15 µL water, and supplemented with, 0.8 µM ssDNA 50nt, 1.5 µM extra non-labeled Smt3 (wild type or D68R) in the presence of increasing concentrations of cp53 (0-8 µM), and 400 nM wild type or Δ4 E3 ($^{1-267 \text{ or } 1-263}$Nse2/Arm-Smc5$^{309-815}$). Reactions were performed on ice-bath (2°C).

Samples were taken and mixed with a 4X Laemmeli non-reducing sample buffer (BioRad). Products of the time-course reactions were analyzed by 12.5% SDS-PAGE (in reducing or non-reducing conditions as indicated in the figures legends) and visualized by Alexa488 fluorescence emission in a Molecular Imager Versadoc MP4000 System (BioRad). Curves were fitted with the Michaelis-Menten equation using Prism (GraphPad).

Analysis and quantification of SUMOylation products

Band densitometry was calculated by Quantity One 1-D (Bio-Rad). Reaction rates of SUMOylation of cNse4 were quantified with ImageJ 1.49v software using the built-in gel-

analyzer function (Schneider, Rasband, & Eliceiri, 2012). Briefly, relative band intensities (fraction of SUMOylated protein) were calculated using a graphical method that involves generating lane profile plots, manually delineating peaks of interest, and then integrating peak areas. The calculations were performed at least in three different independent experiments. Data values are mean ± s.e.m.; and n=3 technical replicates. Significance was measured by a two-tailed unpaired t-test relative to wild-type. *P < 0.05, **P < 0.01, ***P < 0.001.

Kinetic curves using purified Ubc9^{K153R}-Smt3$^{K11C/D68R}$-Alexa488 thioester

In Chapter III, to follow the kinetics of thioester discharge mediated by Nse2/Arm-Smc5 constructs (non-fusion and Smt3-fusioned E3), the purified Ubc9^{K153R}-Smt3$^{K11C/D68R}$-Alexa488 thioester was serial diluted in 20 mM NaCitrate pH 5.5, 100 mM NaCl, and 5% glycerol. Then, 10 μL of diluted thioester (ranging from 0.625 – 25 μM) were incubated 40 μL reaction mixture containing 40 mM HEPES pH 7.5, 25 mM NaCl, 0.1% Tween-20, 4 or 400 nM E3, and 32 μM cp53, 0.8 μM ssDNA 50nt. In indicated reactions, 1.5-fold excess of non-conjugatable Smt3 over thioester was added to the mixture. Also, ssDNA was removed in some experiments, as indicated. Reactions were incubated at 30°C and samples were taken and quenched with a 4X Laemmeli non-reducing sample buffer (BioRad). Curves were fitted with Allosteric-Sigmoidal equation using Prism (GraphPad).

Electrophoretic mobility shift assay (EMSA)

Circular 5 kb ssDNA template was used in EMSA reactions as provided by the supplier using a similar protocol reported by Roy et $al.$, 2011. For DNA binding experiments, reaction mixtures contained 10 mM HEPES pH 7.5, DNA substrate (200 ng, 10 nM), and Arm/Smc5-Nse2 (wild-type or mutants) or kleisin domain of Nse4 (cNse4) in a 0- to 4,000-fold molar excess over DNA; molar ratios were indicated on figure legends. After incubation at 30°C for 40 min, the reactions were stopped by addition of an equal volume of 1.6% low melting point (LMP) agarose containing loading buffer (0.6% glycerol, 0.005% bromophenol blue final concentrations). Mixtures were loaded on 0.5% agarose-TAE gels, and the DNA was resolved by electrophoresis at 2.5 V/cm for 19 h at 4°C. DNA bands

were visualized after staining the gel with GelRed (Biotium) and documented by Gel Doc XR System (BioRad). The experiments were performed in triplicate.

Spectroscopic measurements

Circular dichroism (CD) measurements were performed using a Jasco-715 spectropolarimeter. Arm/Smc5-Nse2 (wild-type and mutants) were diluted in 4 mM HEPES pH 7.5 buffer to a final concentration of 3 µM. Circular 5 kb ssDNA was titrated at various ratios, and the contribution of buffer and DNA to the spectra was subtracted for background correction. Spectra were recorded as an average of ten scan accumulations with a scan rate of 200 nm/min, with 0.1 nm steps in a 1-mm path length cuvette at 30°C. Raw data were converted to mean residue ellipticity.

Intrinsic fluorescence spectra were recorded using a Jasco FP- 8200 spectrofluorimeter. Tryptophan emission spectra were obtained by setting the excitation wavelength at 295 nm and collecting emission in the 310–400 nm range. These spectra were quantified as the center of spectral mass (v) according to equation: $v = \Sigma m_i F_i / \Sigma F_i$ where F_i stands for the fluorescence emission at a given wavelength (v_i) and the summation is carried out over the range of appreciable values of F (Foguel & Silva, 1994). Arm/Smc5-Nse2 (wild-type and mutants) were diluted to achieve 1 µM in 20 mM HEPES pH 7.5 buffer containing 0, 0.05 or 0.1 M NaCl. In the titration experiments, circular ssDNA (5 kb) was tittered up to 5 nM, and the linear ssDNA (50b) was tittered up to 5 µM. In the measurements with Arm/Smc5-Nse2 mutants, a linear ssDNA (60b) was added to the reaction mixture to a final concentration of 0.2 µM in 20 mM HEPES pH 7.5 buffer. The temperature was maintained at 30°C. Kd were calculated with GraphPad Prism4 using ligand binding mode with triplicates.

Analysis of conformational changes

ΔMRE at 222 nm (%) induced by 5 kb circular ssDNA was quantified by ligand titration until signal change achieved saturation, which was assumed to displays 100% of change. Reactions for wild-type protein were performed in three different independent experiments, and data values are mean ± s.d.

ΔCM(%) of fluorescence in the presence of 60b linear ssDNA was quantified by calculating the difference between the Center of Mass of the samples (wild type and mutants) before and after addition of a DNA concentration able to induce half of transitions seen in titration experiments using wild-type protein ($D_{1/2}$=4 nm). This value was considered as 100% of change. Reactions were performed in three different independent experiments. Data values are mean ± s.d. and n = 3 technical replicates. Significance was measured by a two-tailed unpaired t-test relative to wild-type. ****P < 0.0001.
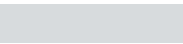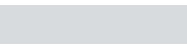
Varejão, N., Ibars, E., **Lascorz, J.**, Colomina, N., Torres-Rosell, J., & Reverter, D. (2018). DNA activates the Nse 2/Mms 21 SUMO E3 ligase in the Smc 5/6 complex. *The EMBO Journal*, *37*(12), e98306. https://doi.org/10.15252/embj.201798306

Gil-Garcia, M., Bano-Polo, M., Varejão, N., Jamroz, M., Kuriata, A., Díaz-Caballero, M., **Lascorz, J.**, Morel, B., Navarro, S., Reverter, D., Kmiecik, S., & Ventura, S. (2018). Combining structural aggregation propensity and stability predictions to redesign protein solubility. *Molecular pharmaceutics*, *15*(9), 3846-3859. https://doi.org/10.1021/acs.molpharmaceut.8b00341

Varejão, N., **Lascorz, J.**, Li, Y., & Reverter, D. (2020). Molecular mechanisms in SUMO conjugation. *Biochemical Society Transactions*, *48*(1), 123–135. https://doi.org/10.1042/bst20190357

Lascorz, J., Codina-Fabra, J., Reverter, D., & Torres-Rosell, J. (2021). SUMO-SIM interactions: From structure to biological functions. *Seminars in Cell & Developmental Biology*. https://doi.org/10.1016/j.semcdb.2021.11.007

Varejão, N.*, **Lascorz, J.***, Codina-Fabra, J., Bellí, G., Borràs-Gas, H., Torres-Rosell, J., & Reverter, D. (2021). Structural basis for the E3 ligase activity enhancement of yeast Nse2 by SUMO-interacting motifs. *Nature Communications, 12*(1), 7013. https://doi.org/10.1038/s41467-021-27301-9
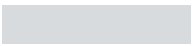
Adams, P. D., Afonine, P. V., Bunkóczi, G., Chen, V. B., Davis, I. W., Echols, N., … Zwart, P. H. (2010). PHENIX: A comprehensive Python-based system for macromolecular structure solution. *Acta Crystallographica Section D: Biological Crystallography*, *66*(2), 213–221. https://doi.org/10.1107/S0907444909052925

Adamus, M., Lelkes, E., Potesil, D., Ganji, S. R., Kolesar, P., Zabrady, K., … Palecek, J. J. (2020). Molecular Insights into the Architecture of the Human SMC5/6 Complex. *Journal of Molecular Biology*, *432*(13), 3820–3837. https://doi.org/10.1016/j.jmb.2020.04.024

Almedawar, S., Colomina, N., Bermúdez-López, M., Pociño-Merino, I., & Torres-Rosell, J. (2012). A SUMO-dependent step during establishment of sister chromatid cohesion. *Current Biology*, *22*(17), 1576–1581. https://doi.org/10.1016/j.cub.2012.06.046

Alt, A., Dang, H. Q., Wells, O. S., Polo, L. M., Smith, M. A., McGregor, G. A., … Oliver, A. W. (2017). Specialized interfaces of Smc5/6 control hinge stability and DNA association. *Nature Communications*, *8*. https://doi.org/10.1038/ncomms14011

Ampatzidou, E., Irmisch, A., O'Connell, M. J., & Murray, J. M. (2006). Smc5/6 Is Required for Repair at Collapsed Replication Forks. *Molecular and Cellular Biology*, *26*(24), 9387–9401. https://doi.org/10.1128/mcb.01335-06

Anamika, & Spyracopoulos, L. (2016). Molecular basis for phosphorylation-dependent SUMO recognition by the DNA repair protein RAP80. *Journal of Biological Chemistry*, *291*(9), 4417–4428. https://doi.org/10.1074/jbc.M115.705061

Andrews, E. A., Palecek, J., Sergeant, J., Taylor, E., Lehmann, A. R., & Watts, F. Z. (2005). Nse2, a Component of the Smc5-6 Complex, Is a SUMO Ligase Required for the Response to DNA Damage. *Molecular and Cellular Biology*, *25*(1), 185–196. https://doi.org/10.1128/MCB.25.1.185-196.2005

Barker, P. A., & Salehi, A. (2002). The MAGE proteins: Emerging roles in cell cycle progression, apoptosis, and neurogenetic disease. *Journal of Neuroscience Research*, *67*(6), 705–712. https://doi.org/10.1002/jnr.10160

Beasley, M., Xu, H., Warren, W., & Mckay, M. (2002). Conserved Disruptions in the Predicted Coiled-Coil Domains of Eukaryotic SMC Complexes : Implications for Structure and Function Conserved Disruptions in the Predicted Coiled-Coil Domains of Eukaryotic SMC Complexes : Implications for Structure and Functi. *Genome Research*, 1201–1209. https://doi.org/10.1101/gr107302

Behlke-Steinert, S., Touat-Todeschini, L., Skoufias, D. A., & Margolis, R. L. (2009). SMC5 and MMS21 are required for chromosome cohesion and mitotic progression. *Cell Cycle*, *8*(14), 2211–2218. https://doi.org/10.4161/cc.8.14.8979

Bergink, S., & Jentsch, S. (2009). Principles of ubiquitin and SUMO modifications in DNA repair. *Nature*, *458*(7237), 461–467. https://doi.org/10.1038/nature07963

Bermúdez-López, M., Pociño-Merino, I., Sánchez, H., Bueno, A., Guasch, C., Almedawar, S., … Torres-Rosell, J. (2015). ATPase-Dependent Control of the Mms21 SUMO Ligase during DNA Repair. *PLoS Biology*, *13*(3). https://doi.org/10.1371/journal.pbio.1002089

Bermúdez-López, M., Villoria, M. T., Esteras, M., Jarmuz, A., Torres-Rosell, J., Clemente-Blanco, A., & Aragon, L. (2016). Sgs1's roles in DNA end resection, HJ dissolution, and crossover suppression require a two-step SUMO regulation dependent on Smc5/6. *Genes and Development*, *30*(11), 1339–1356. https://doi.org/10.1101/gad.278275.116

Berndsen, C. E., Wiener, R., Yu, I. W., Ringel, A. E., & Wolberger, C. (2013). A conserved asparagine has a structural role in ubiquitin-conjugating enzymes. *Nature Chemical Biology*, *9*(3), 154–156. https://doi.org/10.1038/nchembio.1159

Berndsen, C. E., & Wolberger, C. (2014). New insights into ubiquitin E3 ligase mechanism. *Nature Structural and Molecular Biology*, *21*(4), 301–307. https://doi.org/10.1038/nsmb.2780

Bernier-Villamor, V., Sampson, D. A., Matunis, M. J., & Lima, C. D. (2002). Structural basis for E2-mediated SUMO conjugation revealed by a complex between ubiquitin-conjugating enzyme Ubc9 and RanGAP1. *Cell*, *108*(3), 345–356. https://doi.org/10.1016/S0092-8674(02)00630-X

Biegert, A., Mayer, C., Remmert, M., Söding, J., & Lupas, A. N. (2006). The MPI Bioinformatics Toolkit for protein sequence analysis. *Nucleic Acids Research*, *34*(WEB. SERV. ISS.), 335–339. https://doi.org/10.1093/nar/gkl217

Bonner, J. N., Choi, K., Xue, X., Torres, N. P., Szakal, B., Wei, L., … Zhao, X. (2016). Smc5/6 Mediated Sumoylation of the Sgs1-Top3-Rmi1 Complex Promotes Removal of Recombination Intermediates. *Cell Reports*, *16*(2), 368–378. https://doi.org/10.1016/j.celrep.2016.06.015

Branzei, D., Sollier, J., Liberi, G., Zhao, X., Maeda, D., Seki, M., … Foiani, M. (2006). Ubc9- and Mms21-Mediated Sumoylation Counteracts Recombinogenic Events at Damaged Replication Forks. *Cell*, *127*(3), 509–522. https://doi.org/10.1016/j.cell.2006.08.050

Buetow, L., Gabrielsen, M., Anthony, N. G., Dou, H., Patel, A., Aitkenhead, H., … Huang, D. T. (2015). Activation of a Primed RING E3-E2-Ubiquitin Complex by Non-Covalent Ubiquitin. *Molecular Cell*, *58*(2), 297–310. https://doi.org/10.1016/j.molcel.2015.02.017

Bustard, D. E., Ball, L. G., Cobb, J. A., Albuquerque, C. P., Wang, G., Lee, N. S., … Blobel, G. (2016). Non-Smc element 5 (Nse5) of the Smc5/6 complex interacts with SUMO pathway components. *Biology Open*, *5*(6), 777–785. https://doi.org/10.1242/bio.018440

Bustard, D. E., Menolfi, D., Jeppsson, K., Ball, L. G., Dewey, S. C., Shirahige, K., … Cobb, J. A. (2012). During replication stress, non-Smc element 5 (Nse5) is required for Smc5/6 protein complex functionality at stalled forks. *Journal of Biological Chemistry*, *287*(14), 11374–11383. https://doi.org/10.1074/jbc.M111.336263

Capili, A. D., & Lima, C. D. (2007). Structure and Analysis of a Complex between SUMO and Ubc9 Illustrates Features of a Conserved E2-Ubl Interaction. *Journal of Molecular Biology*, *369*(3), 608–618. https://doi.org/10.1016/j.jmb.2007.04.006

Cappadocia, L., & Lima, C. D. (2018). Ubiquitin-like Protein Conjugation: Structures, Chemistry, and Mechanism. *Chemical Reviews*, *118*(3), 889–918. https://doi.org/10.1021/acs.chemrev.6b00737

Cappadocia, L., Pichler, A., & Lima, C. D. (2015). Structural basis for catalytic activation by the human ZNF451 SUMO E3 ligase. *Nature Structural and Molecular Biology*, *22*(12), 968–975. https://doi.org/10.1038/nsmb.3116

Chang, C. C., Naik, M. T., Huang, Y. S., Jeng, J. C., Liao, P. H., Kuo, H. Y., … Shih, H. M. (2011). Structural and Functional Roles of Daxx SIM Phosphorylation in SUMO Paralog-Selective Binding and Apoptosis Modulation. *Molecular Cell*, *42*(1), 62–74. https://doi.org/10.1016/j.molcel.2011.02.022

Chavez, A., George, V., Agrawal, V., & Johnson, F. B. (2010). Sumoylation and the structural maintenance of chromosomes (Smc) 5/6 complex slow senescence through recombination intermediate resolution. *Journal of Biological Chemistry*, *285*(16), 11922–11930. https://doi.org/10.1074/jbc.M109.041277

Cubeñas-Potts, C., & Matunis, M. J. (2013). SUMO: A Multifaceted Modifier of Chromatin Structure and Function. *Developmental Cell*, *24*(1), 1–12. https://doi.org/10.1016/j.devcel.2012.11.020

Cuylen, S., Metz, J., & Haering, C. H. (2011). Condensin structures chromosomal DNA through topological links. *Nature Structural and Molecular Biology*, *18*(8), 894–901. https://doi.org/10.1038/nsmb.2087

De Piccoli, G., Cortes-Ledesma, F., Ira, G., Torres-Rosell, J., Uhle, S., Farmer, S., … Aragón, L. (2006). Smc5-Smc6 mediate DNA double-strand-break repair by promoting sister-chromatid recombination. *Nature Cell Biology*, *8*(9), 1032–1034. https://doi.org/10.1038/ncb1466

Deshaies, R. J., & Joazeiro, C. A. P. (2009). RING Domain E3 Ubiquitin Ligases Key Words. https://doi.org/10.1146/annurev.biochem.78.101807.093809

Dou, H., Buetow, L., Sibbet, G. J., Cameron, K., & Huang, D. T. (2012). BIRC7-E2 ubiquitin conjugate structure reveals the mechanism of ubiquitin transfer by a RING dimer. *Nature Structural and Molecular Biology*, *19*(9), 876–883. https://doi.org/10.1038/nsmb.2379

Doyle, J. M., Gao, J., Wang, J., Yang, M., & Potts, P. R. (2010). MAGE-RING protein complexes comprise a family of E3 ubiquitin ligases. *Molecular Cell*, *39*(6), 963–974. https://doi.org/10.1016/j.molcel.2010.08.029

Droescher, M., Chaugule, V. K., & Pichler, A. (2013). SUMO rules: Regulatory concepts and their implication in neurologic functions. *NeuroMolecular Medicine*, *15*(4), 639–660. https://doi.org/10.1007/s12017-013-8258-6

Duan, X., Sarangi, P., Liu, X., Rangi, G. K., Zhao, X., & Ye, H. (2009). Structural and Functional Insights into the Roles of the Mms21 Subunit of the Smc5/6 Complex. *Molecular Cell*, *35*(5), 657–668. https://doi.org/10.1016/j.molcel.2009.06.032

Duan, X., Yang, Y., Chen, Y. H., Arenz, J., Rangi, G. K., Zhao, X., & Ye, H. (2009). Architecture of the Smc5/6 complex of Saccharomyces cerevisiae reveals a unique interaction between the Nse5-6 subcomplex and the hinge regions of Smc5 and Smc6. *Journal of Biological Chemistry*, *284*, 8507–8515. https://doi.org/10.1074/jbc.M809139200

Eisenhardt, N., Chaugule, V. K., Koidl, S., Droescher, M., Dogan, E., Rettich, J., … Pichler, A. (2015). A new vertebrate SUMO enzyme family reveals insights into SUMO-chain assembly. *Nature Structural and Molecular Biology*, *22*(12), 959–967. https://doi.org/10.1038/nsmb.3114

Emsley, P., Lohkamp, B., Scott, W. G., & Cowtan, K. (2010). Features and development of Coot. *Acta Crystallographica Section D: Biological Crystallography*, *66*(4), 486–501. https://doi.org/10.1107/S0907444910007493

Flotho, A., & Melchior, F. (2013). Sumoylation: A regulatory protein modification in health and disease. *Annual Review of Biochemistry*, *82*, 357–385.

https://doi.org/10.1146/annurev-biochem-061909-093311

Foguel, D., & Silva, J. L. (1994). Cold denaturation of a repressor-operator complex: The role of entropy in protein-DNA recognition. *Proceedings of the National Academy of Sciences of the United States of America*, *91*(17), 8244–8247. https://doi.org/10.1073/pnas.91.17.8244

Fousteri, M. I., & Lehmann, A. R. (2000). A novel SMC protein complex in Schizosaccharomyces pombe contains the Rad18 DNA repair protein. *The EMBO Journal*, *19*(7), 1691–1702. https://doi.org/10.1093/emboj/19.7.1691

García-Rodríguez, N., Wong, R. P., & Ulrich, H. D. (2016). Functions of ubiquitin and SUMO in DNA replication and replication stress. *Frontiers in Genetics*, *7*(MAY), 1–28. https://doi.org/10.3389/fgene.2016.00087

Gutierrez-Escribano, P., Hormeño, S., Madariaga-Marcos, J., Solé-Soler, R., O'Reilly, F. J., Morris, K., … Aragon, L. (2020). Purified Smc5/6 Complex Exhibits DNA Substrate Recognition and Compaction. *Molecular Cell*, *80*(6), 1039-1054.e6. https://doi.org/10.1016/j.molcel.2020.11.012

Haering, C. H., Farcas, A. M., Arumugam, P., Metson, J., & Nasmyth, K. (2008). The cohesin ring concatenates sister DNA molecules. *Nature*, *454*(7202), 297–301. https://doi.org/10.1038/nature07098

Hallett, S. T., Schellenberger, P., Zhou, L., Beuron, F., Morris, E., Murray, J. M., & Oliver, A. W. (2021). Nse5/6 is a negative regulator of the ATPase activity of the Smc5/6 complex. *Nucleic Acids Research*, *49*(8), 4534–4549. https://doi.org/10.1093/nar/gkab234

Hay, R. T. (2005). SUMO: A history of modification. *Molecular Cell*, *18*(1), 1–12. https://doi.org/10.1016/j.molcel.2005.03.012

Hecker, C. M., Rabiller, M., Haglund, K., Bayer, P., & Dikic, I. (2006). Specification of SUMO1- and SUMO2-interacting motifs. *Journal of Biological Chemistry*, *281*(23), 16117–16127. https://doi.org/10.1074/jbc.M512757200

Hendriks, I. A., Lyon, D., Young, C., Jensen, L. J., Vertegaal, A. C. O., & Nielsen, M. L. (2017). Site-specific mapping of the human SUMO proteome reveals co-modification with phosphorylation. *Nature Structural and Molecular Biology*, *24*(3), 325–336. https://doi.org/10.1038/nsmb.3366

Hendriks, I. A., & Vertegaal, A. C. O. (2016). A comprehensive compilation of SUMO proteomics. *Nature Reviews Molecular Cell Biology*, *17*(9), 581–595. https://doi.org/10.1038/nrm.2016.81

Heras, B., & Martin, J. L. (2005). Post-crystallization treatments for improving diffraction quality of protein crystals. *Acta Crystallographica Section D: Biological Crystallography*, *61*(9), 1173–1180. https://doi.org/10.1107/S0907444905019451

Hershko, A., & Ciechanover, A. (1998). The ubiquitin system. *Annual Review of Biochemistry*, *67*, 425–479. https://doi.org/10.1146/annurev.biochem.67.1.425

Hickey, C. M., Wilson, N. R., & Hochstrasser, M. (2012). Function and regulation of SUMO proteases. *Nature Reviews Molecular Cell Biology*, *13*(12), 755–766. https://doi.org/10.1038/nrm3478

Hietakangas, V., Anckar, J., Blomster, H. A., Fujimoto, M., Palvimo, J. J., Nakai, A., & Sistonen, L. (2006). PDSM, a motif for phosphorylation-dependent SUMO modification. *Proceedings of the National Academy of Sciences of the United States of America*, *103*(1), 45–50. https://doi.org/10.1073/pnas.0503698102

Hirano, T. (2006). At the heart of the chromosome: SMC proteins in action. *Nature*

Reviews. Molecular Cell Biology, *7*(5), 311–322. https://doi.org/10.1038/nrm1909

Hirano, T., & Mitchison, T. J. (1994). A heterodimeric coiled-coil protein required for mitotic chromosome condensation in vitro. *Cell*, *79*(3), 449–458. https://doi.org/10.1016/0092-8674(94)90254-2

Ho, C. W., Chen, H. T., & Hwang, J. (2011). UBC9 autosumoylation negatively regulates sumoylation of septins in Saccharomyces cerevisiae. *Journal of Biological Chemistry*, *286*(24), 21826–21834. https://doi.org/10.1074/jbc.M111.234914

Hsieh, Y. L., Kuo, H. Y., Chang, C. C., Naik, M. T., Liao, P. H., Ho, C. C., … Shih, H. M. (2013). Ubc9 acetylation modulates distinct SUMO target modification and hypoxia response. *EMBO Journal*, *32*(6), 791–804. https://doi.org/10.1038/emboj.2013.5

Jacome, A., Gutierrez-Martinez, P., Schiavoni, F., Tenaglia, E., Martinez, P., Rodríguez-Acebes, S., … Fernandez-Capetillo, O. (2015). NSMCE 2 suppresses cancer and aging in mice independently of its SUMO ligase activity. *The EMBO Journal*, *34*(21), 2604–2619. https://doi.org/10.15252/embj.201591829

Jeppsson, K., Kanno, T., Shirahige, K., & Sjögren, C. (2014). The maintenance of chromosome structure: Positioning and functioning of SMC complexes. *Nature Reviews Molecular Cell Biology*. https://doi.org/10.1038/nrm3857

Jo, A., Li, S., Shin, J. W., Zhao, X., & Cho, Y. (2021). Structure Basis for Shaping the Nse4 Protein by the Nse1 and Nse3 Dimer within the Smc5/6 Complex. *Journal of Molecular Biology*, *433*(9), 166910. https://doi.org/10.1016/j.jmb.2021.166910

Johnson, E. S., & Blobel, G. (1997). Ubc9p is the conjugating enzyme for the ubiquitin-like protein Smt3p. *Journal of Biological Chemistry*, *272*(43), 26799–26802. https://doi.org/10.1074/jbc.272.43.26799

Johnson, E. S., & Gupta, A. A. (2001). An E3-like factor that promotes SUMO conjugation to the yeast septins. *Cell*, *106*(6), 735–744. https://doi.org/10.1016/S0092-8674(01)00491-3

Juanhuix, J., Gil-Ortiz, F., Cuní, G., Colldelram, C., Nicolás, J., Lidón, J., … Benach, J. (2014). Developments in optics and performance at BL13-XALOC, the macromolecular crystallography beamline at the Alba Synchrotron. *Journal of Synchrotron Radiation*, *21*(4), 679–689. https://doi.org/10.1107/S160057751400825X

Jumper, J., Evans, R., Pritzel, A., Green, T., Figurnov, M., Ronneberger, O., … Hassabis, D. (2021). Highly accurate protein structure prediction with AlphaFold. *Nature*, *596*(7873), 583–589. https://doi.org/10.1038/s41586-021-03819-2

Kabsch, W. (2010). Integration, scaling, space-group assignment and post-refinement. *Acta Crystallographica Section D: Biological Crystallography*, *66*(2), 133–144. https://doi.org/10.1107/S0907444909047374

Kahyo, T., Nishida, T., & Yasuda, H. (2001). Involvement of PIAS1 in the sumoylation, *8*, 1–6. Retrieved from papers2://publication/uuid/4D74FBCC-37A9-488C-85FA-BD3B9275E62D

Kanno, T., Berta, D. G., & Sjögren, C. (2015). The Smc5/6 Complex Is an ATP-Dependent Intermolecular DNA Linker. *Cell Reports*, *12*(9), 1471–1482. https://doi.org/10.1016/j.celrep.2015.07.048

Kelly, S. M., Jess, T. J., & Price, N. C. (2005). How to study proteins by circular dichroism, *1751*, 119–139. https://doi.org/10.1016/j.bbapap.2005.06.005

Klug, H., Xaver, M., Chaugule, V. K., Koidl, S., Mittler, G., Klein, F., & Pichler, A. (2013). Ubc9 sumoylation controls SUMO chain formation and meiotic synapsis in

saccharomyces cerevisiae. *Molecular Cell*, *50*(5), 625–636. https://doi.org/10.1016/j.molcel.2013.03.027

Knipscheer, P., Flotho, A., Klug, H., Olsen, J. V., van Dijk, W. J., Fish, A., … Pichler, A. (2008). Ubc9 Sumoylation Regulates SUMO Target Discrimination. *Molecular Cell*, *31*(3), 371–382. https://doi.org/10.1016/j.molcel.2008.05.022

Knipscheer, P., Van Dijk, W. J., Olsen, J. V., Mann, M., & Sixma, T. K. (2007). Noncovalent interaction between Ubc9 and SUMO promotes SUMO chain formation. *EMBO Journal*, *26*(11), 2797–2807. https://doi.org/10.1038/sj.emboj.7601711

Koidl, S., Eisenhardt, N., Fatouros, C., Droescher, M., Chaugule, V. K., & Pichler, A. (2016). The SUMO2/3 specific E3 ligase ZNF451-1 regulates PML stability. *International Journal of Biochemistry and Cell Biology*, *79*, 478–487. https://doi.org/10.1016/j.biocel.2016.06.011

Kotaja, N., Karvonen, U., Jänne, O. A., & Palvimo, J. J. (2002). PIAS Proteins Modulate Transcription Factors by Functioning as SUMO-1 Ligases. *Molecular and Cellular Biology*, *22*(14), 5222–5234. https://doi.org/10.1128/mcb.22.14.5222-5234.2002

Lamoliatte, F., Caron, D., Durette, C., Mahrouche, L., Maroui, M. A., Caron-Lizotte, O., … Thibault, P. (2014). Large-scale analysis of lysine SUMOylation by SUMO remnant immunoaffinity profiling. *Nature Communications*, *5*. https://doi.org/10.1038/ncomms6409

Lascorz, J., Codina-Fabra, J., Reverter, D., & Torres-Rosell, J. (2021). SUMO-SIM interactions: From structure to biological functions. *Seminars in Cell & Developmental Biology*. https://doi.org/https://doi.org/10.1016/j.semcdb.2021.11.007

Lehmann, A. R., Walicka, M., Griffiths, D. J., Murray, J. M., Watts, F. Z., McCready, S., & Carr, A. M. (1995). The rad18 gene of Schizosaccharomyces pombe defines a new subgroup of the SMC superfamily involved in DNA repair. *Molecular and Cellular Biology*, *15*(12), 7067–7080. https://doi.org/10.1128/MCB.15.12.7067

Li, S. J., & Hochstrasser, M. (1999). A new protease required for cell-cycle progression in yeast. *Nature*, *398*(6724), 246–251. https://doi.org/10.1038/18457

Liang, Y. C., Lee, C. C., Yao, Y. L., Lai, C. C., Schmitz, M. L., & Yang, W. M. (2016). SUMO5, a novel poly-SUMO isoform, regulates PML nuclear bodies. *Scientific Reports*, *6*, 1–15. https://doi.org/10.1038/srep26509

Lin, D. Y., Huang, Y. S., Jeng, J. C., Kuo, H. Y., Chang, C. C., Chao, T. T., … Shih, H. M. (2006). Role of SUMO-Interacting Motif in Daxx SUMO Modification, Subnuclear Localization, and Repression of Sumoylated Transcription Factors. *Molecular Cell*, *24*(3), 341–354. https://doi.org/10.1016/j.molcel.2006.10.019

Lindroos, H. B., Ström, L., Itoh, T., Katou, Y., Shirahige, K., & Sjögren, C. (2006). Chromosomal Association of the Smc5/6 Complex Reveals that It Functions in Differently Regulated Pathways. *Molecular Cell*, *22*(6), 755–767. https://doi.org/10.1016/j.molcel.2006.05.014

Liu, B., Lois, L. M., & Reverter, D. (2019). Structural insights into SUMO E1–E2 interactions in Arabidopsis uncovers a distinctive platform for securing SUMO conjugation specificity across evolution. *Biochemical Journal*, *476*(14), 2127–2139. https://doi.org/10.1042/BCJ20190232

Lois, L. M., & Lima, C. D. (2005). Structures of the SUMO E1 provide mechanistic insights into SUMO activation and E2 recruitment to E1. *EMBO Journal*, *24*(3), 439–451. https://doi.org/10.1038/sj.emboj.7600552

Losada, A., & Hirano, T. (2005). Dynamic molecular linkers of the genome: The first decade of SMC proteins. *Genes and Development*, *19*(11), 1269–1287. https://doi.org/10.1101/gad.1320505

Lupas, A., Van Dyke, M., & Stock, J. (1991). Predicting coiled coils from protein sequences. *Science*, *252*(5009), 1162–1164. https://doi.org/10.1126/science.252.5009.1162

Lussier-Price, M., Mascle, X. H., Cappadocia, L., Kamada, R., Sakaguchi, K., Wahba, H. M., & Omichinski, J. G. (2020). Characterization of a C-Terminal SUMO-Interacting Motif Present in Select PIAS-Family Proteins. *Structure*, *28*(5), 573-585.e5. https://doi.org/10.1016/j.str.2020.04.002

Matic, I., Schimmel, J., Hendriks, I. A., van Santen, M. A., van de Rijke, F., van Dam, H., … Vertegaal, A. C. O. (2010). Site-Specific Identification of SUMO-2 Targets in Cells Reveals an Inverted SUMOylation Motif and a Hydrophobic Cluster SUMOylation Motif. *Molecular Cell*, *39*(4), 641–652. https://doi.org/10.1016/j.molcel.2010.07.026

McAleenan, A., Cordon-Preciado, V., Clemente-Blanco, A., Liu, I. C., Sen, N., Leonard, J., … Aragón, L. (2012). SUMOylation of the α-kleisin subunit of cohesin is required for DNA damage-induced cohesion. *Current Biology*, *22*(17), 1564–1575. https://doi.org/10.1016/j.cub.2012.06.045

Meulmeester, E., Kunze, M., Hsiao, H. H., Urlaub, H., & Melchior, F. (2008). Mechanism and Consequences for Paralog-Specific Sumoylation of Ubiquitin-Specific Protease 25. *Molecular Cell*, *30*(5), 610–619. https://doi.org/10.1016/j.molcel.2008.03.021

Michaelis, C., Ciosk, R., & Nasmyth, K. (1997). Cohesins: Chromosomal proteins that prevent premature separation of sister chromatids. *Cell*, *91*(1), 35–45. https://doi.org/10.1016/S0092-8674(01)80007-6

Minty, A., Dumont, X., Kaghad, M., & Caput, D. (2000). Covalent modification of p73α by SUMO-1: Two-hybrid screening with p73 identifies novel SUMO-1-interacting proteins and a SUMO-1 interaction motif. *Journal of Biological Chemistry*, *275*(46), 36316–36323. https://doi.org/10.1074/jbc.M004293200

Mohideen, F., Capili, A. D., Bilimoria, P. M., Yamada, T., Bonni, A., & Lima, C. D. (2009). A molecular basis for phosphorylation-dependent SUMO conjugation by the E2 UBC9. *Nature Structural and Molecular Biology*, *16*(9), 945–952. https://doi.org/10.1038/nsmb.1648

Müller, S., Ledl, A., & Schmidt, D. (2004). SUMO: A regulator of gene expression and genome integrity. *Oncogene*, *23*(11 REV. ISS. 1), 1998–2008. https://doi.org/10.1038/sj.onc.1207415

Murray, J. M., & Carr, A. M. (2008). Smc5/6: a link between DNA repair and unidirectional replication? *Nature Reviews. Molecular Cell Biology*, *9*, 177–182. https://doi.org/10.1038/nrm2309

Namanja, A. T., Li, Y. J., Su, Y., Wong, S., Lu, J., Colson, L. T., … Chen, Y. (2012). Insights into high affinity small ubiquitin-like modifier (SUMO) recognition by SUMO-interacting motifs (SIMs) revealed by a combination of NMR and peptide array analysis. *Journal of Biological Chemistry*, *287*(5), 3231–3240. https://doi.org/10.1074/jbc.M111.293118

Nasmyth, K., & Haering, C. H. (2005). The structure and function of SMC and kleisin complexes. *Annual Review of Biochemistry*, *74*, 595–648. https://doi.org/10.1146/annurev.biochem.74.082803.133219

Olsen, S. K., & Lima, C. D. (2013). Structure of a Ubiquitin E1-E2 Complex: Insights to E1-E2 Thioester Transfer. *Molecular Cell*, *49*(5), 884–896. https://doi.org/10.1016/j.molcel.2013.01.013

Page, R. C., Pruneda, J. N., Amick, J., Klevit, R. E., & Misra, S. (2012). Structural insights into the conformation and oligomerization of e2~ubiquitin conjugates. *Biochemistry*, *51*(20), 4175–4187. https://doi.org/10.1021/bi300058m

Palecek, J. J., & Gruber, S. (2015). Kite Proteins: A Superfamily of SMC/Kleisin Partners Conserved Across Bacteria, Archaea, and Eukaryotes. *Structure*, *23*(12), 2183–2190. https://doi.org/10.1016/j.str.2015.10.004

Palecek, J., Vidot, S., Feng, M., Doherty, A. J., & Lehmann, A. R. (2006). The Smc5-Smc6 DNA repair complex: Bridging of the Smc5-Smc6 heads by the kleisin, nse4, and non-kleisin subunits. *Journal of Biological Chemistry*, *281*, 36952–36959. https://doi.org/10.1074/jbc.M608004200

Payne, F., Colnaghi, R., Rocha, N., Seth, A., Harris, J., Carpenter, G., … Semple, R. (2014). Hypomorphism in human NSMCE2 linked to primordial dwarfism and insulin resistance. *Journal of Clinical Investigation*, *124*(9), 4028–4038. https://doi.org/10.1172/JCI73264

Pebernard, S., Wohlschlegel, J., McDonald, W. H., Yates, J. R., & Boddy, M. N. (2006). The Nse5-Nse6 Dimer Mediates DNA Repair Roles of the Smc5-Smc6 Complex. *Molecular and Cellular Biology*, *26*(5), 1617–1630. https://doi.org/10.1128/MCB.26.5.1617-1630.2006

Pebernard, Stephanie, Perry, J. J. P., Tainer, J. A., & Boddy, M. N. (2008). Nse1 RING-like Domain Supports Functions of the Smc5-Smc6 Holocomplex in Genome Stability. *Molecular Biology of the Cell*, *19*(10), 4099–4109. https://doi.org/10.1091/mbc.e08-02-0226

Pichler, A. (2018). How DNA vicinity controls SUMO E3 ligase activity. *The EMBO Journal*, *37*(12), 2–3. https://doi.org/10.15252/embj.201899705

Pichler, A., Fatouros, C., Lee, H., & Eisenhardt, N. (2017). SUMO conjugation - A mechanistic view. *Biomolecular Concepts*, *8*(1), 13–36. https://doi.org/10.1515/bmc-2016-0030

Plechanovová, A., Jaffray, E. G., Tatham, M. H., Naismith, J. H., & Hay, R. T. (2012). Structure of a RING E3 ligase and ubiquitin-loaded E2 primed for catalysis. *Nature*, *489*(7414), 115–120. https://doi.org/10.1038/nature11376

Potts, P. R., Porteus, M. H., & Yu, H. (2006). Human SMC5/6 complex promotes sister chromatid homologous recombination by recruiting the SMC1/3 cohesin complex to double-strand breaks. *EMBO Journal*, *25*(14), 3377–3388. https://doi.org/10.1038/sj.emboj.7601218

Potts, P. R., & Yu, H. (2005). Human MMS21 / NSE2 Is a SUMO Ligase Required for DNA Repair †. *Molecular and Cellular Biology*, *25*(16), 7021–7032. https://doi.org/10.1128/MCB.25.16.7021

Potts, P. R., & Yu, H. (2007). The SMC5/6 complex maintains telomere length in ALT cancer cells through SUMOylation of telomere-binding proteins. *Nature Structural and Molecular Biology*, *14*(7), 581–590. https://doi.org/10.1038/nsmb1259

Prakash, L., & Prakash, S. (1977). Isolation and characterization of MMS-sensitive mutants of Saccharomyces cerevisiae. *Genetics*, *86*(1), 33–55. https://doi.org/10.1093/genetics/86.1.33

Pruneda, J. N., Stoll, K. E., Bolton, L. J., Brzovic, P. S., & Klevit, R. E. (2011). Ubiquitin in

motion: Structural studies of the ubiquitin-conjugating enzyme~ubiquitin conjugate. *Biochemistry*, *50*(10), 1624–1633. https://doi.org/10.1021/bi101913m

Psakhye, I., & Jentsch, S. (2012). Protein group modification and synergy in the SUMO pathway as exemplified in DNA repair. *Cell*, *151*(4), 807–820. https://doi.org/10.1016/j.cell.2012.10.021

Ranjha, L., Levikova, M., Altmannova, V., Krejci, L., & Cejka, P. (2019). Sumoylation regulates the stability and nuclease activity of Saccharomyces cerevisiae Dna2. *Communications Biology*, *2*(1). https://doi.org/10.1038/s42003-019-0428-0

Reverter, D., & Lima, C. D. (2004). A basis for SUMO protease specificity provided by analysis of human Senp2 and a Senp2-SUMO complex. *Structure*, *12*(8), 1519–1531. https://doi.org/10.1016/j.str.2004.05.023

Reverter, D., & Lima, C. D. (2005). Insights into E3 ligase activity revealed by a SUMO-RanGAP1-Ubc9-Nup358 complex. *Nature*, *435*(7042), 687–692. https://doi.org/10.1038/nature03588

Roy, M. A., & D'Amours, D. (2011). DNA-binding properties of Smc6, a core component of the Smc5-6 DNA repair complex. *Biochemical and Biophysical Research Communications*, *416*(1–2), 80–85. https://doi.org/10.1016/j.bbrc.2011.10.149

Roy, M. A., Dhanaraman, T., & D'Amours, D. (2015). The Smc5-Smc6 heterodimer associates with DNA through several independent binding domains. *Scientific Reports*, *5*, 1–12. https://doi.org/10.1038/srep09797

Roy, M. A., Siddiqui, N., & D'Amours, D. (2011). Dynamic and selective DNA-binding activity of Smc5, a core component of the Smc5-Smc6 complex. *Cell Cycle*, *10*(4), 690–700. https://doi.org/10.4161/cc.10.4.14860

Sachdev, S., Bruhn, L., Sieber, H., Pichler, A., Melchior, F., & Grosschedl, R. (2001). PIASy, a nuclear matrix-associated SUMO E3 ligase, represses LEF1 activity by sequestration into nuclear bodies. *Genes and Development*, *15*(23), 3088–3103. https://doi.org/10.1101/gad.944801

Saitoh, H., & Hinchey, J. (2000). Functional heterogeneity of small ubiquitin-related protein modifiers SUMO-1 versus SUMO-2/3. *Journal of Biological Chemistry*, *275*(9), 6252–6258. https://doi.org/10.1074/jbc.275.9.6252

Sampson, D. A., Wang, M., & Matunis, M. J. (2001). The Small Ubiquitin-like Modifier-1 (SUMO-1) Consensus Sequence Mediates Ubc9 Binding and is Essential for SUMO-1 Modification. *Journal of Biological Chemistry*, *276*(24), 21664–21669. https://doi.org/10.1074/jbc.M100006200

Sapetschnig, A., Rischitor, G., Braun, H., Doll, A., Schergaut, M., Melchior, F., & Suske, G. (2002). Transcription factor Sp3 is silenced through SUMO modification by PIAS1. *EMBO Journal*, *21*(19), 5206–5215. https://doi.org/10.1093/emboj/cdf510

Schmidt, D., & Müller, S. (2002). Members of the PIAS family act as SUMO ligases for c-Jun and p53 and repress p53 activity. *Proceedings of the National Academy of Sciences of the United States of America*, *99*(5), 2872–2877. https://doi.org/10.1073/pnas.052559499

Schneider, C. A., Rasband, W. S., & Eliceiri, K. W. (2012). NIH Image to ImageJ: 25 years of image analysis. *Nature Methods*, *9*(7), 671–675. https://doi.org/10.1038/nmeth.2089

Schulman, B. A., & Wade Harper, J. (2009). Ubiquitin-like protein activation by E1 enzymes: The apex for downstream signalling pathways. *Nature Reviews Molecular Cell Biology*, *10*(5), 319–331. https://doi.org/10.1038/nrm2673

Sergeant, J., Taylor, E., Palecek, J., Fousteri, M., Andrews, E. A., Sweeney, S., … Lehmann, A. R. (2005). Composition and Architecture of the Schizosaccharomyces pombe Rad18 (Smc5-6) Complex. *Molecular and Cellular Biology*, *25*(1), 172–184. https://doi.org/10.1128/mcb.25.1.172-184.2005

Serrano, D., Cordero, G., Kawamura, R., Sverzhinsky, A., Sarker, M., Roy, S., … D'Amours, D. (2020). The Smc5/6 Core Complex Is a Structure-Specific DNA Binding and Compacting Machine. *Molecular Cell*, *80*(6), 1025-1038.e5. https://doi.org/10.1016/j.molcel.2020.11.011

Song, J., Durrin, L. K., Wilkinson, T. A., Krontiris, T. G., & Chen, Y. (2004). Identification of a SUMO-binding motif that recognizes SUMO-modified proteins. *Proceedings of the National Academy of Sciences of the United States of America*, *101*(40), 14373–14378. https://doi.org/10.1073/pnas.0403498101

Song, J., Zhang, Z., Hu, W., & Chen, Y. (2005). Small ubiquitin-like modifier (SUMO) recognition of a SUMO binding motif: A reversal of the bound orientation. *Journal of Biological Chemistry*, *280*(48), 40122–40129. https://doi.org/10.1074/jbc.M507059200

Stewart, M. D., Ritterhoff, T., Klevit, R. E., & Brzovic, P. S. (2016). E2 enzymes: More than just middle men. *Cell Research*, *26*(4), 423–440. https://doi.org/10.1038/cr.2016.35

Streich, F. C., & Lima, C. D. (2014). Structural and functional insights to ubiquitin-like protein conjugation. *Annual Review of Biophysics*, *43*(1), 357–379. https://doi.org/10.1146/annurev-biophys-051013-022958

Streich, F. C., & Lima, C. D. (2016). Capturing a substrate in an activated RING E3/E2-SUMO complex. *Nature*, *536*(7616), 304–308. https://doi.org/10.1038/nature19071

Streich, F. C., & Lima, C. D. (2018). Strategies to Trap Enzyme-Substrate Complexes that Mimic Michaelis Intermediates During E3-Mediated Ubiquitin-Like Protein Ligation. *Methods in Molecular Biology*, *1844*, 169–196. https://doi.org/10.1007/978-1-4939-8706-1_12,

Taschner, M., Basquin, J., Steigenberger, B., Schäfer, I. B., Soh, Y., Basquin, C., … Gruber, S. (2021). Nse5/6 inhibits the Smc5/6 ATPase and modulates DNA substrate binding. *The EMBO Journal*, *40*(15), 1–23. https://doi.org/10.15252/embj.2021107807

Tatham, M. H., Matic, I., Mann, M., & Hay, R. T. (2011). Comparative proteomic analysis identifies a role for SUMO in protein quality control. *Science Signaling*, *4*(178). https://doi.org/10.1126/scisignal.2001484

Torres-Rosell, J., Mahín, F., Farmer, S., Jarmuz, A., Eydmann, T., Dalgaard, J. Z., … Branzei, D. (2005). SMC5 and SMC6 genes are required for the segregation of repetitive chromosome regions. *Nature Cell Biology*, *7*(4), 412–419. https://doi.org/10.1038/ncb1239

Varejão, N., Ibars, E., Lascorz, J., Colomina, N., Torres-rosell, J., & Reverter, D. (2018). DNA activates the Nse2/Mms21 SUMO E3 ligase in the Smc 5/6 complex. *EMBO Journal*, 1–16. https://doi.org/10.15252/embj.201798306

Varejão, N., Lascorz, J., Codina-Fabra, J., Bellí, G., Borràs-Gas, H., Torres-Rosell, J., & Reverter, D. (2021). Structural basis for the E3 ligase activity enhancement of yeast Nse2 by SUMO-interacting motifs. *Nature Communications*, *12*(1), 1–14. https://doi.org/10.1038/s41467-021-27301-9

Varejão, N., Lascorz, J., Li, Y., & Reverter, D. (2020). Molecular mechanisms in SUMO conjugation. *Biochemical Society Transactions*, 1–13. https://doi.org/10.1042/bst20190357

Verver, D. E., Hwang, G. H., Jordan, P. W., & Hamer, G. (2016). Resolving complex chromosome structures during meiosis: versatile deployment of Smc5/6. *Chromosoma*, *125*(1), 15–27. https://doi.org/10.1007/s00412-015-0518-9

Walter, T. S., Meier, C., Assenberg, R., Au, K. F., Ren, J., Verma, A., … Grimes, J. M. (2006). Lysine Methylation as a Routine Rescue Strategy for Protein Crystallization. *Structure*, *14*(11), 1617–1622. https://doi.org/10.1016/j.str.2006.09.005

Wei, W., Yang, P., Pang, J., Zhang, S., Wang, Y., Wang, M. H., … Wang, C. Y. (2008). A stress-dependent SUMO4 sumoylation of its substrate proteins. *Biochemical and Biophysical Research Communications*, *375*(3), 454–459. https://doi.org/10.1016/j.bbrc.2008.08.028

Welchman, R. L., Gordon, C., & Mayer, R. J. (2005). Ubiquitin and ubiquitin-like proteins as multifunctional signals. *Nature Reviews Molecular Cell Biology*, *6*(8), 599–609. https://doi.org/10.1038/nrm1700

Winn, M. D., Ballard, C. C., Cowtan, K. D., Dodson, E. J., Emsley, P., Evans, P. R., … Wilson, K. S. (2011). Overview of the CCP4 suite and current developments. *Acta Crystallographica Section D: Biological Crystallography*, *67*(4), 235–242. https://doi.org/10.1107/S0907444910045749

Yeh, E. T. H. (2009). SUMOylation and De-SUMOylation: Wrestling with life's processes. *Journal of Biological Chemistry*, *284*(13), 8223–8227. https://doi.org/10.1074/jbc.R800050200

Yong-Gonzales, V., Hang, L. E., Castellucci, F., Branzei, D., & Zhao, X. (2012). The Smc5-Smc6 Complex Regulates Recombination at Centromeric Regions and Affects Kinetochore Protein Sumoylation during Normal Growth. *PLoS ONE*, *7*. https://doi.org/10.1371/journal.pone.0051540

Yu, Y., Li, S., Ser, Z., Sanyal, T., Choi, K., Wan, B., … Zhao, X. (2021). Integrative analysis reveals unique structural and functional features of the Smc5/6 complex. *Proceedings of the National Academy of Sciences of the United States of America*, *118*(19). https://doi.org/10.1073/pnas.2026844118

Yunus, A. A., & Lima, C. D. (2005). Purification and activity assays for Ubc9, the ubiquitin-conjugating enzyme for the small ubiquitin-like modifier SUMO. *Methods in Enzymology*, *398*(05), 74–87. https://doi.org/10.1016/S0076-6879(05)98008-7

Yunus, A. A., & Lima, C. D. (2006). Lysine activation and functional analysis of E2-mediated conjugation in the SUMO pathway. *Nature Structural and Molecular Biology*, *13*(6), 491–499. https://doi.org/10.1038/nsmb1104

Yunus, A. A., & Lima, C. D. (2009). Structure of the Siz/PIAS SUMO E3 Ligase Siz1 and Determinants Required for SUMO Modification of PCNA. *Molecular Cell*, *35*(5), 669–682. https://doi.org/10.1016/j.molcel.2009.07.013

Zabrady, K., Adamus, M., Vondrova, L., Liao, C., Skoupilova, H., Novakova, M., … Palecek, J. J. (2016). Chromatin association of the SMC5/6 complex is dependent on binding of its NSE3 subunit to DNA. *Nucleic Acids Research*, *44*(3), 1064–1079. https://doi.org/10.1093/nar/gkv1021

Zhao, X., & Blobel, G. (2005). A SUMO ligase is part of a nuclear multiprotein complex that affects DNA repair and chromosomal organization. *Proceedings of the National Academy of Sciences*, *102*(13), 4777–4782.

https://doi.org/10.1073/pnas.0500537102

Zhen, Y., Knobel, P. A., Stracker, T. H., & Reverter, D. (2014). Regulation of USP28 deubiquitinating activity by SUMO conjugation. *Journal of Biological Chemistry*, *289*(50), 34838–34850. https://doi.org/10.1074/jbc.M114.601849

Zheng, N., & Shabek, N. (2017). Ubiquitin ligases: Structure, function, and regulation. *Annual Review of Biochemistry*, *86*, 129–157. https://doi.org/10.1146/annurev-biochem-060815-014922

Zhu, J., Zhu, S., Guzzo, C. M., Ellis, N. A., Ki, S. S., Cheol, Y. C., & Matunis, M. J. (2008). Small ubiquitin-related modifier (SUMO) binding determines substrate recognition and paralog-selective SUMO modification. *Journal of Biological Chemistry*, *283*(43), 29405–29415. https://doi.org/10.1074/jbc.M803632200

Zhu, S., Goeres, J., Sixt, K. M., Békés, M., Zhang, X. D., Salvesen, G. S., & Matunis, M. J. (2009). Protection from Isopeptidase-Mediated Deconjugation Regulates Paralog-Selective Sumoylation of RanGAP1. *Molecular Cell*, *33*(5), 570–580. https://doi.org/10.1016/j.molcel.2009.02.008

Zimmermann, L., Stephens, A., Nam, S. Z., Rau, D., Kübler, J., Lozajic, M., … Alva, V. (2018). A Completely Reimplemented MPI Bioinformatics Toolkit with a New HHpred Server at its Core. *Journal of Molecular Biology*, *430*(15), 2237–2243. https://doi.org/10.1016/j.jmb.2017.12.007